

NASA/TM—2003—212236, Vol. 7



**Topography Experiment (TOPEX)
Software Document Series**

Volume 7

**TOPEX Mission Radar Altimeter
Engineering Assessment Report**

February 1994

D.W. Hancock III

G.S. Hayne

C.L. Purdy

R.L. Brooks

TOPEX Contact:

D.W. Hancock III

The NASA STI Program Office ... in Profile

Since its founding, NASA has been dedicated to the advancement of aeronautics and space science. The NASA Scientific and Technical Information (STI) Program Office plays a key part in helping NASA maintain this important role.

The NASA STI Program Office is operated by Langley Research Center, the lead center for NASA's scientific and technical information. The NASA STI Program Office provides access to the NASA STI Database, the largest collection of aeronautical and space science STI in the world. The Program Office is also NASA's institutional mechanism for disseminating the results of its research and development activities. These results are published by NASA in the NASA STI Report Series, which includes the following report types:

- **TECHNICAL PUBLICATION.** Reports of completed research or a major significant phase of research that present the results of NASA programs and include extensive data or theoretical analysis. Includes compilations of significant scientific and technical data and information deemed to be of continuing reference value. NASA's counterpart of peer-reviewed formal professional papers but has less stringent limitations on manuscript length and extent of graphic presentations.
- **TECHNICAL MEMORANDUM.** Scientific and technical findings that are preliminary or of specialized interest, e.g., quick release reports, working papers, and bibliographies that contain minimal annotation. Does not contain extensive analysis.
- **CONTRACTOR REPORT.** Scientific and technical findings by NASA-sponsored contractors and grantees.
- **CONFERENCE PUBLICATION.** Collected papers from scientific and technical conferences, symposia, seminars, or other meetings sponsored or cosponsored by NASA.
- **SPECIAL PUBLICATION.** Scientific, technical, or historical information from NASA programs, projects, and mission, often concerned with subjects having substantial public interest.
- **TECHNICAL TRANSLATION.** English-language translations of foreign scientific and technical material pertinent to NASA's mission.

Specialized services that complement the STI Program Office's diverse offerings include creating custom thesauri, building customized databases, organizing and publishing research results . . . even providing videos.

For more information about the NASA STI Program Office, see the following:

- Access the NASA STI Program Home Page at <http://www.sti.nasa.gov/STI-homepage.html>
- E-mail your question via the Internet to help@sti.nasa.gov
- Fax your question to the NASA Access Help Desk at (301) 621-0134
- Telephone the NASA Access Help Desk at (301) 621-0390
- Write to:
NASA Access Help Desk
NASA Center for AeroSpace Information
7121 Standard Drive
Hanover, MD 21076-1320

NASA/TM—2003—212236, Vol. 7



**Topography Experiment (TOPEX)
Software Document Series**

Volume 7

**TOPEX Mission Radar Altimeter
Engineering Assessment Report**

February 1994

*D.W. Hancock III, G.S. Hayne, C.L. Purdy, R.L. Brooks
NASA GSFC Wallops Flight Facility, Wallops Island, VA*

*TOPEX Contact:
David W. Hancock III
NASA GSFC Wallops Flight Facility, Wallops Island, VA*

National Aeronautics and
Space Administration

Goddard Space Flight Center
Greenbelt, Maryland 20771

September 2003

About the Series

The TOPEX Radar Altimeter Technical Memorandum Series is a collection of performance assessment documents produced by the NASA Goddard Space Flight Center Wallops Flight Facility over a period starting before the TOPEX launch in 1992 and continuing over greater than the 10 year TOPEX lifetime. Because of the mission's success over this long period and because the data are being used internationally to redefine many aspects of ocean knowledge, it is important to make a permanent record of the TOPEX radar altimeter performance assessments which were originally provided to the TOPEX project in a series of internal reports over the life of the mission. The original reports are being printed in this series without change in order to make the information more publicly available as the original investigators become less available to explain the altimeter operation and details of the various data anomalies that have been resolved.

Available from:

NASA Center for AeroSpace Information
7121 Standard Drive
Hanover, MD 21076-1320
Price Code: A17

National Technical Information Service
5285 Port Royal Road
Springfield, VA 22161
Price Code: A10

February 1994

ACKNOWLEDGMENTS

The authors gratefully acknowledge the contributions of the members of the Wallops TOPEX Software Development Team and TOPEX Hardware Development Team:

Ronald Forsythe (NASA)

Hayden Gordon (CSC)

Jeff Lee (CSC)

Dennis Lockwood (CSC)

Carol Purdy (CSC)

Rob Ryan (CSC)

Bill Shoemaker (SMSRC)

TABLE OF CONTENTS

1.0	INTRODUCTION	1
2.0	RELATIONSHIPS TO OTHER DOCUMENTS.....	2
3.0	RADAR ALTIMETER DESCRIPTION.....	5
4.0	ON-ORBIT INSTRUMENT PERFORMANCE REQUIREMENTS	10
4.1	Height Measurements	10
4.2	Height Measurement Drift Rate.....	11
4.3	Sea State (H1/3).....	11
4.4	Altitude Velocity and Acceleration	11
4.5	Acquisition and Data Quality Settling Time	11
4.6	Absolute Internal Calibration.....	11
4.7	Radar Reflectivity (Backscatter Coefficient).....	12
4.8	Ancillary Altimeter System Specifications	12
5.0	ON-ORBIT INSTRUMENT PERFORMANCE ASSESSMENT.....	14
5.1	Height Measurements	14
5.2	Height Measurement Drift Rate.....	16
5.3	Sea State (H1/3).....	16
5.4	Altitude Velocity and Acceleration	19
5.5	Acquisition and Data Quality Settling Time	19
5.6	Absolute Internal Calibration.....	23
5.7	Radar Reflectivity (Backscatter Coefficient).....	29
5.8	Ancillary Altimeter Systems Performance	31
6.0	WAVEFORM SAMPLES ASSESSMENT.....	43
6.1	Introduction	43
6.2	Digital Filter Bank	43
6.3	Correction/Compensation for Waveform Effects.....	63
6.4	Waveform Effects Status	64
7.0	ENGINEERING MONITORS.....	69
7.1	Temperatures	69
7.2	Voltages, Powers and Currents.....	69
8.0	SYNOPSIS OF ENGINEERING ASSESSMENT	89

LIST OF FIGURES

Figure 3.0	Altimeter Block Diagram	7
Figure 4.8.2	Relationships of Onboard Waveform Samplers and Telemetered Tracking Gates	13
Figure 5.1.2	Calculated Ionospheric Corrections for a Daytime Pass and a Nighttime Pass	17
Figure 5.3a	Histogram of SWH for a 10-Day Cycle	18
Figure 5.3b	SWH Intercomparison	20
Figure 5.4	Altitude Velocities for Typical Ascending Groundtrack and Typical Descending Groundtrack	21
Figure 5.4b	Altitude Accelerations for Typical Ascending Groundtrack and Typical Descending Groundtrack	22
Figure 5.6a	Ku Height and C Height Calibration Results Since Launch	25
Figure 5.6b	Ku AGC and C AGC Calibration Results Since Launch	26
Figure 5.6c	Ku and C AGC Calibration Plots for CAL2	27
Figure 5.6d	Ku and C Transmit Power During Calibration, Converted to Watts to dB	28
Figure 5.7	Histogram of Sigma-Zero for a 10-Day Cycle	30
Figure 5.8.1	Frequency Reference Unit Performance	32
Figure 5.8.3	Locations of Single Event Upsets	35
Figure 5.8.4	Command Block Mode Switching	36
Figure 6.2.1	TOPEX Altimeter Data Processing	44
Figure 6.2.2.2a	TOPEX Ku Waveform for 1993 Day 257 Data	48
Figure 6.2.2.2b	TOPEX Ku Waveform for 1993 Day 257 Data	49
	(Magnified Portion)	

LIST OF FIGURES
(continued)

Figure 6.2.2.2c	Calibration Mode 2 Waveform Data for TOPEX Ku-Band Altimeter	50
Figure 6.2.2.2d	Jensen Simulation Cal-II Waveforms	51
Figure 6.2.2.2e	Jensen Simulation Cal-II Waveforms	52
Figure 6.2.2.2f	Modeling Results for TOPEX Ku Altimeter	53
Figure 6.2.2.2g	Modeling Results for TOPEX Ku Altimeter	55
Figure 6.2.2.2h	Modeling Results for TOPEX Ku Altimeter	56
Figure 6.2.3.1	Sketch of Height Location Within Fine Height Word	57
Figure 6.2.3.2	TOPEX Video Shape for Different Values of the Fine Height Word	59
Figure 6.2.3.4	TOPEX Altimeter Gates and Center Locations of Leakage Spikes	61
Figure 6.3.2	TOPEX Altimeter Gates and Smeared Locations of Leakage	65
Figure 6.3.3	Comparison of Input, Corrected, and Fitted Ku Waveforms for 1993 Day 257 Data	67
Figure 7.1	Temperature History Plots	70
Figure 7.2	Monitor History Plots	80

LIST OF TABLES

Table 3.0a	TOPEX Technical Characteristics.....	6
Table 3.0b	Telemetry Produced in Each Altimeter Mode	8
Table 3.0c	Definition of Altimeter Modes	9
Table 4.1a	Height Measurement Noise Specifications for Three-Second Averaging Interval.....	10
Table 4.1b	Height Measurement Noise Specifications for One-Second Averaging Interval	10
Table 5.1.1a	One-Second Range Measurement Noise Performance	15
Table 5.1.1b	One-Second Pooled Range Measurement Noise Performance	15
Table 5.6a	AGC Corrections for GDR Production	24
Table 5.6b	AGC Calibration Comparisons: Launch to Date	29
Table 5.8.4	Comparison of Initial (PARMC320) and Present (C35028SL) Programmable Parameter Sets	38
Table 6.2.1	TOPEX Waveform to Telemetry Sample Compression in Different Modes.....	45
Table 6.2.3.1	Fine Height Word Value Summary	58
Table 6.2.3.4	Characterization of TOPEX Waveform Leakage Spikes.....	62
Table 6.3.2	TOPEX Waveform Multiplicative and Additive Correction Factors	66
Table 7.1	Thermistor Minimum/Maximum Temperatures During Track Mode	79
Table 7.2	Comparison of Pre-Launch and On-Orbit Engineering Parameters During Track Mode.....	86

1.0 INTRODUCTION

The primary objective of the NASA Ocean Topography Experiment (TOPEX) project is to develop, launch, and operate a satellite-borne dual-frequency radar altimeter; the altimeter is to provide ocean topographic range measurements with a nominal precision of ± 2.4 cm and an overall accuracy of ± 14 cm. The Johns Hopkins University Applied Physics Laboratory (JHU/APL) developed the altimeter hardware for NASA's Goddard Space Flight Center/Wallops Flight Facility (GSFC/WFF). The TOPEX altimeter was integrated into the TOPEX/POSEIDON spacecraft by Fairchild Space (FS) Company.

POSEIDON is a single-frequency solid-state altimeter developed by the Centre National d'Etudes Spatiales (CNES) of France. TOPEX and POSEIDON share a NASA-provided antenna on the spacecraft. The TOPEX/POSEIDON launch date was August 10, 1992.

This document describes the GSFC/WFF analysis of the on-orbit engineering data from the TOPEX radar altimeter, to establish altimeter performance. In accordance with Project guidelines, neither surface truth nor precision orbital data are used for the engineering assessment of the altimeter. The use of such data would imply not only a more intensive and complete performance evaluation, but also a calibration. Such evaluations and calibrations are outside the scope of this document and will be presented in a separate Verification Report.

2.0 RELATIONSHIPS TO OTHER DOCUMENTS

The *TOPEX Project Plan* (Reference 1) is the controlling document for Project and Mission goals, and specifies the methods to be used to achieve those goals. *TOPEX Project Requirements and Constraints* (Reference 2) and *TOPEX Project Mission and Systems Requirements* (Reference 3) are the controlling documents for requirements and constraints placed on the Project. *TOPEX/POSEIDON Project Joint Verification Plan* (Reference 4) is in consonance with these plans and is the controlling document for specifying verification activities and plans. References 5 through 28 are supporting documents for this verification effort.

- (1) *TOPEX Project Plan*, July 1989, Jet Propulsion Laboratory (JPL), JPL D-3635, 633-100.
- (2) *TOPEX Project Requirements and Constraints*, Rev. B, October 1988, JPL D-2555, 633-102.
- (3) *TOPEX Project Mission and Systems Requirements*, April 1989, JPL D-5901, 633-103.
- (4) *TOPEX/POSEIDON Joint Verification Plan*, June 15, 1992, JPL92-9
- (5) *TOPEX Mission Radar Altimeter Engineering Support Plan*, May 1992, NASA GSFC WFF.
- (6) *TOPEX Project Radar Altimeter Development Requirements and Specifications*, August 1988, NASA GSFC WFF 672-85-004.
- (7) *TOPEX Ground System Algorithm Specification Document*, September 1990, JPL D-7075 (Rev. A), TOPEX 633-708.
- (8) *Interface Control Document between the TOPEX Ground System and the Goddard Space Flight Center/Wallops Flight Facility Oceans Laboratory*, (Rev. 2.0), July 1990, TOPEX 633-712J.
- (9) *Wallops Flight Facility TOPEX Project Software Products Specification for Engineering Assessment Software*, January 1991.
- (10) Hayne, G. S., and D. W. Hancock, III, March 1990, *Corrections for The Effects of Significant Wave Height and Attitude on GEOSAT Radar Altimeter Measurements*, Journal of Geophysical Research, Vol. 95, No. C3, pp. 2837-2842.

- (11) Hancock, D. W., III, R. L. Brooks and D. W. Lockwood, March 1990, *Effects of Height Acceleration on GEOSAT Heights*, Journal of Geophysical Research, Vol. 95, No. C3, pp. 2843-2848.
- (12) Callahan, P. S., 1984, *Ionospheric Variations Affecting Altimeter Measurements: A Brief Synopsis*, Marine Geodesy, Volume 8.
- (13) Dodson, A.H., 1986, *Refraction and Propagation Delays in Space Geodesy*, International Journal of Remote Sensing, 7, pp. 515-524.
- (14) Goldhirsh, J. and J. R. Rowland, 1982, *A Tutorial Assessment of Atmospheric Height Uncertainties for High-Precision Satellite Altimeter Missions to Monitor Ocean Currents*, IEEE Transactions on Geoscience and Remote Sensing, GE-20, pp. 418-434.
- (15) Hagfors, T., 1976, *Atmospheric Effects: The Ionosphere*, in *Methods of Experimental Physics*, Volume 12, Astrophysics, Part B: Radio Telescopes, edited by M. L. Meeks, pp. 119-135.
- (16) Lawrence, R. S., C. G. Little, and H. J.A. Chivers, 1964, *A Survey of Ionospheric Effects upon Earth-Space Radio Propagation*, Proceedings IEEE, 52, pp. 4-27.
- (17) Lorell, J., E. Colquitt, and R. J. Anderle, 1982, *Ionospheric Corrections for SEASAT Altimeter Height Measurement*, Journal of Geophysical Research, Res. 87, pp. 3207-3212.
- (18) Rush, C. M., *Ionospheric Radio Propagation Models and Predictions - A Mini-Review*, IEEE Transactions, Antennas & Propagation, AP-34, pp. 1163-1170, 1986.
- (19) Spoelstra, T. A., 1986, *Correcting Ionospheric Effects in Radio Astronomy and Satellite Geodesy*, International Beacon Satellites Symposium on Radio Beacon Contribution to The Study of Ionization and Dynamics of The Ionosphere and to Corrections to Geodesy and Technical Workshop, Oulu, Finland, June 9-14, 1986, Proceedings, Part 2, pp. 253-275.
- (20) Hancock, D. W., III, 1989, *Studies in Support of The NASA Ocean Topography Experiment (Report 1)*, NASA TM-100766.
- (21) Zieger, Alfred R., David W. Hancock, III, George S. Hayne, and Craig L. Purdy, June 1991, *NASA Radar Altimeter for The TOPEX/POSEIDON Project*, Proceedings of The IEEE, Vol. 79, No. 6, pp. 810-826.

- (22) Marth, P. C., J. R. Jensen, C.C.Kilgus, J. A. Perschy, and J. L. MacArthur of The Johns Hopkins University Applied Physics Laboratory; D. W. Hancock, III, G. S. Hayne, C. L. Purdy, and L. C. Rossi of NASA GSFC WFF; and C.J. Koblinsky of NASA GSFC, *Pre-Launch Performance of the NASA TOPEX/POSEIDON Altimeter*, IEEE Transactions on Geoscience and Remote Sensing, 31(2), pp. 315-332, 1993.
- (23) Hancock, D. W., III, Memorandum to Craig L. Purdy, June 1992, *Pre-Ship TOPEX Height Bias Calibration*, NASA GSFC WFF.
- (24) Hancock, D. W., III, R. L. Brooks and H. A. Goldberg, June 1992, Performance Parameters for The TOPEX Radar Altimeter from Bench Testing through Spacecraft Thermal Vacuum Testing, NASA GSFC WFF.
- (25) Applied Physics Laboratory, *TOPEX Radar Altimeter System Specification*. APL Document 7301-9028.
- (26) Hayne, G.S., March 1993, *Estimating Ku Range Noise*, WFF TOPEX Informal Memorandum.
- (27) Hayne, G.S., September 1993, *Current Status of Work on σ^0 Blooms*, WFF TOPEX Informal Memorandum.
- (28) Hayne, G.S., D.W. Hancock III, C.L. Purdy, and P.S. Callahan, 1994, *The Corrections for Significant Waveheight and Attitude Effects in the TOPEX Radar Altimeter*. Draft submitted to Journal of Geophysical Research.

3.0 RADAR ALTIMETER DESCRIPTION

TOPEX is a dual-frequency radar altimeter with complete redundancy of all active circuitry. It is a nadir-looking radar which transmits RF energy towards the earth's surface, then receives and processes the reflected energy. It measures height above the earth's surface (pulse transmit time), ocean significant waveheight (via return pulse shape characteristics), and surface radar backscatter coefficient (via received energy).

The TOPEX radar altimeter design has evolved from a number of previous designs (for example, Seasat and Geosat), but also includes a second frequency to yield information on propagation delay due to the ionosphere. The two frequencies are Ku-Band (13.6 GHz) and C-Band (5.3 GHz); the height of the altimeter above the ocean surface will be measured at each frequency. The desired bandwidth for Ku-Band and for C-Band is 320 MHz. However, because of discrete geographic areas where 320 MHz may produce interference with ground-based C-Band systems, the contingency capability exists to change the C-Band bandwidth to 100 MHz for those geographic areas. The technical characteristics of the TOPEX radar altimeter are summarized in Table 3.0a, and a block diagram of the altimeter appears in Figure 3.0.

The TOPEX spacecraft has an onboard recording capability. Altimeter data are telemetered in two streams, the engineering stream and the science stream. The engineering stream includes engineering measurements, and is transmitted approximately every eight seconds. The science stream, which is transmitted at approximately one-second intervals, includes: Ku heights, C-minus-Ku height differences, significant waveheight voltage, waveform samples, and Automatic Gain Control values (signal strength measurement). The altimeter waveforms are processed to calculate significant wave height and provide corrected off-nadir angles. The Automatic Gain Control (AGC) is converted to sigma naught for windspeed estimation. Table 3.0b lists the availability of altimeter data streams for each altimeter mode.

Initiation of altimeter modes occurs by ground command, either real-time or delayed. The altimeter modes are defined in Table 3.0c.

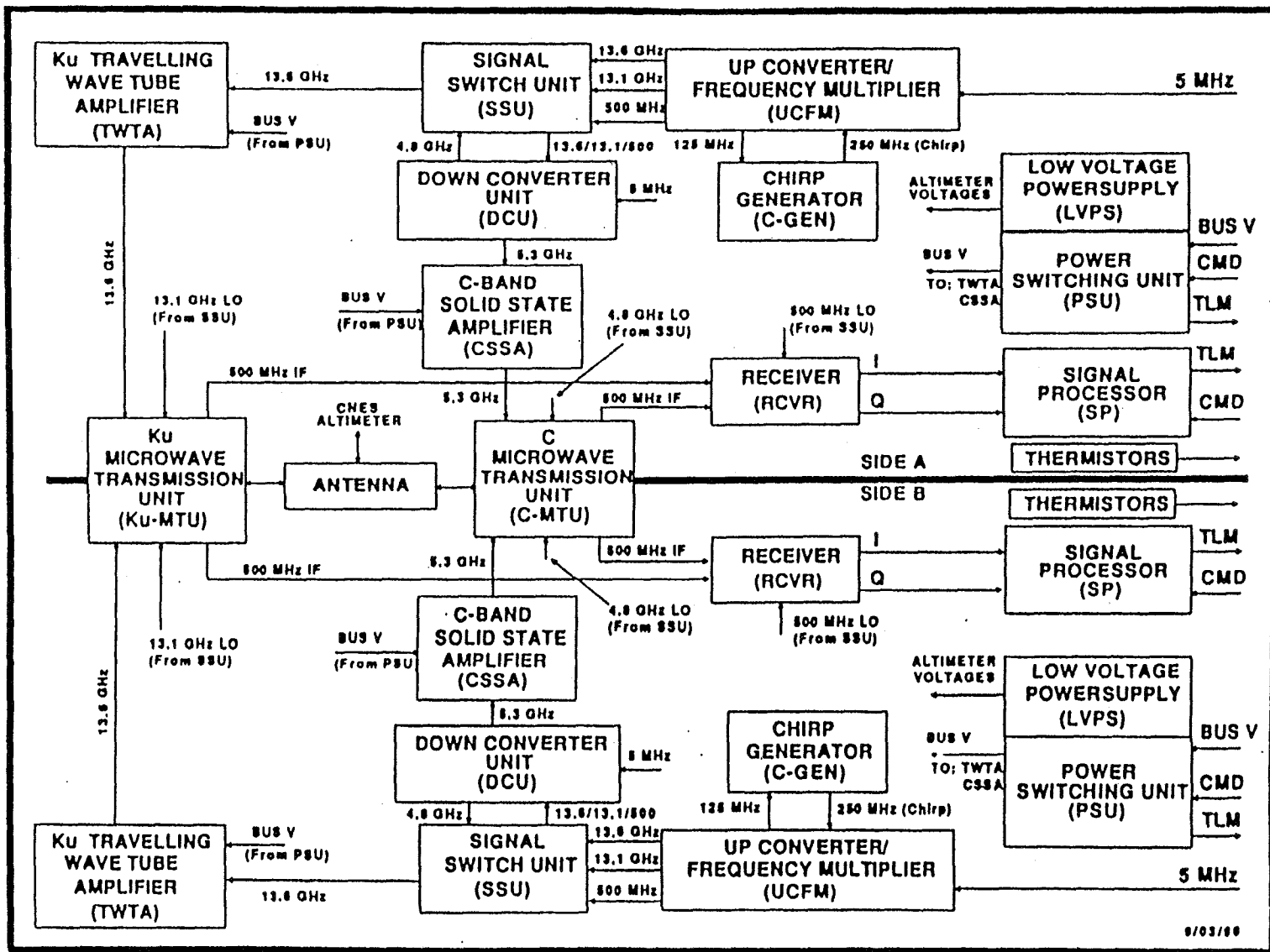
Parameter	Ku/C
Mean Altitude (KM)	1336
Frequency (GHz)	13.6/5.3
Antenna Beamwidth (deg)	1.0/2.7
Peak RF Power (W)	20
Average RF Power (W)	9.2/2.3
Pulsewidth (uncompressed)	102.4 msec*
Pulsewidth (nsec) (compressed)	3.125*
Repetition Frequency (Hz)	4500/1100 **
Mission Duration (yrs)	3-5
Inclination (deg)	66.0
Repeat Cycle (days)	10
Beam Limited Footprint Diameter (KM)	24.3/63 ***
Pulse Limited Footprint Diameter (KM)	2.2 ***

* Nominal pulsewidth

** Varies with altitude.

*** 320 MHz, varies with pulsewidth and seastate.

Table 3.0a TOPEX Technical Characteristics



TOPEX RADAR ALTIMETER - BLOCK DIAGRAM

Figure 3.0 Altimeter Block Diagram (from APL Document 7301-9028)

Altimeter Mode	Telemetry Produced	
	Engineering	Science
OFF	No	No
IDLE	Yes	No
STANDBY	Yes	Yes
CALIBRATION	Yes	Yes
TRACK	Yes	Yes

Table 3.0b - Telemetry Produced in Each Altimeter Mode

Altimeter Mode	Definition
OFF 1	The spacecraft power system is not applying 28 volts to the radar altimeter. The spacecraft power bus relay to the altimeter is open.
OFF 2	The spacecraft power system is applying 28 volts to the radar altimeter, but all systems within the altimeter are in the OFF state. The internal altimeter relays are open. Power is supplied to the charging capacitors.
IDLE	The altimeter does not transmit. Primarily used when the CNES altimeter is on.
STANDBY	The altimeter does not transmit.
CALIBRATION	CAL-I is the first of two internal calibration modes. The transmitted pulse is fed back to the altimeter through a series of attenuators in 17 discrete steps. Provides monitoring of height bias, total loop gain characteristics, and waveform sample operations.
- CAL-I	
- CAL-II	This is the second of two internal calibration modes. CAL-II is a single-step process wherein the AGC operates on noise only. Provides receiver and waveform characteristics.
TRACK	The flight software searches for a return signal from the surface in low resolution (50 ns pulsewidth).
- COARSE ACQUISITION	
- COARSE TRACK	Surface return waveforms are tracked in coarse resolution.
- FINE ACQUISITION	After a signal is detected in coarse resolution, fine resolution acquisition (3.125 ns) begins. If the tracking performance in the Coarse Track mode is of sufficient quality, this step is omitted and the altimeter goes directly to Fine Track mode.
- FINE TRACK	Surface return waveforms are tracked in fine resolution.

Table 3.0c Definition of Altimeter Modes

4.0 ON-ORBIT INSTRUMENT PERFORMANCE REQUIREMENTS

The source for the requirements that follow is the *TOPEX Project Radar Altimeter Development Requirements and Specification* document, August 25, 1988, WFF-672-85-004.

4.1 Height Measurements

The term "height measurement", as used in this document, is synonymous with the term "range measurement." It refers to the fundamental process of the altimeter, the precise measurement of the distance between the sensor and the Earth's surface at nadir.

At an averaged output rate of height measurement over a minimum duration of one minute, the combined and single channel noise level of the Ku- and C-Band data shall be such that 68% of the height data will be within the specifications listed in Tables 4.1a and 4.1b.

H 1/3	Combined Ku/C Bands	Ku - Band 320 MHz BW	C-Band 320 MHz BW	C-Band 100 MHz BW
2m	2.4cm	2.0cm	3.1cm	6.3cm
4m	2.7cm	2.2cm	3.5cm	8.0cm
8m	3.2cm	2.6cm	4.3cm	8.4cm

Table 4.1a Height Measurement Noise Specifications for Three-Second Averaging Interval

H 1/3	Combined Ku/C Bands	Ku - Band 320 MHz BW	C-Band 320 MHz BW	C-Band 100 MHz BW
2m	4.1cm	3.5cm	5.4cm	10.9cm
4m	4.6cm	3.8cm	6.1cm	13.9cm
8m	5.5cm	4.5cm	7.4cm	14.5cm

Table 4.1b Height Measurement Noise Specifications for One-Second Averaging Interval

On-orbit measurement specifications assume a wave skewness value of 0.1, and a rainfall rate of less than 2 mm/hour.

4.2 Height Measurement Drift Rate

After appropriate internal calibration, the maximum residual height drift rate shall be less than 2 cm per 10 days, during combined or single channel operation.

4.3 Sea State (H1/3)

At an averaged output rate of one per second, the accuracy of H1/3 shall be within 10% or 50 cm, whichever value is larger, of the true sea state. This accuracy is to be attainable over a wave height range of 1 to 20 m, and pertains to both Ku- and C-Band measurements.

4.4 Altitude Velocity and Acceleration

The altimeter is to provide a measurement of the height velocity for combined or single channel operation to ± 1 cm/s over the range of 0 to ± 50 m/s. The derived acceleration lag values, after ground-processing, are to have an accuracy of ≤ 0.2 cm under height acceleration conditions of ≤ 1 m/s/s for combined or single channel operation.

4.5 Acquisition and Data Quality Settling Time

The altimeter shall provide data of the specified quality within 5 seconds of the initiation of acquisition over the ocean. This is applicable to combined or single channel operation for height accelerations of -1 to +1 m/s/s.

4.6 Absolute Internal Calibration

An absolute internal calibration capability will be provided for both the Ku- and C-Band channels. This calibration will be performed twice per day, and will monitor:

- Changes in internal height bias to ± 1.5 cm or less.
- Gate bias and gain to $\pm 1\%$ of maximum average value at nadir and zero H1/3.
- Transmit power to ± 1 dB.
- Loop Gain Changes in Automatic Gain Control values related to Radio Frequency (RF) path loss, RF output power, receiver gain, or processor performance with precision and accuracy of ± 0.25 dB.

4.7 Radar Reflectivity (Backscatter Coefficient)

The ocean backscatter coefficient, sigma-zero, is to be determined within a measurement precision of ± 0.25 dB, with a measurement accuracy of ± 1.0 dB in both the Ku- and C-Band channels.

4.8 Ancillary Altimeter System Specifications

4.8.1 Time-Tag Precision and Accuracy

The Frequency Reference Unit (FRU) specifications are to provide a frequency stability of 1 part in 7×10^{11} in a 24-hour period, and an absolute frequency accuracy of 1 part in 7×10^8 over a 3-year period, for the 5 MHz altimeter input.

The maximum time-tag bias error within the altimeter will be ≤ 10 μ sec. The time-tag bias is defined as the difference between the spacecraft time when a particular altitude measurement is performed by the altimeter and the time inserted in the telemetry data within the altimeter. Time-tag bias error in this assessment context does not include clock errors which may exist in the timing system of the spacecraft. The overall time-tag error, including spacecraft timing errors, is to be ≤ 100 μ sec.

4.8.2 Waveform Samples

The altimeter will acquire 128 waveform samples of the ocean surface return in each of the two channels. Sixty-four amalgamations of the waveform samples, as shown in Figure 4.8.2 (Item 2), will be telemetered in the data stream. The 64 samples are telemetered at a 10-per-frame rate (primary channel) and a 5-per-frame rate (secondary channel) with a selection available to designate which channel is to be high or low rate. Figure 4.8.2 pertains to Ku-Band waveforms; the C-Band waveform relationships are identical except that C-Band waveforms are shifted three gates to the right (later in time).

4.8.3 Command Capability and Programmability

The altimeter will be commandable to various modes through the spacecraft interface via ground uplink. The ground uplink may also be used to reprogram the onboard altimeter operational programs.

Relationships of Onboard waveform samplers and Telemetered Tracking Gates

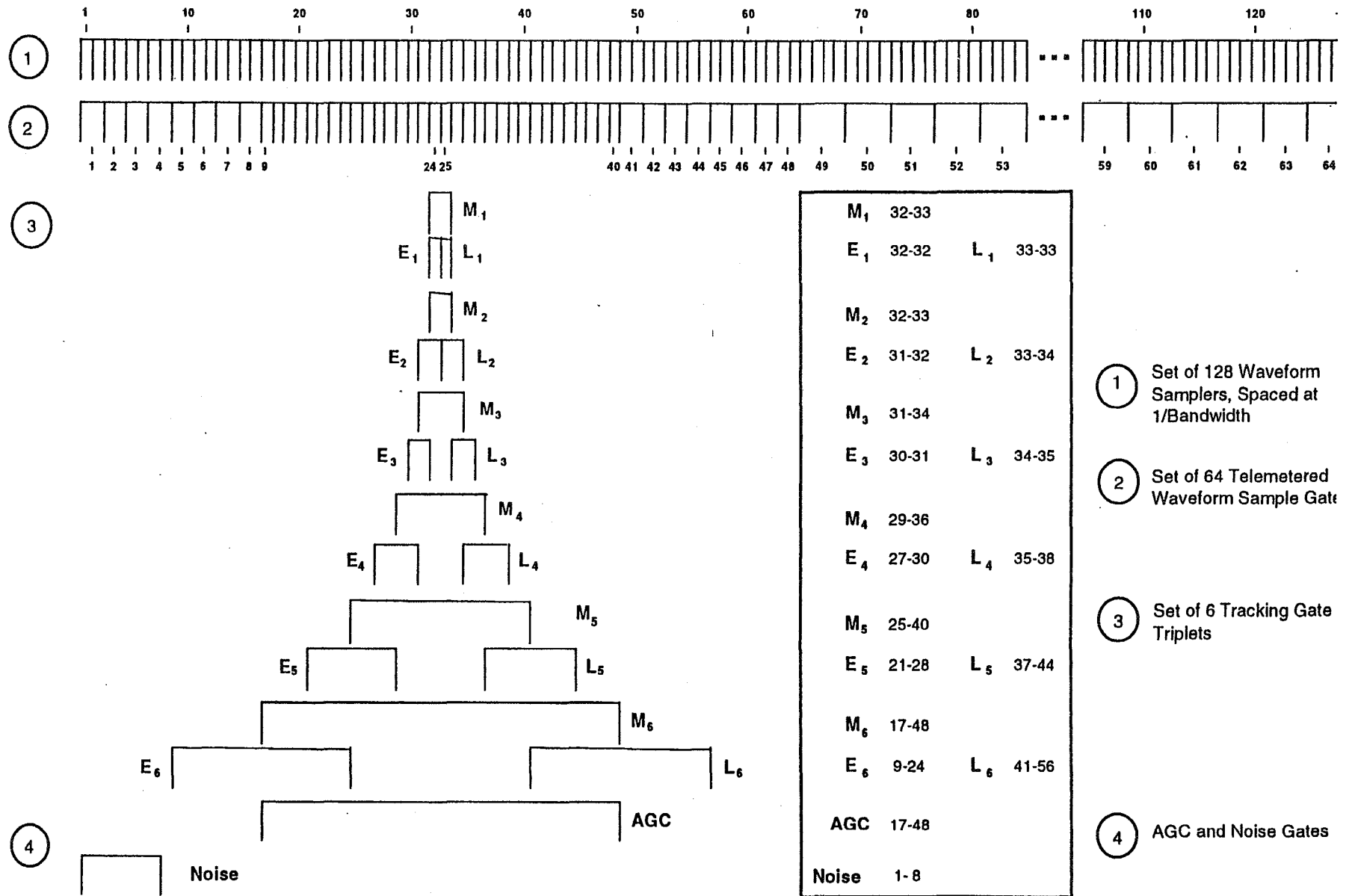


Figure 4.8.2

5.0 ON-ORBIT INSTRUMENT PERFORMANCE ASSESSMENT

The TOPEX Altimeter (ALT) was initially turned on to IDLE mode, on August 21, 1992, eleven days after launch. It was switched to TRACK mode for the first time on-orbit on August 26, 1992. From initial turn-on to February 1, 1994, the ALT track status has been:

<u>Mode</u>	<u>Total Hours</u>
OFF	72
IDLE	1490
TRACK	11,130

The ALT is switched to IDLE whenever the CNES Altimeter is turned ON.

The performance assessment which follows is based solely on Side A. Side B of the altimeter has not been turned on since pre-launch testing. The Project plan is that Side B will not be turned on unless Side A fails.

The C bandwidth used throughout the performance assessment is 320 MHz. The 100 MHz bandwidth was very briefly tested after launch to affirm its operability.

The performance assessment shown below is keyed, by section numbering, to the performance requirements of Section 4.0.

5.1 Height Measurements

5.1.1 Measurement Noise

The measurement noise of the ALT heights has been estimated by calculating the rms of one-per-frame Ku-minus-C height differences, after a linear fit over a 60-second interval (Hayne, 1993). The height rms for each of Ku, C, and combined Ku-and-C was then determined by scaling the rms-of-fit by the ratio of the Ku/C noise.

This method takes the effects of geoid noise out of the calculation that would be present on a straight fit to either frequency, since both frequencies follow the same geoid tracking.

The height measurement noise estimates resulting from this technique are listed in Table 5.1.1a, where the rms specification is for one-second averaging intervals as listed in Table 4.1b.

	SIGNIFICANT WAVEHEIGHT					
	2M		4M		8M	
	<u>SPEC</u>	<u>ON-ORBIT</u>	<u>SPEC</u>	<u>ON-ORBIT</u>	<u>SPEC</u>	<u>ON-ORBIT</u>
	Min.	Max.	Min.	Max.	Min.	Max.
Combined	4.1	1.4 - 2.9	4.6	2.2 - 3.3	5.5	3.7 - 4.5
Ku	3.5	1.2 - 2.4	3.8	1.8 - 2.7	4.5	3.1 - 3.8
C320	5.4	1.8 - 3.7	6.1	2.9 - 4.4	7.4	5.1 - 6.3

Table 5.1.1a One-Second Range Measurement Noise Performance (in cm)

The pooled height measurement noise estimates from this technique are shown in Table 5.1.1b. Although this is a new noise-estimation technique, the results are in good agreement with those presented by Purdy and Marth at the February 1993 Verification Workshop; for that presentation, noise estimates were based on the use of repeating groundtracks to subtract the geoid signatures. These estimates are also similar to noise spectra computed by Richard Sailor, which were part of a presentation by Hayne, et al, at the same Workshop, and are generally within $\pm 10\%$ of the estimates emanating from pre-launch thermal-vacuum testing. C100 range measurement noise estimates for 2 m and 4 m SWH are included in Table 5.1.1b, based on an analysis of the small amount of C100 on-orbit tracking data; no C100 data are available for 8 m SWH.

	SIGNIFICANT WAVEHEIGHT					
	2M		4M		8M	
	<u>SPEC</u>	<u>ON-ORBIT</u>	<u>SPEC</u>	<u>ON-ORBIT</u>	<u>SPEC</u>	<u>ON-ORBIT</u>
Combined	4.1	2.1	4.6	2.9	5.5	4.0
Ku	3.5	1.7	3.8	2.4	4.5	3.4
C320	5.4	2.6	6.1	3.8	7.4	5.6
C100	10.9	4.1	13.9	6.5	14.5	n/a

Table 5.1.1b One-Second Pooled Range Measurement Noise Performance (in cm)

5.1.2 Ku/C Height Differences

The ionosphere introduces an error in height because of increased propagation delay; the propagation delay is proportional to the electron constant of the ionosphere and is also related to the frequency of the radar pulse. The C-Band is affected more by the ionosphere than Ku-Band and therefore C heights are generally greater than Ku heights. The height differences are much larger in daylight hours when the total electron content (TEC) along the radar propagation path is larger. Ionospheric effects are also latitude-dependent.

The Ku/C height differences provide a means of determining the TEC, and thus provide a technique for calculating the corrections for height errors attributed to the ionosphere. The Ku height corrections are equal to the Ku-minus-C heights multiplied by 0.179065468, per TOPEX Algorithm G1043: Combined Height/Ionospheric Correction.

An analysis of calculated ionospheric height corrections, performed shortly after launch, revealed that the altimeter-derived corrections were generally +1.8 cm during nighttime passes when the corrections should have been near-zero, and should have been about 1.8 cm more negative during daytime passes. A +100 mm offset was added to the C-Band heights to rectify this observed effect. The effective date of this C-Band offset was day 238 of 1992, at 23:12:00 UTC.

Two typical plots of height corrections based on ionospheric effects, subsequent to the implementation of the +100 mm C-Band height offset, are illustrated in Figure 5.1.2. The top plot in Figure 5.1.2 is for a daytime pass; the shape of the corrections appropriately contains the classic ionospheric maxima at about ± 15 degrees latitude, and the minima are at the high latitudes. The bottom plot in Figure 5.1.2 is for a nighttime pass, with appropriately smaller ionospheric effects.

5.2 Height Measurement Drift Rate

The ALT has an internal Calibration Mode, which is routinely initiated twice per day, at approximately 12-hour intervals. A review of the internal height calibration results, discussed later in Section 5.6, indicates that there has not been any discernible height measurement drift with respect to the specified interval of 10 days.

5.3 Sea State (H1/3)

The ALT determination of H 1/3, significant waveheight, appears to be quite good; it is in good agreement with H 1/3 derived from waveform fitting. A representative histogram of Ku significant wave height (SWH) for a full 10-day cycle is shown in Figure 5.3a; the distribution of measured wave heights is comparable with those of the earlier Geosat mission. The C SWH is typically 5 cm higher than the Ku SWH.

IONOSPHERIC CORRECTION (METERS)

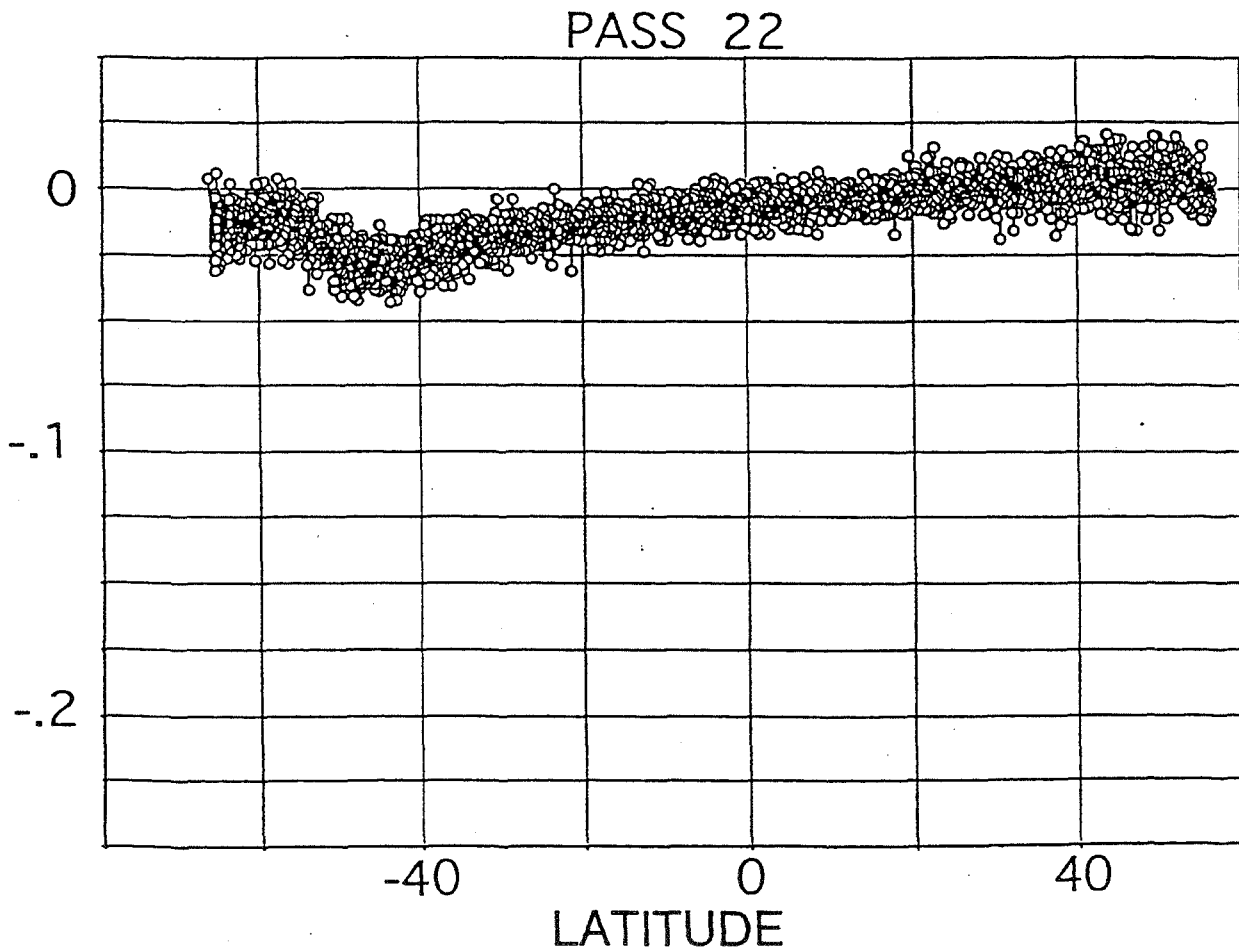
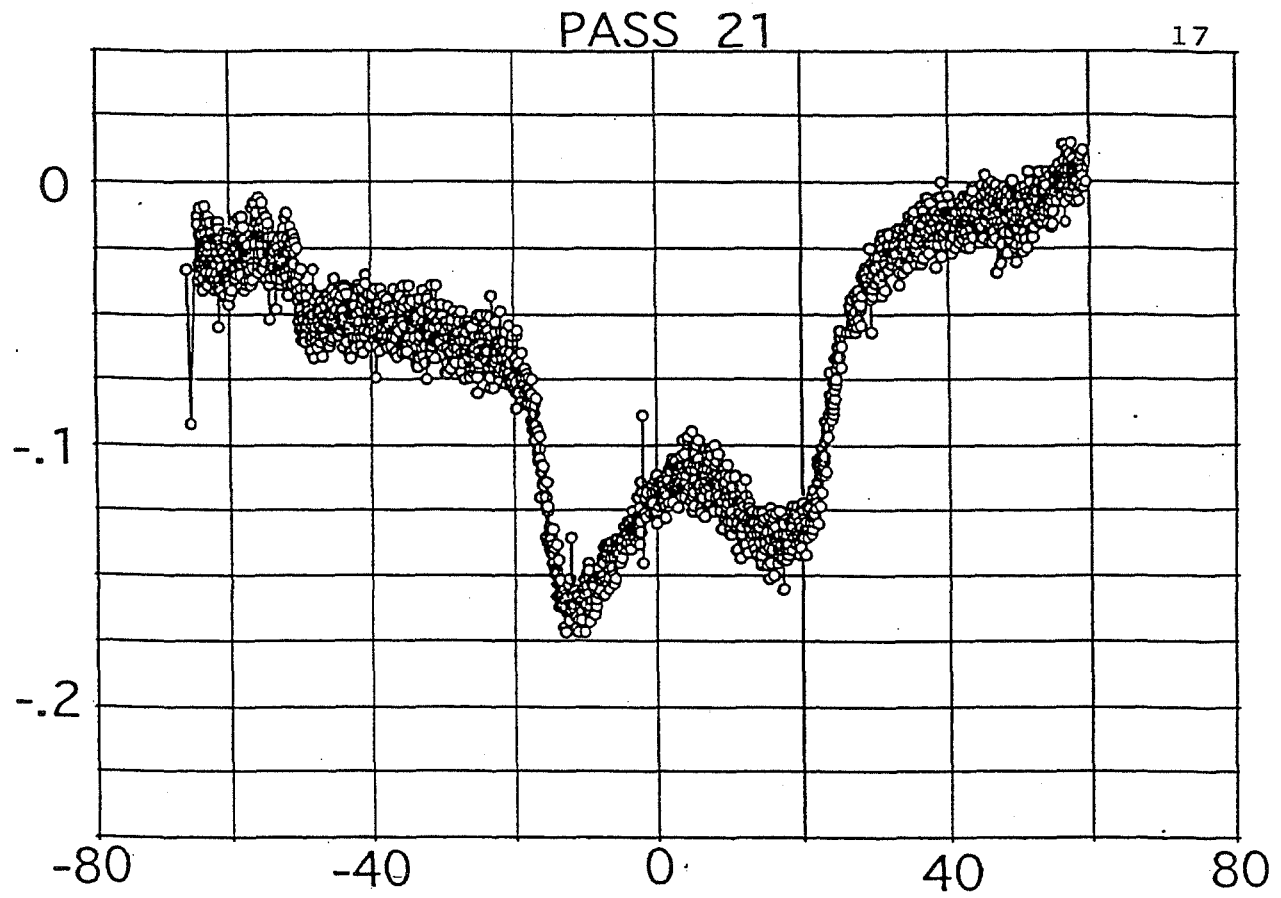
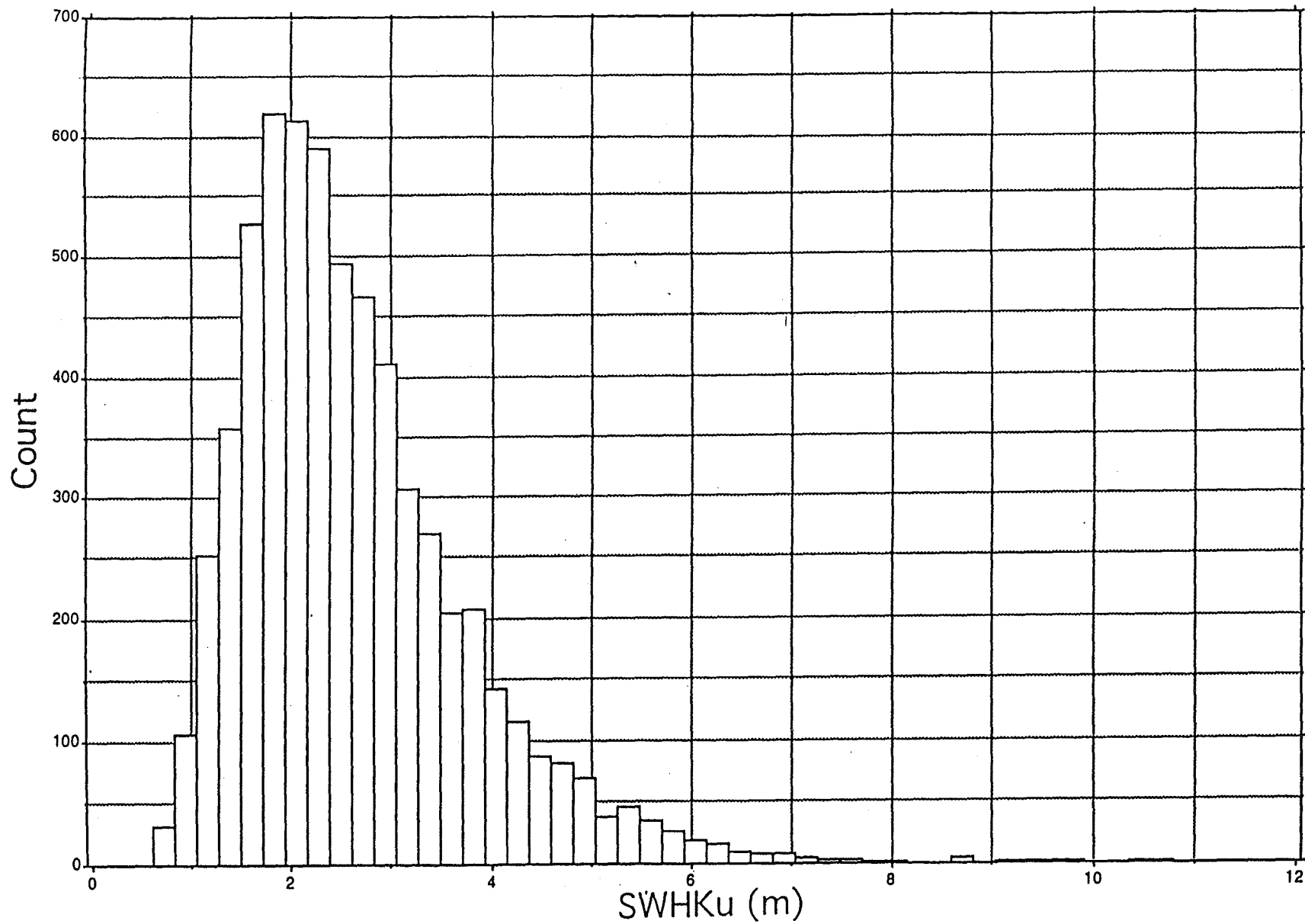


Figure 5.1.2 Calculated ionospheric Corrections for a Daytime Pass (top) and a Nighttime Pass (bottom)



Frequency Distribution of 1-Min Avgs, Cycle 14

Figure 5.3.a Histogram of SWH for a 10-Day Cycle

Morris and Callahan of JPL have compared ALT-derived significant wave heights with wave heights independently measured by a NOAA buoy and by the Colorado University tide gauge, all in the vicinity of the Harvest platform. Their results, based on analysis of Cycles 1-10, were presented at the Verification Workshop in February 1993, and are shown here as Figure 5.3b. The agreement is excellent, with the ALT measurement generally about 10 cm high, but well within the specification of 50 cm.

5.4 Altitude Velocity and Acceleration

The achieved orbit for the TOPEX/POSEIDON spacecraft is very circular (mean eccentricity <0.0001); therefore, the orbital parameters contribute very little to altitude velocity or altitude acceleration. The altitude velocities as measured by the altimeter are, for the most part, due to the oblateness of the earth. The altitude accelerations, computed on the ground, are primarily due to localized changes in geoid slopes.

Typical measured altitude velocities, in m/s, for an ascending groundtrack (pass 21) and for a descending groundtrack (pass 22) are plotted vs. latitude in Figure 5.4a. The velocity is zero at the equator where the earth flattening effect changes sign, and approaches zero at the extreme orbital latitude of +66 degrees where the orbit levels out with respect to latitude. The maximum rates are at +40 degrees latitude where the earth flattening rate-of-change is the greatest. The absolute altitude velocity is slightly higher at -40 degrees than at +40 degrees latitude due to the different flattening characteristics between the southern and northern hemispheres.

Typical altitude accelerations, in m/s/s, are shown in Figure 5.4b for the same two passes as the previous Figure. The accelerations were computed by first-differencing the velocities of Figure 5.4a. The accelerations are observed to have a mean of zero, are generally banded within $+0.3$ m/s/s, and tend to be more variable near latitude -50 degrees. Studies by Hancock *et al.* (1990), using Geosat measurements, concluded that the effects of tracker lag on the altimeter range (dR), in meters, due to altitude acceleration (a), in m/s/s, are correctable by $dR=at^2/B$, where t is the tracker update interval in seconds, and B is the tracker parameter Beta (typically $B = 1/64$). Algorithm S1039: Acceleration Correction to Height computes a range correction for the effects of acceleration. Based on simulations, the calculated acceleration corrections have an accuracy of -0.05 ± 0.04 cm.

5.5 Acquisition and Data Quality Settling Time

During the first week after the on-orbit ALT was initially commanded to TRACK mode, acquisition tests were performed. The altimeter was commanded into 15 acquisition test sequences for each of seven different parameter sets. These parameter sets varied acquisition bandwidth, sweep range and threshold levels.

ALT, NOAA Buoy, and CU Tide Gauge SWH at Platform Harvest

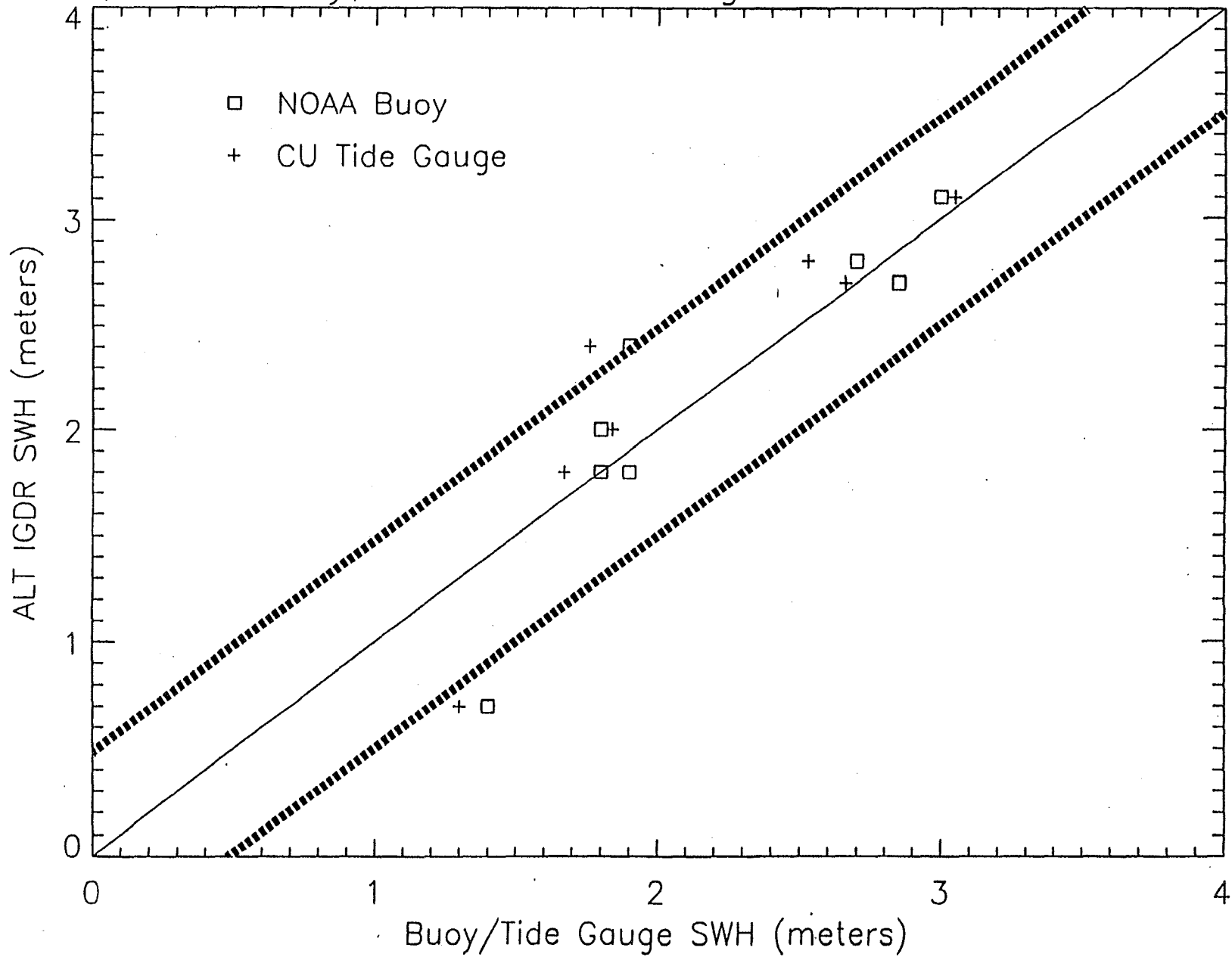


Figure 5.3b SWH Intercomparison (Morris and Callahan, 1993)

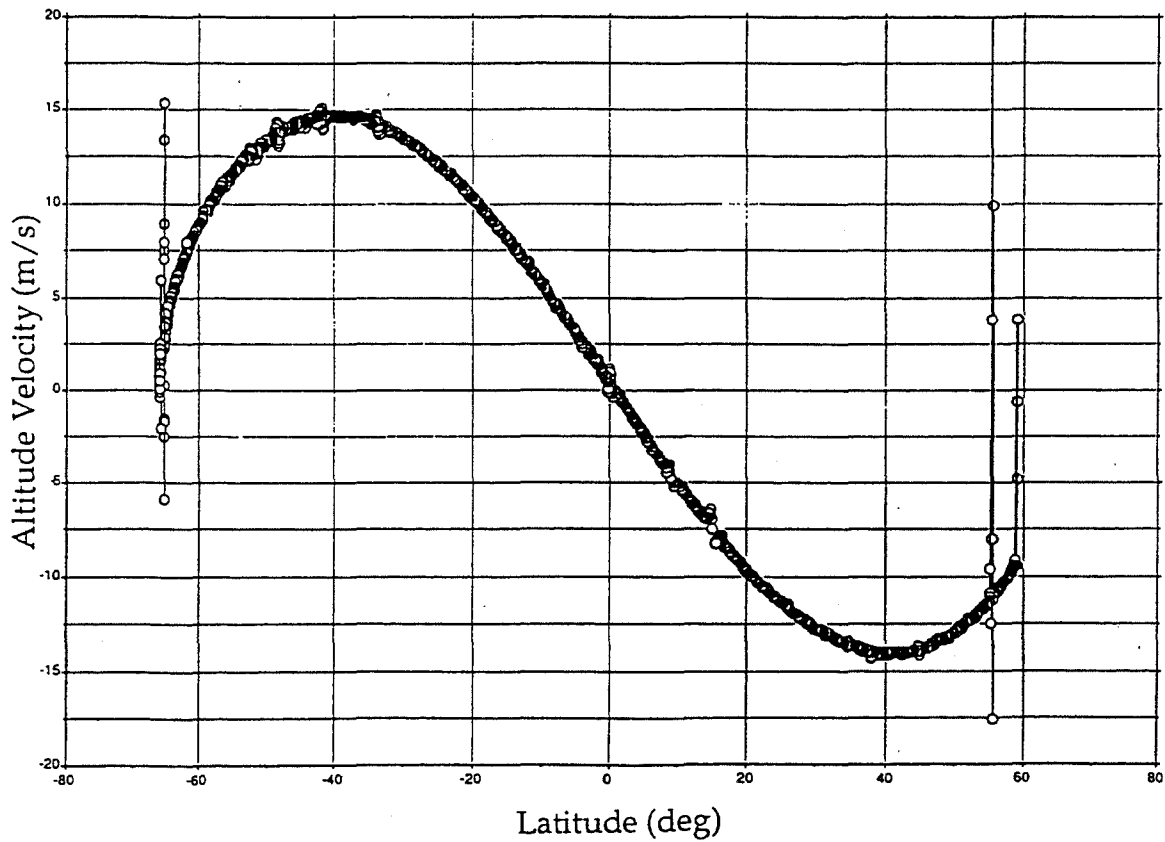
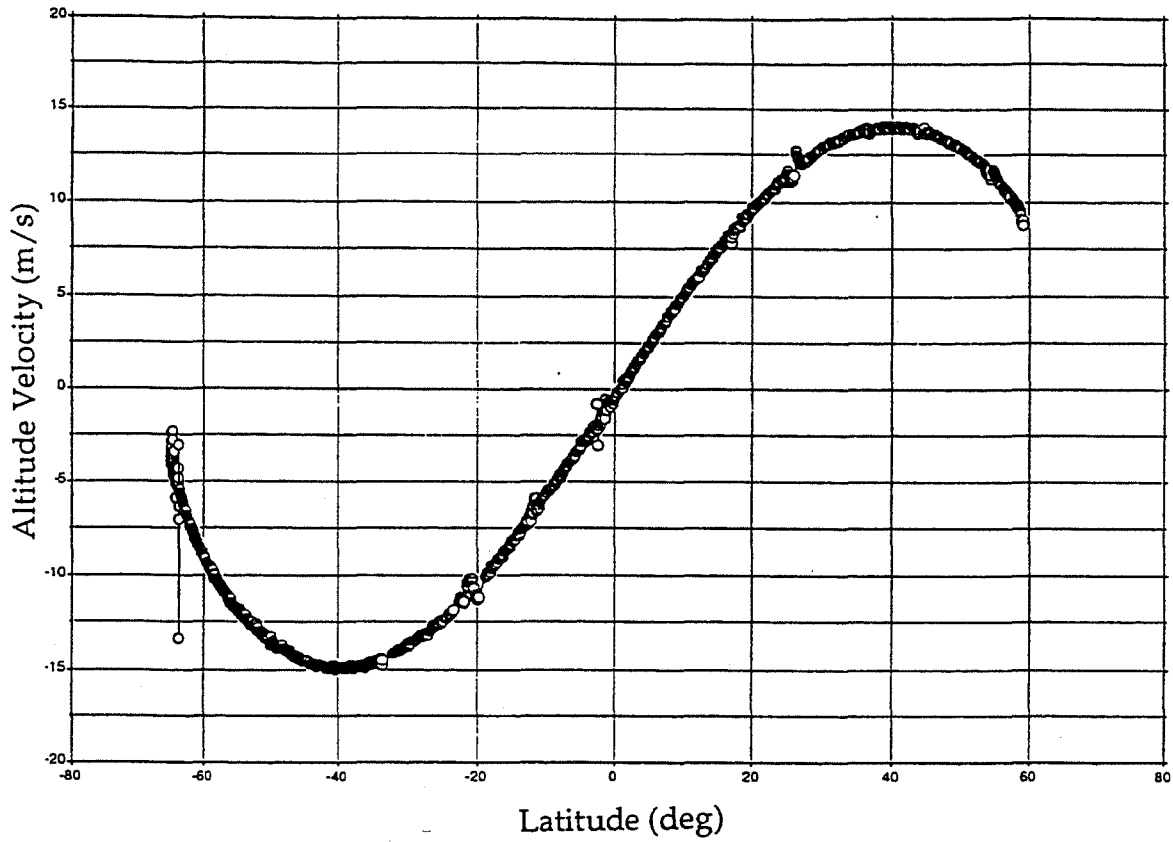


Figure 5.4a Altitude Velocities for Typical Ascending Groundtrack (Pass 21, top) and Typical Descending Groundtrack (Pass 22, bottom). In the Bottom Plots, the Groundtrack Moves from Right-to-Left.

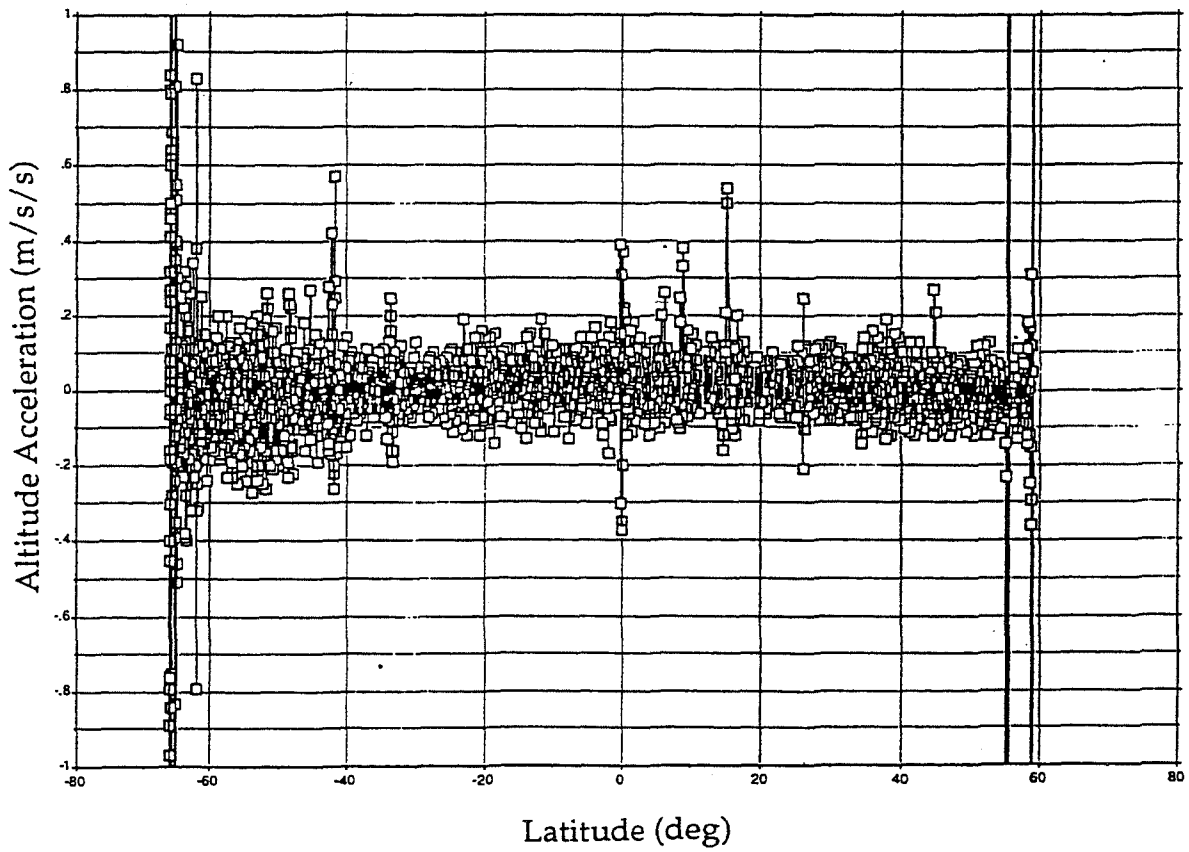
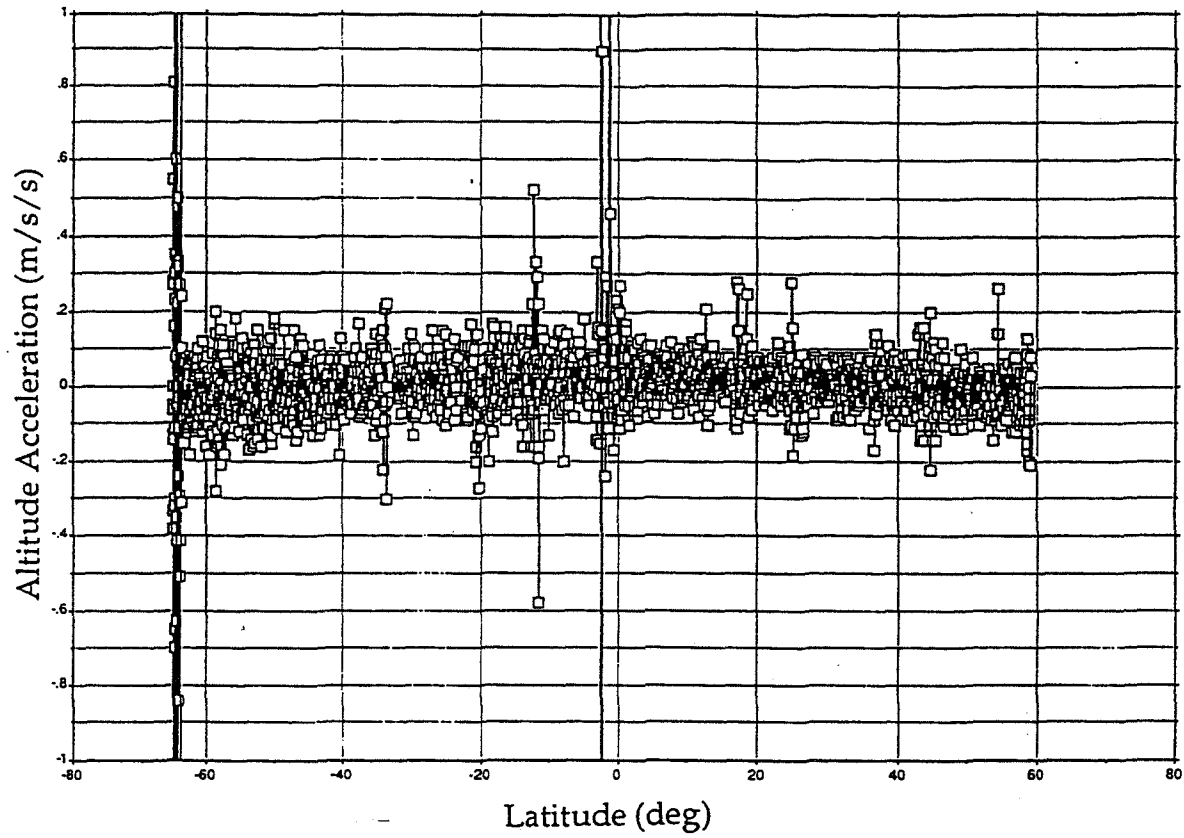


Figure 5.4b - Altitude Accelerations for Typical Ascending Groundtrack (Pass 21, top) and Typical Descending Groundtrack (Pass 22, bottom).

The results of the acquisition analyses were as follows:

1. For a cold start (no lock-on), the acquisition and data quality settling time varies from 3-7 seconds, depending on the particular parameter file configuration.
2. For a cold start, for the parameter file which is operationally in use, the acquisition and data quality settling time varies from 4-5 seconds.
3. Generally, the 20 MHz (50 ns equivalent pulse width) acquisition bandwidth performed better than the 5 MHz (200 ns equivalent pulse width) acquisition.
4. For the situation where the altimeter groundtrack goes from land to water, the acquisition and data quality settling time is usually 0-1.5 seconds depending on the land characteristics.
5. For many of the analyzed land-to-water transitions, the altimeter was already in FINE TRACK over the land areas.

The TOPEX altimeter uses an acquisition scheme which allows it to degrade from high resolution tracking to coarser tracking over land or ice without completely losing lock. This allows the altimeter to bypass much of the acquisition time when coming off land or ice.

5.6 Absolute Internal Calibration

The altimeter has an internal calibration which provides for in-flight self-calibration. Currently it is scheduled two times per day at approximately 12-hour intervals (over land).

The calibrate command causes the altimeter to exercise two distinct calibration modes. In the first, CAL1, the transmitted pulse is fed back through digital attenuators with 17 sequential steps; the duration of each step is approximately ten seconds. The pulse is tracked during each of the steps. When all CAL1 attenuator steps are completed, the flight processor automatically changes to CAL2. CAL2 operates for approximately 60 seconds. Of the seventeen steps of CAL1, it has been observed that the initial seven steps have a larger signal level so are more reliable for calibration than the later steps.

The CAL1 mode allows for monitoring changes in height bias, changes in system loop gain and waveform sample operation.

In CAL2, the transmit pulse is not linked to the receiver, so it has a noise input only. The AGC is active and adjusts to the noise level. This allows for monitoring the receiver health and waveform sampler operation.

The CAL1, step 5, Ku height and C height calibration results since launch are plotted in Figure 5.6a, along with the Ku MTU Cal Attenuator temperature. In all the plots of calibration results, the reference is the average of nine consecutive calibrations during cycle 001 (days 270-275 of 1992). The Ku height is observed to have decreased about 1.0 mm during these 530 days. The 5 mm height spikes in the Figure are assumed to be the effects of bit toggling when the altimeter was switched from IDLE Mode to TRACK Mode after an interval during which the French altimeter was turned on or when the spacecraft had a problem or did a maneuver. Normal stable operation shows none of these spikes. The C height has decreased about 5.0 mm since launch; the apparent recent increase in measurement noise is an artifact of bit toggling.

The CAL1, step 5, Ku AGC and C AGC calibration results since launch are plotted in Figure 5.6b, along with the AGC Receiver Section temperature. The Ku AGC is observed to have linearly decreased about 0.25 dB, from launch to day 242 of 1993; since that time, it has leveled off. The C AGC trend shows a linear decrease of about 0.10 dB since launch. At WFF's recommendation, and with the TOPEX Measurement Systems Engineer's concurrence, calibration-based AGC corrections have been entered into the production of GDR data at JPL. The AGC corrections and their start times are listed in Table 5.6a, where the values are to be added to the calculated sigma-naughts. The AGC corrections were not applied to the GDR data until the beginning of Cycle 48 on January 1, 1994.

<u>Side A</u>	<u>Frequency</u>	<u>Year</u>	<u>Day-of-Year</u>	<u>Time</u>	<u>Correction</u>
A	Ku	1993	39	23:46	+0.10 dB
A	Ku	1993	99	11:37	+0.15 dB
A	Ku	1993	178	19:25	+0.25 dB
A	C	1993	149	01:30	+0.10 dB

Table 5.6a AGC Corrections for GDR Production

The CAL2 Ku AGC and C AGC calibration plots are shown in Figure 5.6c. Early in the mission, Ku AGC increased about 0.1 dB; it is presently about 0.2 dB below its initial value. The C AGC also increased about 0.1 dB early in the mission; it has returned to its original level.

The AGC calibrations for Ku and C-Band, as shown in Figures 5.6b and 5.6c are not in agreement. Table 5.6b summarizes these two results and adds a third result wherein Ku and C-Band transmit power values, during periods of calibration, have been converted from watts to dB. The watts-to-dB calibration results for Ku- and C-Bands are shown in Figure 5.6d.

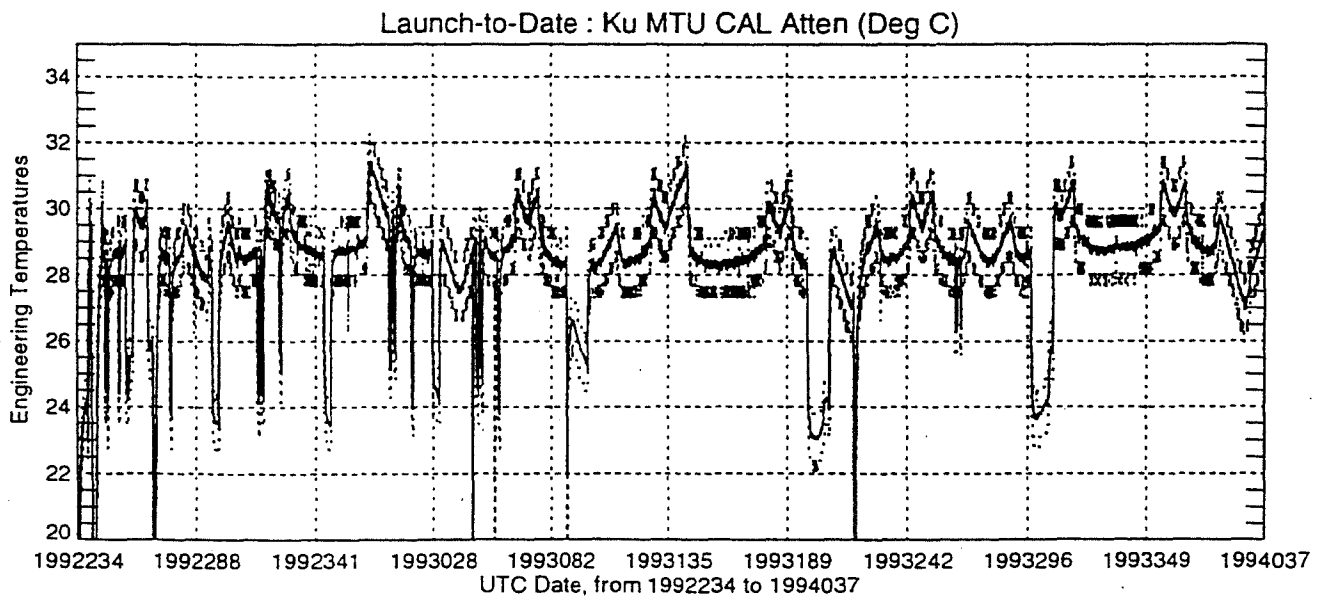
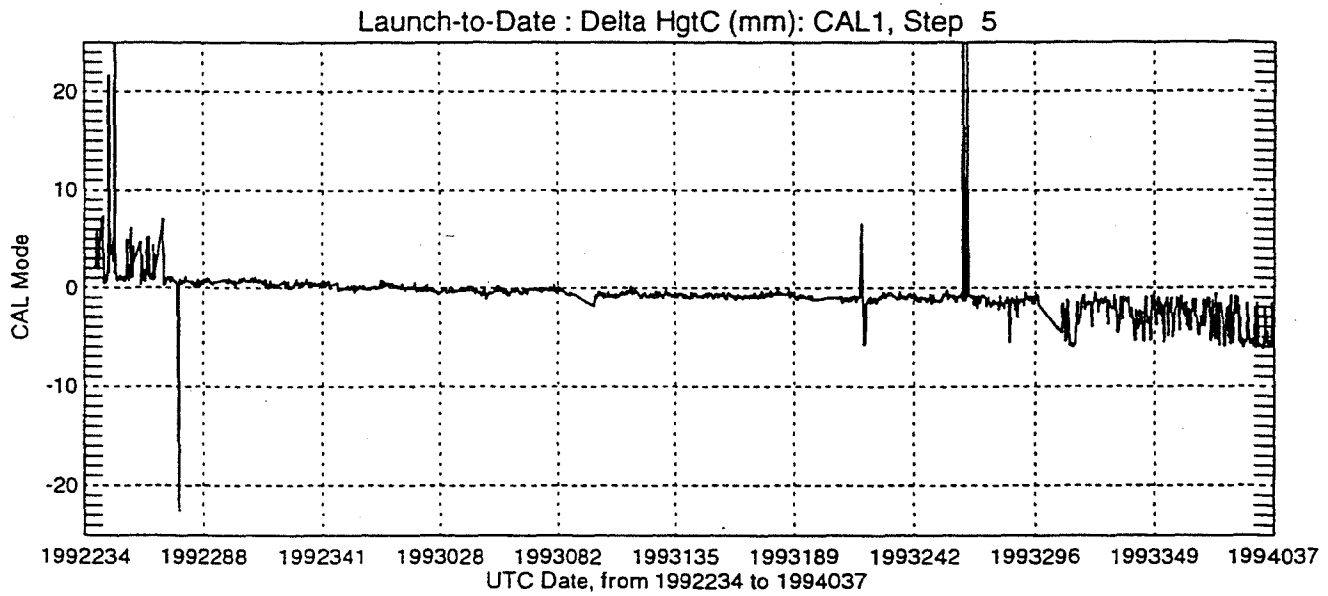
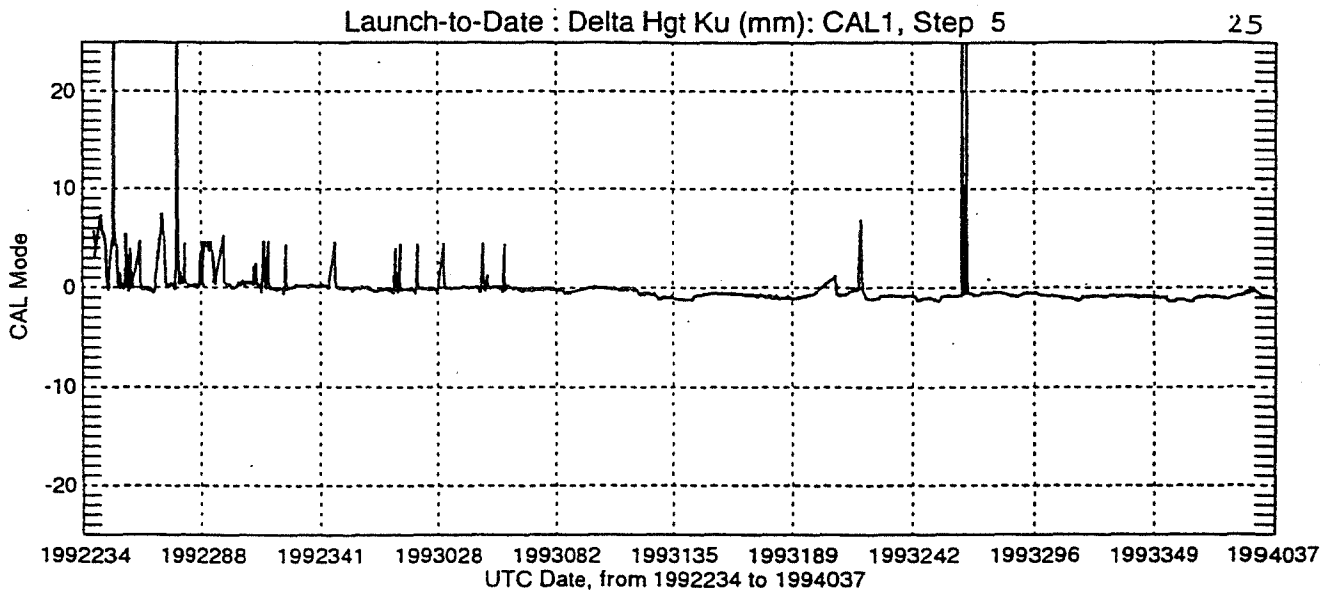


Figure 5.6a Ku Height and C Height Calibration Results Since Launch

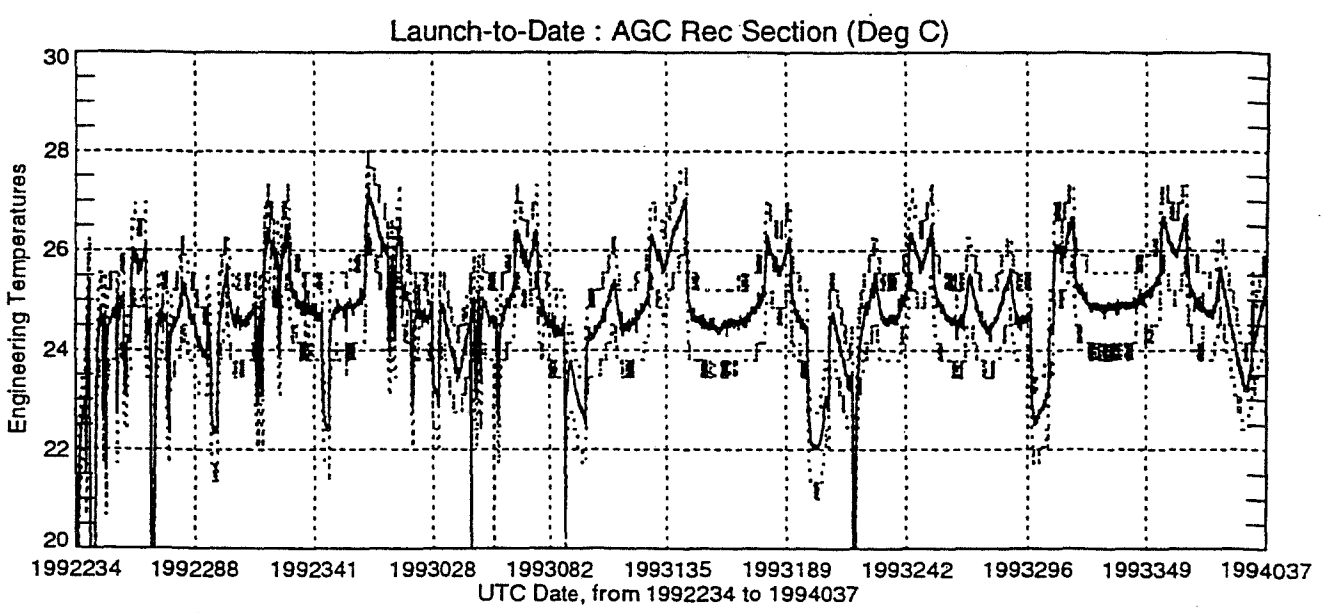
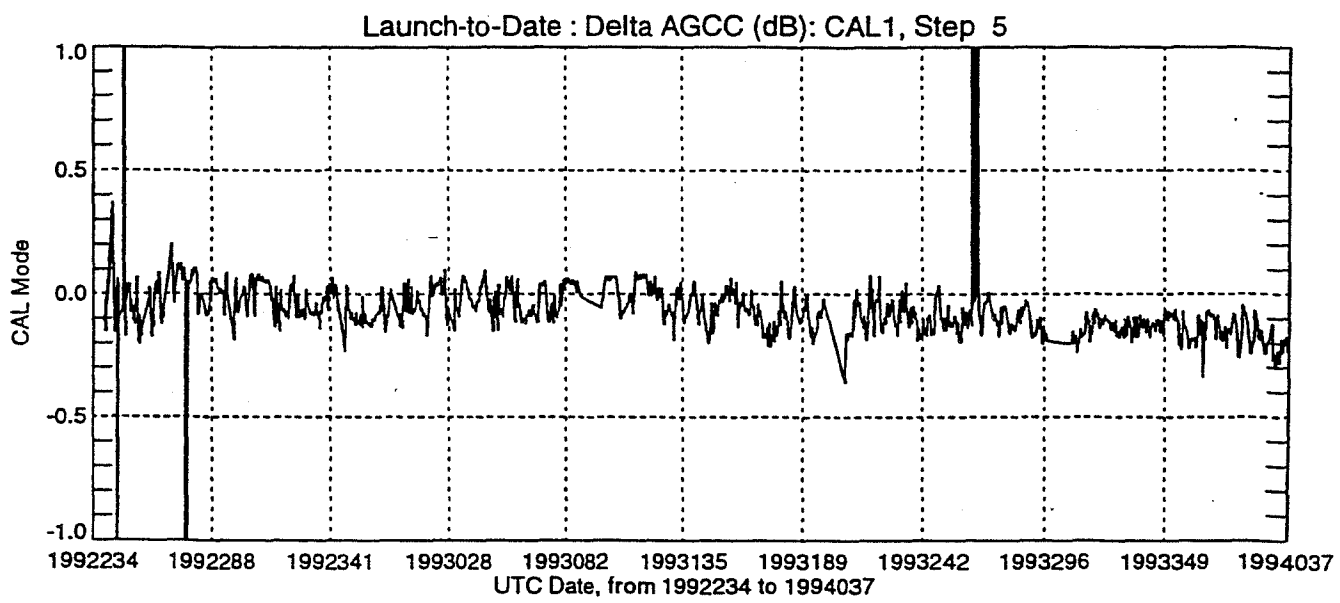
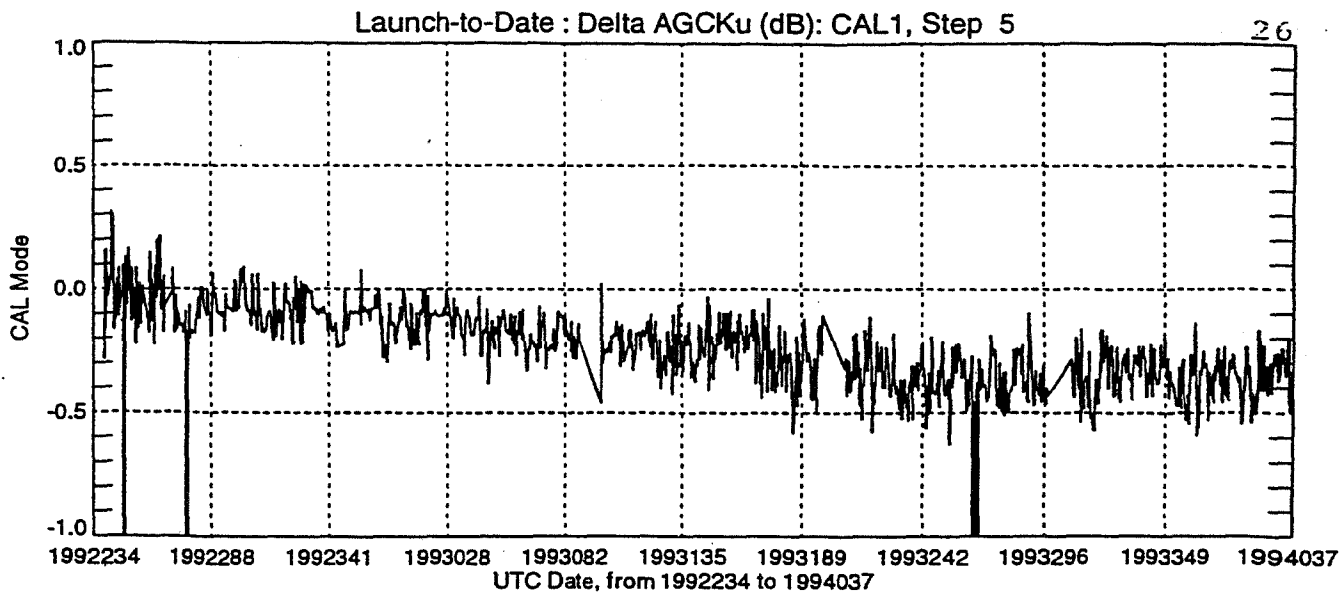
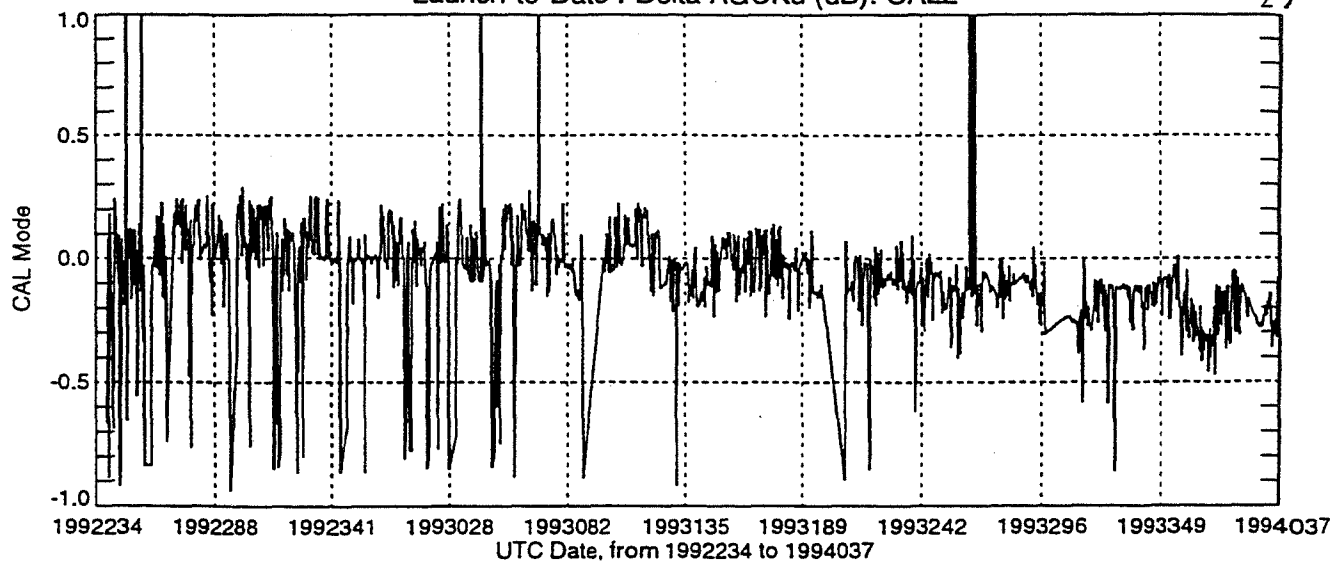
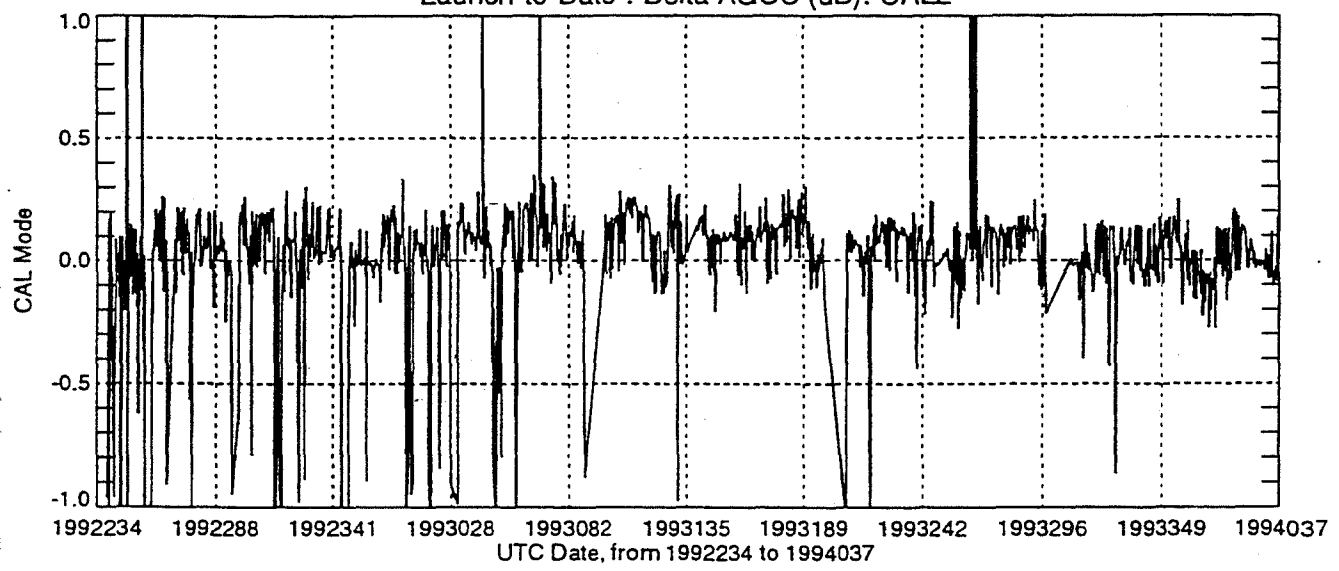


Figure 5.6b Ku AGC and C AGC Calibration Results Since Launch

Launch-to-Date : Delta AGCKu (dB): CAL2



Launch-to-Date : Delta AGCC (dB): CAL2



Launch-to-Date : AGC Rec Section (Deg C)

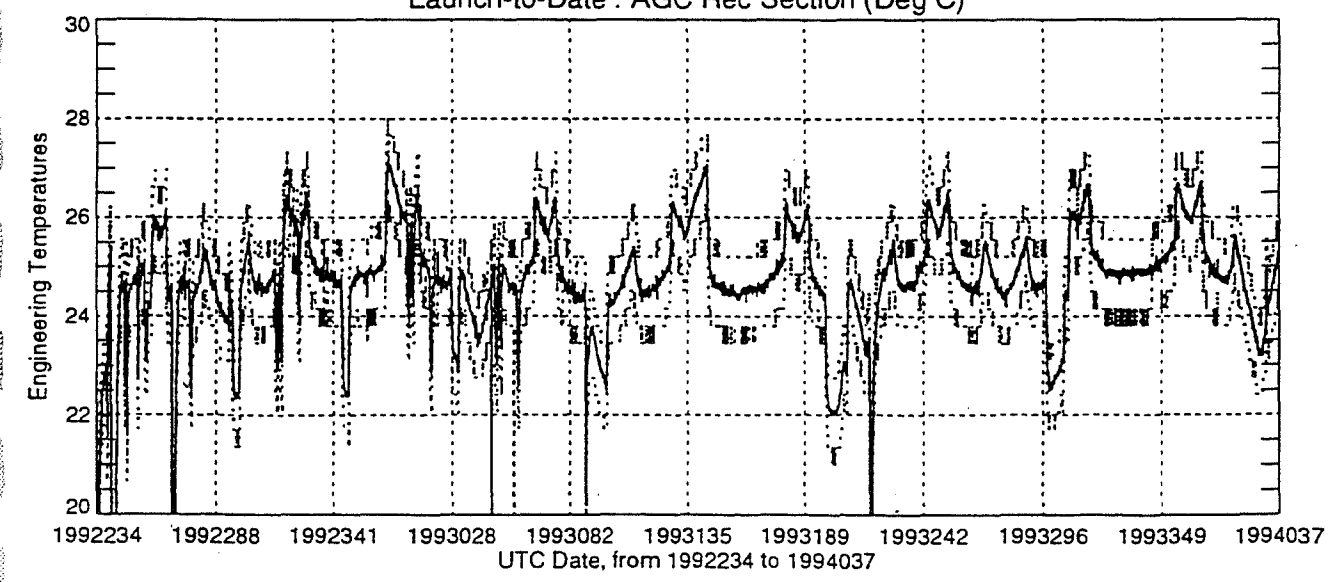


Figure 5.6c Ku and C AGC Calibration Plots for CAL2

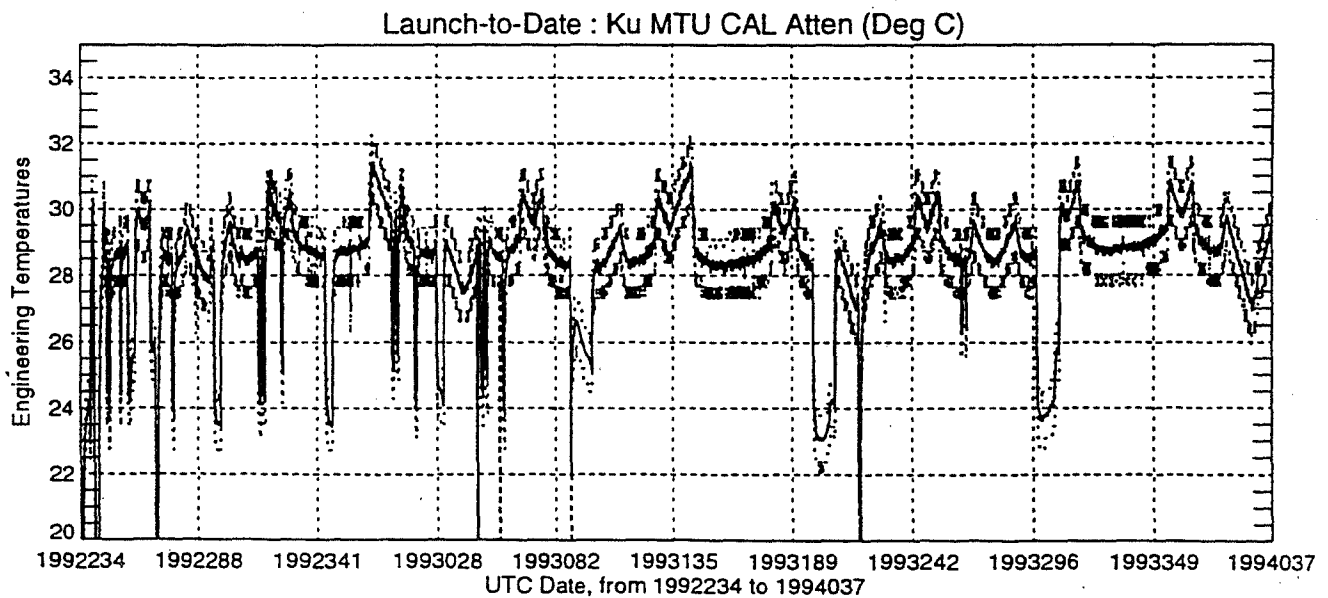
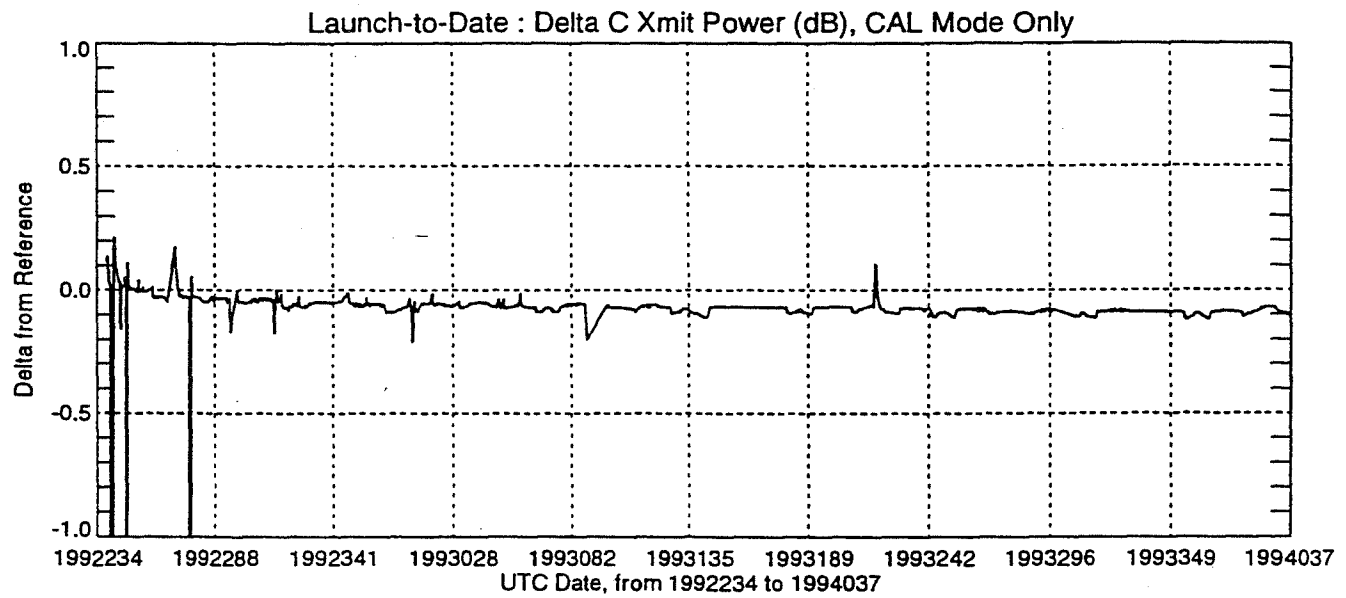
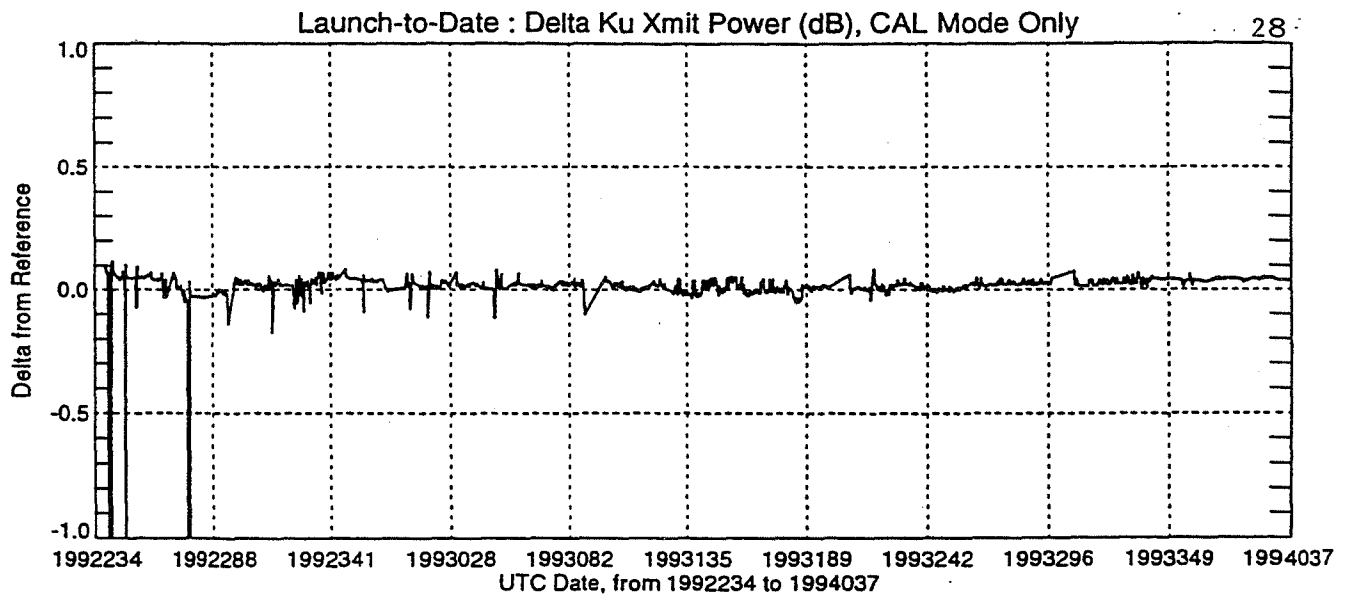


Figure 5.6d Ku and C Transmit Power During Calibration,
Converted from Watts to dB

<u>Method</u>	<u>Ku-Band</u>	<u>C-Band</u>
CAL1	-0.25 dB	-0.10 dB
CAL2	-0.20 dB	0.00 dB
Watts-to-dB	-0.05 dB	-0.10 dB

Table 5.6b AGC Calibration Comparisons: Launch to Date

5.7 Radar Reflectivity (Backscatter Coefficient)

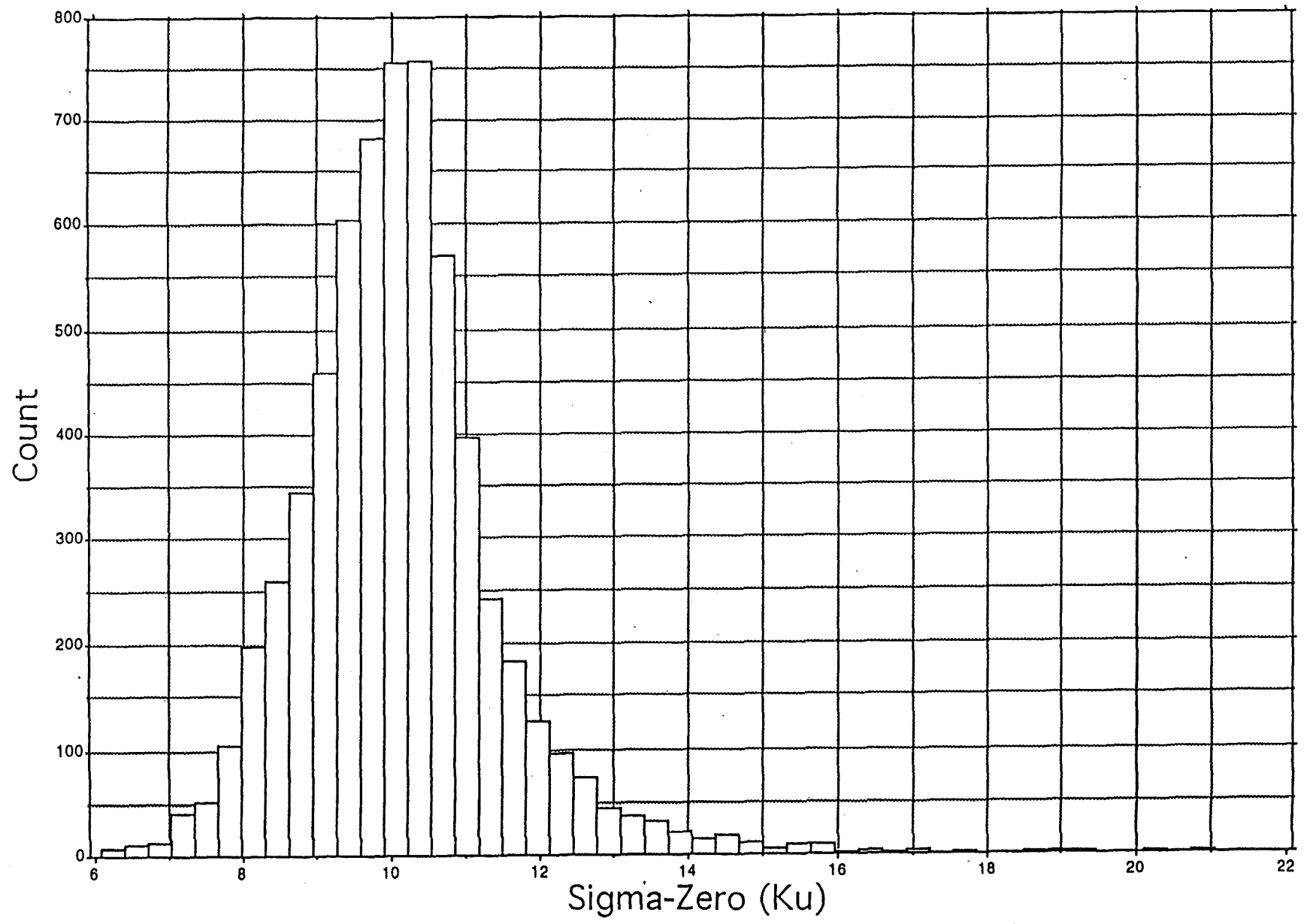
A representative distribution of Ku sigma zero, for a full cycle, is shown in Figure 5.7. While the ALT-derived histograms are similar in shape to those of Geosat, the ALT sigma zero values are shifted about +0.7 dB higher (Callahan, 1993, personal communication). In a June 1993 WFF informal memorandum, Hayne references Shoemaker who attributes 0.5 dB of this difference to the Geosat sigma-naught computations not taking into account the Earth's finite radius of curvature.

The histograms of C sigma zero have a narrower power distribution than the Ku, and the C sigma zero values are typically 3.4 dB higher.

Frequent occurrences of AGC "blooms" have been observed. Over areas of very calm seas, the waveforms become more specular, and the AGC increases by 5-8 dB. The duration of the blooms is typically on the order of a minute, which corresponds to about 350 km alongtrack. The effect of the specular waveforms on the ALT range tracker is to generally increase the noise of the range measurements during those intervals. A study of AGC blooms by Hayne et al (1993) concludes that:

1. The blooms are ocean surface effects, appearing in both Ku and C altimeter data.
2. Most of the affected altimeter measurements in the vicinity of the blooms are being appropriately flagged in the GDR processing.
3. Perhaps 5% of the over-ocean, normal-track data are in the vicinity of AGC blooms.

Hayne (1994) estimated the precision of one-per-frame GDR Ku sigma-naught measurements by fitting five short (70-160 seconds duration) segments to a quadratic. The rms of the residuals from the five fits varied from 0.065 to 0.091 dB. Hayne concludes that 0.08 dB is a conservative estimate of Ku sigma-naught measurement precision.



Frequency Distribution of 1-Min Avgs, Cycle 14

Figure 5.7 Histogram of Sigma-Zero for a 10-Day Cycle

5.8 Ancillary Altimeter Systems Performance

5.8.1 Time-Tag Accuracy

A plot of the Frequency Reference Unit (FRU) frequency stability is shown in Figure 5.8.1. This plot, from Clevon (1993), depicts the difference in milliHertz between the nominal frequency (5 MHz) and the measured frequency. The negative sign indicates that the measured frequency is less than the nominal. A line representing the per-day specification of 1 part in 7×10^{11} is shown in the Figure. The absolute frequency accuracy specification of 1 part in 7×10^8 is being met since the measured frequency offset is well within ± 350 milliHertz. Algorithm S1034: Oscillator Drift corrects the height measurements for the effects of FRU frequency drifts.

Shum *et al*, of the University of Texas, have made estimates of ALT time-tag accuracy determined from crossover analyses. The crossover solution computes the time shift which minimizes the crossover residuals. Their results, based on IGDR data from Cycles 1-12, were presented at the Verification Workshop in February 1993. Their preliminary conclusion, based on all 12 cycles, is that the overall TOPEX time-tag error is -0.1 ± 0.2 msec. The assessments of time-tag accuracy will become more refined as the crossover solutions use additional cycles of altimeter data, and as GDR data are utilized rather than IGDR data.

5.8.2 Waveform Samples

Waveform samples are discussed in Section 6.0.

5.8.3 Single Event Upsets

As of February 1, 1994, there had been 59 Single-Event Upsets (SEUs). The altimeter automatically recovered from 50 of the SEUs, with the loss of a few seconds of data during each of those occurrences. The nine anomalous SEU occurrences were as follows:

- Day 247 of 1992 - The improper SEU recovery on this date was due to the corruption of the Pulse Count Variable. The altimeter was commanded to IDLE mode and then commanded to return to TRACK mode. Approximately seven hours of data were lost. A software patch to refresh the Pulse Counts was made on day 328 of 1992.
- Day 354 of 1992 - On this date, the altimeter recovery from an SEU took 16-1/2 hours. At the end of that interval, another SEU apparently occurred and reset the processor.

FRU Frequency and Drift Spec

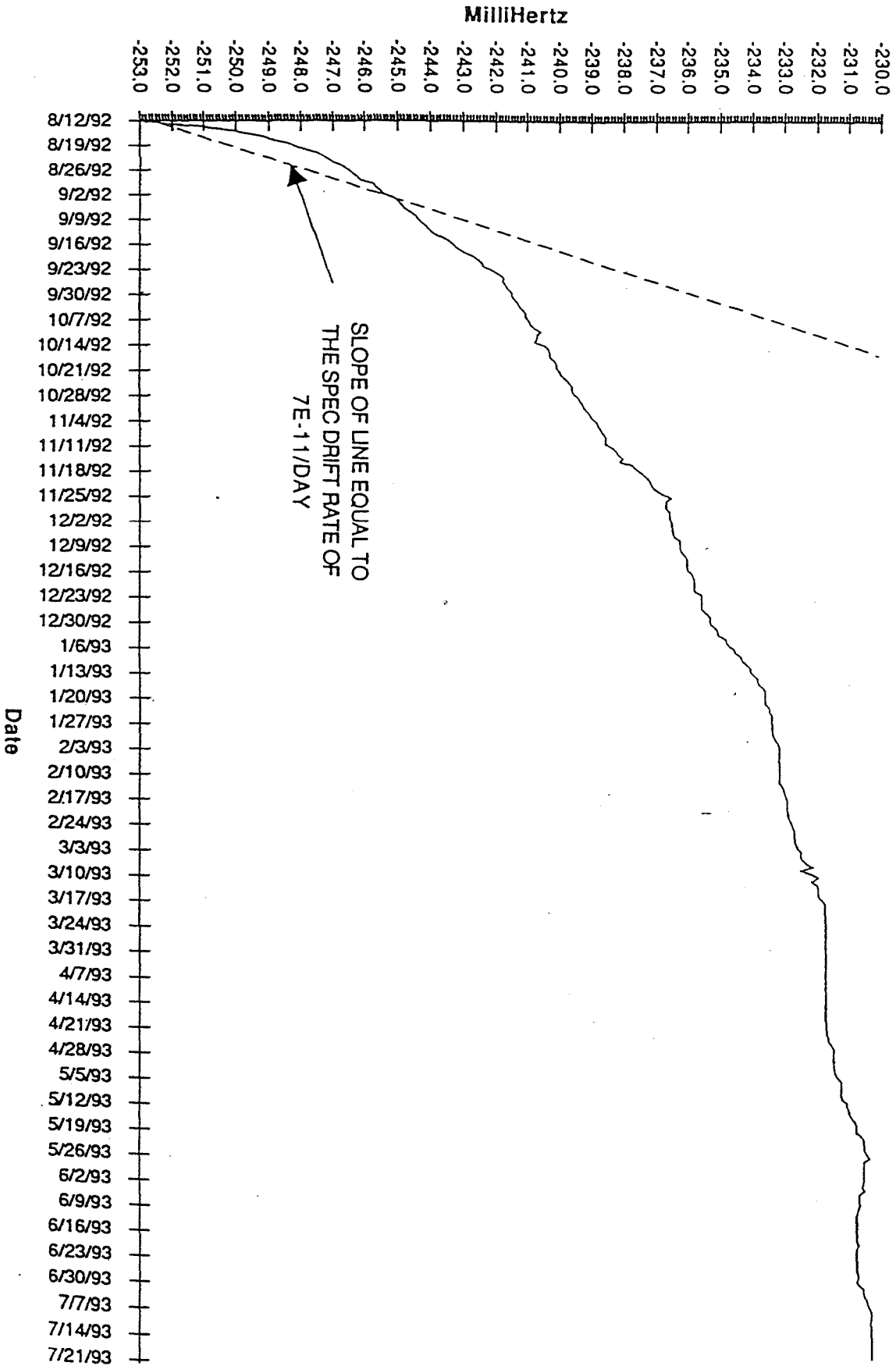


Figure 5.8.1 Frequency Reference Unit Performance
(from C. Clevon, 1993)

- Day 12 of 1993 - The altimeter self-recovered from an SEU on this date, but 12 minutes of data were lost. The hypothesis for this recovery is that the SEU itself was not detected by the processor, but that the range eventually swept to the lower limit causing an internal reset.
- Day 230 of 1993 - This upset was similar to that of day 12, but the altimeter self-recovery took 1-1/4 hours.
- Day 264 of 1993 - Approximately 14.5 hours of data were lost when an interface lockup occurred, apparently due to an SEU. To reset the processor, the altimeter was commanded from TRACK to IDLE mode, a ground reset command was executed, and then the altimeter was commanded back to TRACK mode.
- Day 266 of 1993 - Approximately 7.5 hours of data were lost when an interface lockup occurred, apparently due to an SEU. During this anomalous period, the altimeter generally remained in acquisition mode with some half-frame transfers to coarse track. To reset the processor, the altimeter was commanded from TRACK to IDLE mode, a ground reset command was executed, and then the altimeter was commanded back to TRACK mode.
- Day 307 of 1993 - A science telemetry interface lockup was detected when the ALT was commanded to TRACK after the French Altimeter SSALT had been ON. The science word value remained at zero, even though the altimeter was tracking. The sequence to perform the ground reset was the same as for day 266. A total of 2-1/3 hours of data were lost.
- Day 330 of 1993 - Approximately 8.2 hours of data were lost when an interface lockup occurred, apparently due to an SEU. During this period, the altimeter was tracking but did not transmit science data. To reset the processor, the altimeter was commanded from TRACK to SAFE IDLE mode, a ground reset command was executed, and then the altimeter was commanded back to TRACK mode.
- Day 001 of 1994 - Approximately 3.7 hours of data were lost when an interface lockup occurred, apparently due to an SEU. During this anomalous period, the altimeter generally remained in TRACK mode, but science data were not being telemetered. An error reset command was executed to reset the processor.

The latitude/longitude locations of the 59 SEUs are shown in Figure 5.8.3. Almost all the SEUs have occurred within or near the outlined South Atlantic Anomaly, an area noted for its high solar activity. The circles in Figure 5.8.3 appear at the latitudes and longitudes where SEUs had automatic resets. The diamonds represent the locations of SEUs which required manual resets. The two diamonds at -90 degrees latitude are placed there because the locations of the SEUs could not be discerned.

The ALT is responding appropriately to all commands which it has received. Pre-launch, WFF developed 25 command blocks; three additional command blocks have been developed since launch. Most of the blocks have been transmitted to the altimeter at one time or another. The mode switching aspects of the 28 command blocks are depicted in Figure 5.8.4.

The programmability of the altimeter was demonstrated on November 23, 1993, when a software patch was successfully uploaded. The purpose of the patch is to refresh a pulse counter variable after a Single Event Upset.

The TOPEX onboard flight processor uses an uploaded programmable 274-byte parameter file. Revised parameter files have been sent to the altimeter for special testing and for performance improvement. The initial on-orbit parameter filename was PARMC320; the present parameter file, in operational use since early November 1992, is C35028SL. The contents of these two files are listed side-by-side in Table 5.8.4.

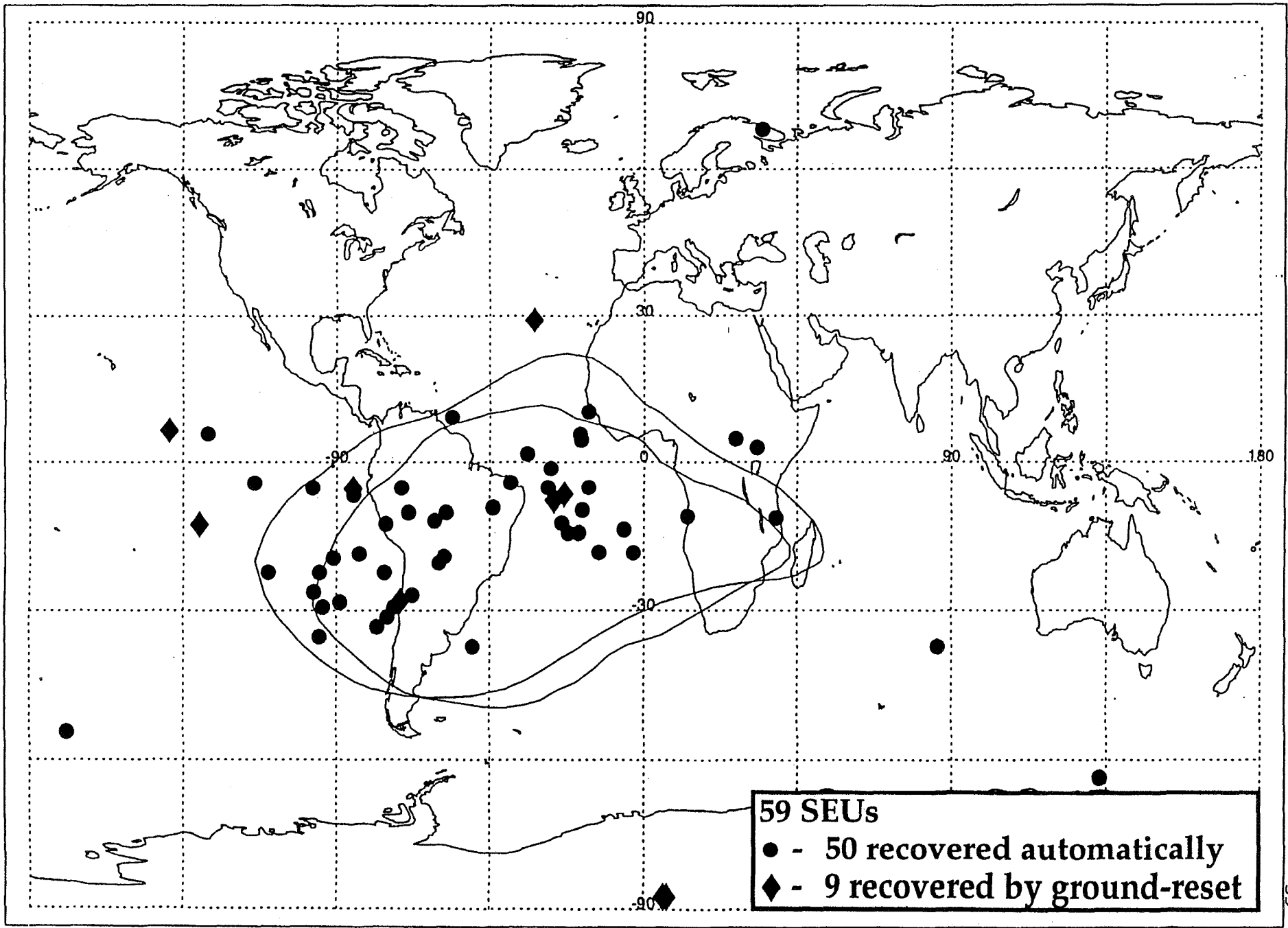


Figure 5.8.3 Locations of Single Event Upsets, in Relation to the South Atlantic Anomaly Area

NASA ALTIMETER COMMAND PROFILE

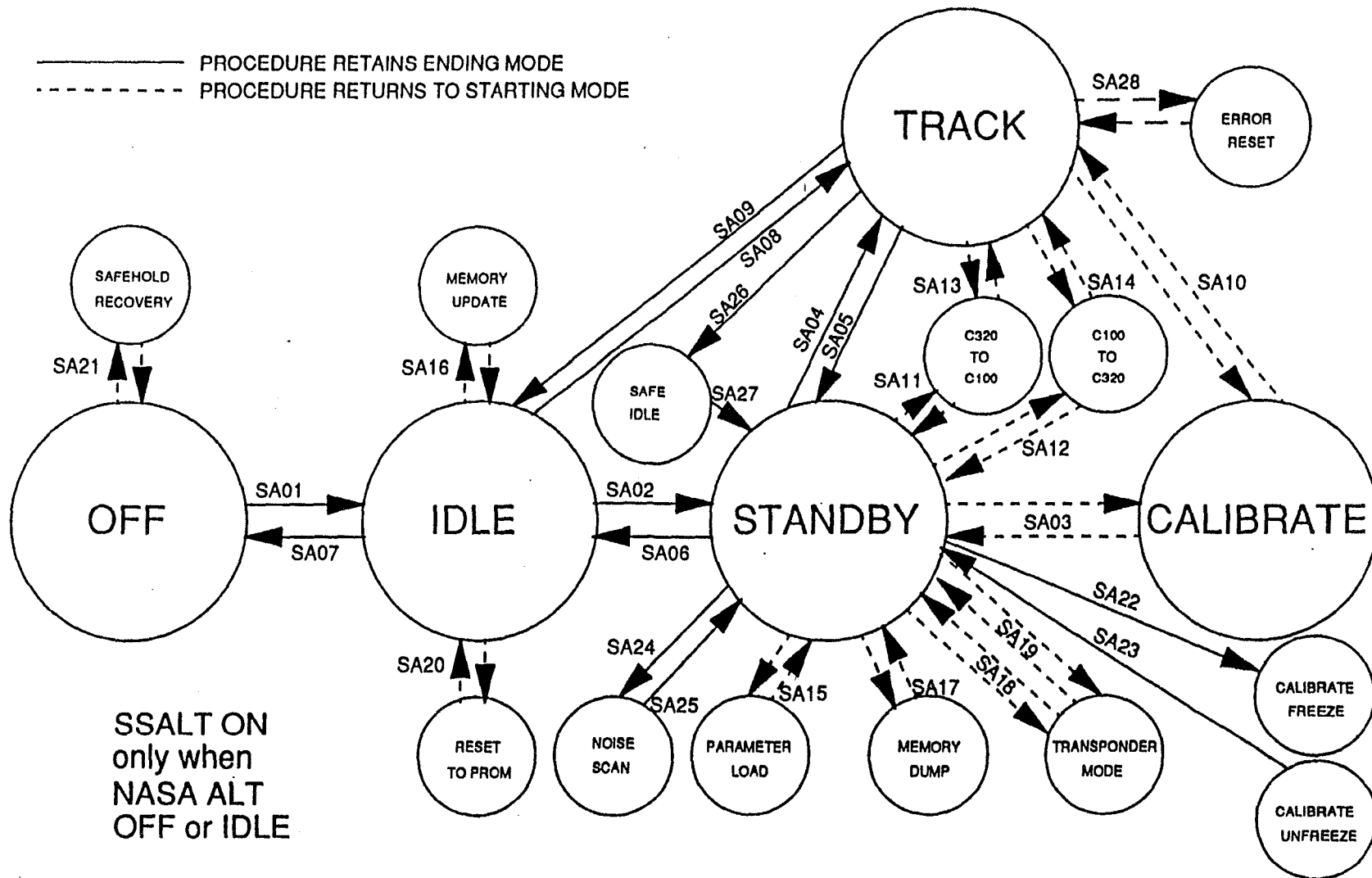


Figure 5.8.4 Command Block Mode Switching

Filename = PARMC320					Filename = C35028SL		
Byte	Parameter		Value	Hex	Value	Hex	Comment
1	Iscan_Min_Hgt	LSB/LSW	8.4992 mSec	00	8.4992 mSec	00	
		MSB/LSW		00		00	
2		LSB/MID		00		00	
3		MSB/MID		00		00	
		LSB/MSW		00		00	
5		MSB/MSW		A6		A6	
6	Iscan_Max_Hgt	LSB/LSW	9.318 mSec	00	9.318 mSec	00	
		MSB/LSW		00		00	
8		LSB/MID		00		00	
9		MSB/MID		00		00	
		LSB/MSW		00		00	
11		MSW/MSW		B6		B6	
12	Iscan_Hgt_Inc	LSB/LSW	200.0 nSec	00	200.0 nSec	00	
		MSB/LSW		00		00	
14		LSB/MID		00		00	
15		MSB/MID		00		00	
		LSB/MSW		01		01	
		MSB/MSW		00		00	
18	Cal-I Index 1		77	4D	77	4D	
19	Cal-I Index 2		78	4E	78	4E	
20	Cal-I Ku Min AGC Gate	LSB	1024	00	1024	00	
21		MSB		04		04	
22	Cal-I C Min AGC Gate	LSB	1024	00	1024	00	
23		MSB		04		04	
24	CI_AGC_Threshold	LSB	16384	00	16384	00	
25		MSB		40		40	
26	CI-AGC_Alpha		2	02	2	02	
27	CI_Track_Alpha		2	02	2	02	
28	CI_Ku_Hgt_Error_Scale		24	18	24	18	
29	CI_C_Hgt_Error_Scale		24	18	24	18	
30	CI_AGC_Error_Scale	LSB	35	23	35	23	
31		MSB		00		00	
32	AGC_Threshold	LSB	4096	00	4096	00	
33		MSB		10		10	
34	Low_Vres		6	06	4	04	Decrease Vres
35	Hgt_Adjustment		0	00	0	00	
36	AGC_Adjustment	LSB/LSW	18 dB	00	10.5 dB	00	Decrease AGC Adjustment
37		MSB/LSW		00		00	
38		LSB/MSW		00		00	
39		MSB/MSW		48		2A	
40	AGC_Error_Scale	LSB	139	8B	139	8B	
41		MSB		00		00	
42	Ku_AGC_Gate_Scale		1	01	1	01	
43	C-100_AGC_Gate_Scale		32	20	32	20	
44	C_320_AGC_Gate_Scale		4	04	4	04	
45	LRA_Min_Height	LSB/LSW	1275 Km	00	1328 Km	00	Trim Range
46		MSB/LSW		00		00	

Table 5.8.4 Comparison of Initial (PARMC320) and Present (C35028SL) Programmable Parameter Sets

Filename = PARMC320				Filename = C35028SL		
Byte	Parameter	Value	Hex	Value	Hex	Comment
47	LSB/MID		14		00	
48	MSB/MID		1E		50	
49	LSB/MSW		04		09	
50	MSB/MSW		A6		AD	
51	LRA_Max_Height	1398 Km	00	1358 Km	00	Trim Range
52	MSB/LSW		00		00	
53	LSB/MID		FB		00	
54	MSB/MID		20		00	
55	LSB/MSW		08		F2	
56	MSB/MSW		B6		B0	
57	LRA_Height_Inc	3.24 Km	00	0.81 Km	00	Decrease Scan Step Size
58	MSB/LSW		00		00	
59	LSB/MID		00		00	
60	MSB/MID		00		00	
61	LSB/MSW		6C		1B	
62	MSB/MSW		00		00	
63	LRA_AGC_Dec	4.25 dB	00	4.25 dB	00	
64	MSB/LSW		00		00	
65	LSB/MSW		00		00	
66	MSB/MSW		11		11	
67	AGC_Minimum	13 dB	00	13 dB	00	
68	MSB/LSW		00		00	
69	LSB/MSW		00		00	
70	MSB/MSW		34		34	
71	Delta_AGC	39 dB	00	30 dB	00	Decrease AGC Adjustment
72	MSB/LSW		00		00	
73	LSB/MSW		00		00	
74	MSB/MSW		9C		78	
75	HRA_Scan_Window	800.0 nSec	08	800.0 nSec	08	
76	HRA_Scan_Hgt_Inc	200.0 nSec	00	200.0 nSec	00	
77	MSB/LSW		00		00	
78	LSB/MID		00		00	
79	MSB/MID		00		00	
80	LSB/MSW		01		01	
81	MSB/MSW		00		00	
82	HRA_AGC_NoiseI1	4	04	4	04	
83	HRA_AGC_NoiseI2	7	07	7	07	
84	HRA_Min_Sig_Thr	1024	00	1024	00	
85	MSB		04		04	
86	LR_Ku_NoiseI1	4	04	4	04	
87	LR_Ku_NoiseI2	7	07	7	07	
88	LR_Ku_Thr_Hgt_Scale	31	1F	29	1D	Decrease Ku Threshold Ht. Scale
89	HR_Ku_AGC_I1	16	10	16	10	
90	HR_Ku_AGC_I2	47	2F	47	2F	
91	HR_Ku_NoiseI1	4	04	4	04	
92	HR_Ku_NoiseI2	7	07	7	07	

Table 5.8.4 (Continued)

Filename = PARMC320				Filename = C35028SL		
Byte	Parameter	Value	Hex	Value	Hex	Comment
93	Ku_HR_Thr_Hgt	25	19	25	19	
94	Fine_Trk_Ku_Alpha	2	02	2	02	
95	Coarse_Trk_Ku_Alpha	1	01	1	01	
96	Ku_AGC_Scale1	33458	B2	33458	B2	
	MSB		82		82	
98	Ku_AGC_Scale2	33458	B2	33458	B2	
99	MSB		82		82	
100	Ku_AGC_Scale3	33511	E7	33511	E7	
101	MSB		82		82	
102	Ku-AGC_Scale4	33479	C7	33479	C7	
103	MSB		82		82	
104	Ku_AGC_Scale5	33309	1D	33309	1D	
105	MSB		82		82	
106	Ku_AGC_Scale6	32768	00	32768	00	
107	MSB		80		80	
108	Ku_EML_Hgt_Scale1	77	4D	77	4D	
109	MSB		00		00	
110	Ku_EML_Hgt_Scale2	105	69	105	69	
111	MSB		00		00	
112	Ku_EML_Hgt_Scale3	262	06	262	06	
113	MSB		01		01	
114	Ku_EML_Hgt_Scale4	696	B8	696	B8	
115	MSB		02		02	
116	Ku_EML_Hgt_Scale5	1882	5A	1882	5A	
117	MSB		07		07	
118	LR_C_NoiseI1	4	04	4	04	
119	LR_C_NoiseI2	7	07	7	07	
120	LR_C_Thr_Hgt_Scale	31	1F	29	1D	Tune Scale
121	HR_C_AGC_I1	16	10	19	13	Shift C Gates +3
122	HR_C_AGC_I2	47	2F	50	32	Shift C Gates +3
123	HR_C_NoiseI1	4	04	7	07	Shift C Gates +3
124	HR_C_NoiseI2	7	07	10	0A	Shift C Gates +3
125	C_HR_Thr_Hgt	25	19	25	19	
126	Fine_Trk_C_Alpha	2	02	2	02	
127	Coarse_Trk_C_Alpha	1	01	1	01	
128	C_AGC_Scale1	32768	00	32768	00	
129	MSB		80		80	
130	C_AGC_Scale2	32768	00	32768	00	
131	MSB		80		80	
132	C_AGC_Scale3	32809	29	32809	29	
133	MSB		80		80	
134	C-AGC_Scale4	32839	47	32839	47	
135	MSB		80		80	
136	C_AGC_Scale5	32829	3D	32829	3D	
137	MSB		80		80	
138	C_AGC_Scale6	32768	00	32768	00	
139	MSB		80		80	
140	C_EML_Hgt_Scale1	312	38	312	38	
141	MSB		01		01	

Table 5.8.4 (Continued)

Filename = PARMC320					Filename = C35028SL		
Byte	Parameter		Value	Hex	Value	Hex	Comment
142	C_EML_Hgt_Scale2	LSB	440	B8	440	B8	
143		MSB		01		01	
144	C_EML_Hgt_Scale3	LSB	1040	10	1040	10	
145		MSB		04		04	
146	C_EML_Hgt_Scale4	LSB	2784	E0	2784	E0	
147		MSB		0A		0A	
148	C_EML_Hgt_Scale5	LSB	7112	C8	7112	C8	
149		MSB		1B		1B	
150	LR_Track_Point		63.5	7F	63.5	7F	
151	T1	LSB	24	18	96	60	Increase Signal Width
152		MSB		00		00	
153	T2	LSB	160	A0	2560	00	Increase Signal Variability
154		MSB		00		0A	
155	T3	LSB	16	10	64	40	Tune Signal Width
156		MSB		00		00	
157	T4	LSB	40	28	640	80	Tune Signal Variability
158		MSB		00		02	
159	T8	LSB	1024	00	1024	00	
160		MSB		04		04	
161	Ku_Early_Index1_1		31	1F	31	1F	
162	Ku_Early_Index2_1		31	1F	31	1F	
163	Ku_Early_Index1_2		30	1E	30	1E	
164	Ku_Early_Index2_2		31	1F	31	1F	
165	Ku_Early_Index1_3		29	1D	29	1D	
166	Ku_Early_Index2_3		30	1E	30	1E	
167	Ku_Early_Index1_4		26	1A	26	1A	
168	Ku_Early_Index2_4		29	1D	29	1D	
169	Ku_Early_Index1_5		20	14	20	14	
170	Ku_Early_Index2_5		27	1B	27	1B	
171	Ku_Early_Index1_6		8	08	8	08	
172	Ku_Early_Index2_6		23	17	23	17	
173	Ku_Middle_Index1_1		31	1F	31	1F	
174	Ku_Middle_Index2_1		32	20	32	20	
175	Ku_Middle_Index1_2		31	1F	31	1F	
176	Ku_Middle_Index2_2		32	20	32	20	
177	Ku_Middle_Index1_3		30	1E	30	1E	
178	Ku_Middle_Index2_3		33	21	33	21	
179	Ku_Middle_Index1_4		28	1C	28	1C	
180	Ku_Middle_Index2_4		35	23	35	23	
181	Ku_Middle_Index1_5		24	18	24	18	
182	Ku_Middle_Index2_5		39	27	39	27	
183	Ku_Middle_Index1_6		24	18	24	18	
184	Ku_Middle_Index2_6		39	27	39	27	
185	Ku_Late_Index1_1		32	20	32	20	
186	Ku_Late_Index2_1		32	20	32	20	
187	Ku_Late_Index1_2		32	20	32	20	
188	Ku_Late_Index2_2		33	21	33	21	
189	Ku_Late_Index1_3		33	21	33	21	

Table 5.8.4 (Continued)

Filename - PARMC320				Filename = C35028SL		
Byte	Parameter	Value	Hex	Value	Hex	Comment
190	Ku_Late_Index2_3	34	22	34	22	
191	Ku_Late_Index1_4	34	22	34	22	
192	Ku_Late_Index2_4	37	25	37	25	
193	Ku_Late_Index1_5	36	24	36	24	
194	Ku_Late_Index2_5	43	2B	43	2B	
195	Ku_Late_Index1_6	40	28	40	28	
196	Ku_Late_Index2_6	55	37	55	37	
197	C_Early_Index1_1	31	1F	34	22	Shift C Gates +3
198	C_Early_Index2_1	31	1F	34	22	Shift C Gates +3
199	C_Early_Index1_2	30	1E	33	21	Shift C Gates +3
200	C_Early_Index2_2	31	1F	34	22	Shift C Gates +3
201	C_Early_Index1_3	29	1D	32	20	Shift C Gates +3
202	C_Early_Index2_3	30	1E	33	21	Shift C Gates +3
203	C_Early_Index1_4	26	1A	29	1D	Shift C Gates +3
204	C_Early_Index2_4	29	1D	32	20	Shift C Gates +3
205	C_Early_Index1_5	20	14	23	17	Shift C Gates +3
206	C_Early_Index2_5	27	1B	30	1E	Shift C Gates +3
207	C_Early_Index1_6	8	08	11	0B	Shift C Gates +3
208	C_Early_Index2_6	23	17	26	1A	Shift C Gates +3
209	C_Middle_Index1_1	31	1F	34	22	Shift C Gates +3
210	C_Middle_Index2_1	32	20	35	23	Shift C Gates +3
211	C_Middle_Index1_2	31	1F	34	22	Shift C Gates +3
212	C_Middle_Index2_2	32	20	35	23	Shift C Gates +3
213	C_Middle_Index1_3	30	1E	33	21	Shift C Gates +3
214	C_Middle_Index2_3	33	21	36	24	Shift C Gates +3
215	C_Middle_Index1_4	28	1C	31	1F	Shift C Gates +3
216	C_Middle_Index2_4	35	23	38	26	Shift C Gates +3
217	C_Middle_Index1_5	24	18	27	1B	Shift C Gates +3
218	C_Middle_Index2_5	39	27	42	2A	Shift C Gates +3
219	C_Middle_Index1_6	24	18	27	1B	Shift C Gates +3
220	C_Middle_Index2_6	39	27	42	2A	Shift C Gates +3
221	C_Late_Index1_1	32	20	35	23	Shift C Gates +3
222	C_Late_Index2_1	32	20	35	23	Shift C Gates +3
223	C_Late_Index1_2	32	20	35	23	Shift C Gates +3
224	C_Late_Index2_2	33	21	36	24	Shift C Gates +3
225	C_Late_Index1_3	33	21	36	24	Shift C Gates +3
226	C_Late_Index2_3	34	22	37	25	Shift C Gates +3
227	C_Late_Index1_4	34	22	37	25	Shift C Gates +3
228	C_Late_Index2_4	37	25	40	28	Shift C Gates +3
229	C_Late_Index1_5	36	24	39	27	Shift C Gates +3
230	C_Late_Index2_5	43	2B	46	2E	Shift C Gates +3
231	C_Late_Index1_6	40	28	43	2B	Shift C Gates +3
232	C_Late_Index2_6	55	37	58	3A	Shift C Gates +3
233	RAVE Time Constant	LSB	8	08	8	08
234		MSB			00	
235	Ku_GI_Scale	82	52	82	52	
236	C_320_GI_Scale	78	4E	78	4E	
237	C_100_GI_Scale	70	46	70	46	
238	HR_Track_Point	63	3F	63	3F	

Table 5.8.4 (Continued)

Filename - PARMC320				Filename = C35028SL		
Byte	Parameter	Value	Hex	Value	Hex	Comment
239	Thr_Hgt_Err_Win1	8	08	8	08	
240	Thr_Hgt_Err_Win2	8	08	8	08	
241	Thr_Hgt_Err_Win3	12	0C	12	0C	
242	Thr_Hgt_Err_Win4	16	10	16	10	
243	Thr_Hgt_Err_Win5	32	20	32	20	
244	Fine_Trk_AGC_Alpha	3	03	3	03	
245	Fine_Track_Beta	6	06	6	06	
246	Coarse_Trk_AGC_Alpha	2	02	2	02	
247	Coarse_Track_Beta	4	04	4	04	
248	T5	LSB	2560	00	2560	00
249		MSB		0A		0A
250	T6	LSB	10240	00	10240	00
251		MSB		28		28
252	T7	LSB	256	00	256	00
253		MSB		01		01
254	Ku_Pulse_Count	25	19	25	19	
255	C_Pulse_Count	26	1A	26	1A	
256	Acq_Pulse_Count	26	1A	26	1A	
257	AGC_Rate	LSB	13	0D	13	0D
258		MSB		00		00
259	Xmit_Test_Height	LSB/LSW	8609.6μSec	00	8609.6μSec	00
260		MSB/LSW		00		00
261		LSB/MID		00		00
262		MSB/MID		00		00
263		LSB/MSW		28		28
264		MSB/MSW		A8		A8
265	Xmit_Test_Hgt_Rate	LSB/LSW	0	00	0	00
266		MSB/LSW		00		00
267		LSB/MID		00		00
268		MSB/MID		00		00
269		LSB/MSW		00		00
270		MSB/MSW		00		00
271	Xmit_Test_AGC	60 dB	F0	60 dB	F0	
272	BC_Init	0	00	0	00	
273	WD_Init	25	19	25	19	

Table 5.8.4 (Continued)

6.0 WAVEFORM SAMPLES ASSESSMENT

6.1 Introduction

The various waveform effects discussed in this section are produced by the TOPEX digital filter bank (DFB), and are present in both the Ku and the C waveforms. The DFB will be described briefly. Several departures of the signal from the ideal will be discussed. Some of the departures depend on the value of the fine-height word, so the relationship between height rate and fine-height word is also described. Sets of multiplicative and additive waveform corrections have been developed which, on average, compensate for the waveform departures from ideal. We acknowledge the efforts of P. C. Marth, Jr. of JHU/APL and W. B. Shoemaker of SM Systems and Research Corporation in trying to understand the details of waveform shape effects arising from the digital filter bank. J. R. Jensen, JHU/APL, contributed important simulations to clarify relationships of FFT hardware details to observed waveform features.

6.2 Digital Filter Bank

6.2.1 Brief Description

The digital filter bank (DFB) lies at the heart of the altimeter and its range tracking loop as shown in **Figure 6.2.1**. The transmitted pulse (320 MHz chirp bandwidth, 102.4 μ sec pulsewidth, from the digital chirp generator) scatters off the ocean surface; the received return signal is dechirped and then mixed down to in-phase (I) and quadrature (Q) signals, filtered with a 625 kHz lowpass filter (the "anti-aliasing filter"), and digitized at a 1.25 MHz sample rate. At 1.25 MHz, the 102.4 μ sec pulse results in 128 complex samples upon which the DFB performs a 128-point fast Fourier transform (FFT). The FFT output is 128 individual waveform samples, spaced effectively 9.765 kHz apart in frequency (equivalent to 3.125 n spacing in the time domain), which are tracked by the adaptive tracker unit (AMU). The tracking error in the tracking loop is nulled by frequency shifting. The frequency shift, controlled by the track loop, is accomplished by (complex) multiplication of the digitized I and Q samples by a rotating phaser just before the FFT is performed. The phaser rotation rate is controlled by the tracking loop's fine-height word. The 128 individual waveform samples are also compressed into 64 samples and placed into the telemetry stream. The compression depends upon mode, as summarized in **Table 6.2.1**. The DFB performs the same operations for both the Ku and the C altimeters in TOPEX.

In radar altimeters prior to TOPEX, the DFB's used the discrete Fourier transform with a maximum of 64 samples. For TOPEX, the FFT was implemented in digital electronics to lessen the time required to perform the full transform for the 128 samples. In a perfect DFB, the output would be a perfect Fourier transform of the

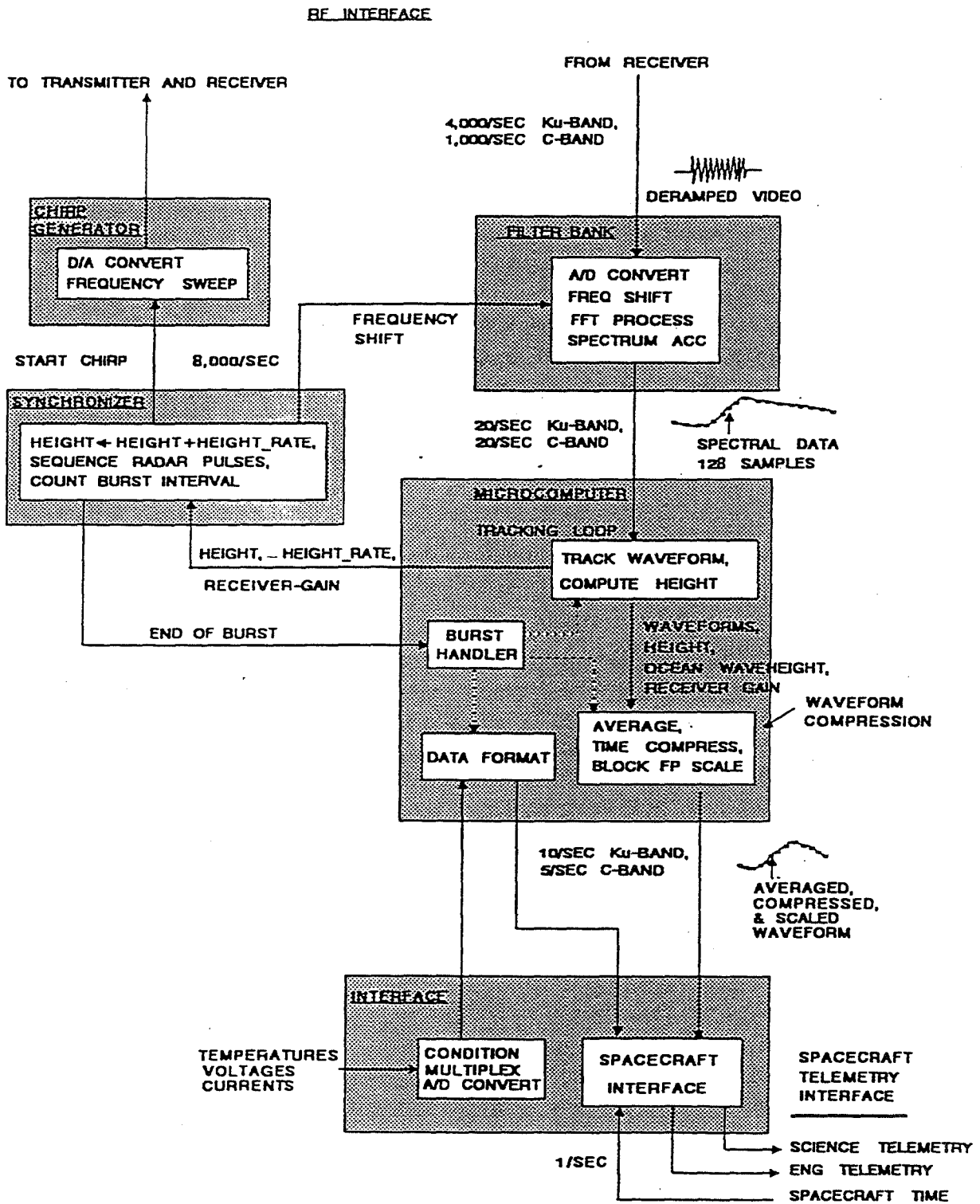


Figure 6.2.1 TOPEX Altimeter Data Processing (from Perschy, JHU/APL)

Table 6.2.1. TOPEX Waveform to Telemetry Sample Compression in Different Modes

TELEMETRY Sample #	CAL MODE 2 or TRACK Waveform Sample #	CAL MODE 1, STANDBY, or TRANSMITTER TEST Waveform Sample #	TELEMETRY Sample #	CAL MODE 2 or TRACK Waveform Sample #	CAL MODE 1, STANDBY, or TRANSMITTER TEST Waveform Sample #
1	1 - 2	33	33	41	65
2	3 - 4	34	34	42	66
3	5 - 6	35	35	43	67
4	7 - 8	36	36	44	68
5	9 - 10	37	37	45	69
6	11 - 12	38	38	46	70
7	13 - 14	39	39	47	71
8	15 - 16	40	40	48	72
9	17	41	41	49 - 50	73
10	18	42	42	51 - 52	74
11	19	43	43	53 - 54	75
12	20	44	44	55 - 56	76
13	21	45	45	57 - 58	77
14	22	46	46	59 - 60	78
15	23	47	47	61 - 62	79
16	24	48	48	63 - 64	80
17	25	49	49	65 - 68	81
18	26	50	50	69 - 72	82
19	27	51	51	73 - 76	83
20	28	52	52	77 - 80	84
21	29	53	53	81 - 84	85
22	30	54	54	85 - 88	86
23	31	55	55	89 - 92	87
24	32	56	56	93 - 96	88
25	33	57	57	97 - 100	89
26	34	58	58	101 - 104	90
27	35	59	59	105 - 108	91
28	36	60	60	109 - 112	92
29	37	61	61	113 - 116	93
30	38	62	62	117 - 120	94
31	39	63	63	120 - 124	95
32	40	64	64	125 - 128	96

input with no extraneous effects being introduced by the DFB itself. The shape of the transformed pulse in amplitude versus frequency would look exactly like the time domain average return from a 3.125 n transmitted pulse. But the TOPEX DFB does not provide a completely perfect transform, and there are several small effects of the DFB hardware/software on the shape of the output. Some of these effects are independent of value of the fine-height word, while others of the effects vary with fine-height word. In this discussion the waveform samples will always be numbered 1 through 128, and the telemetry samples will always be numbered 1 through 64.

6.2.2 DFB Effects Not Depending on Fine-Height Word

6.2.2.1 Zero Leakage

At the center of the filter bank (waveform sample 65 out of the full 128) there appears to be an excess signal, spread across several samples. Waveform sample 65 is the zero-frequency sample. This zero-frequency leakage appears to be present in all the TOPEX filter banks tested (*i.e.*, engineering model, breadboard unit, and both Side A and Side B in the flight unit), and is seen in all modes (standby, calibration, and tracking). The zero-frequency leakage is not affected by AGC or receiver gain, and appears to be an additive effect only. The probable explanation for this is provided by J. R. Jensen of JHU/APL who has done tracker simulations which include details of the mathematics performed in the digital FFT. Jensen has found a right shift-caused truncation in the DFB where round-off should have been used, and when the right shift is corrected in Jensen's simulation the zero leakage disappears. There is a subtle fine-height dependence in that round-off error will go to zero when the fine height is exactly zero with respect to any filter. Since in general the fine height is continually changing, the zero-leakage from round-off error will disappear only a small fraction of the time. The time average over even as short a time as one tracker update interval will exhibit this zero-leakage.

There may also be another DC or zero-frequency leakage from charges retained on the biasing capacitors in the analog to digital conversion; residual charge will appear as a DC bias and therefore appear at the zero-frequency filter and its immediate neighbors. As with wraparound, the way to handle the zero-leakage is to ignore the waveform samples in which it is present.

6.2.2.2 FFT Finite Word Length Effects

The TOPEX FFT word length was 8 bits (a limit set by device availability at the time of the altimeter design), and the DFB output exhibits "sawteeth" and a "plateau excess". Jensen's simulation of DFB details included the effects of the finite word length (8 bits) of the DFB FFT devices. The simulation was able to demonstrate both sawteeth and plateau excess matching that seen in TOPEX data. While these effects

can generally be removed (or compensated for) in ground processing, they are present in the waveforms presented to the TOPEX on-board tracker.

Sawteeth

The (uncompressed) waveform samples exhibit an alternating up-and-down neighbor-to-neighbor variation. This effect is also cyclic in groups of eight samples, so that within each group of eight neighboring sampler there will be one which is noticeably lower than the rest. The eighth sample away will also be lower than its neighbors. The sawteeth are smoothed by the compression from waveform to telemetry samples, so that in fine-tracking the sawteeth are seen only in samples number 17-48. The sawteeth are harder to see in actual fine-track data than in Calibration Mode 2 waveforms because in the latter the signal on which the sawteeth ride is an approximately straight horizontal line. Figure 6.2.2.2a shows the sawteeth in a typical Ku fine-track waveform averaged for 5 seconds, and Figure 6.2.2.2b is a magnified portion of part of the uncompressed waveform region of Figure 6.2.2.2a. Figure 6.2.2.2c shows the sawteeth in Calibration Mode 2. The sawteeth seem to be multiplicative, do not exhibit much variation with fine height, and in ground processing can be removed from waveform samples by using multiplicative compensation-factors derived from Calibration Mode 2 data.

Plateau excess

Model TOPEX waveforms were generated at WFF for 2 meter SWH and attitude values of 0.0, 0.2 and 0.4 degrees: Jensen was supplied values for (internal) waveform samples 1 - 128, uniformly spaced at 3.125 n, with their track-point at sample 32.5, and having a (noise) baseline of zero. These model waveforms were used as input to the Jensen TOPEX simulation, and the simulation output waveform samples (1-128) were compared to the input. Jensen also produced a simulated set of Calibration Mode 2 output waveform samples.

The Jensen model can only do Cal-II at fixed values of the fine-height word, but the actual, on-board TOPEX hardware performs Cal-II using a continuous sweep of the height. Jensen supplied three simulated different Cal-II waveforms, for fine-height values of 0 and +/- three samples (*i.e.*, +/- 9.375 n). These simulated Cal-II waveforms are shown in Figure 6.2.2.2d, and with a magnified vertical scale in Figure 6.2.2.2e. These three different results were averaged, and that average used in subsequent waveform figures. The Cal-II average is shown by the solid line on Figures 6.2.2.2d and 6.2.2.2e.

Figure 6.2.2.2f summarizes the waveforms in and out of the Jensen simulation for the TOPEX Ku altimeter at 0.0 degrees attitude angle. The "+" symbols show the model waveform which was sent to Jensen, and the diamond symbols show the output from the Jensen simulation. The Figure 6.2.2.2d Cal-II result was converted into a set of gains used to "correct" the Jensen output, with the result shown by the solid line in Figure 6.2.2.2f. The Figure 6.2.2.2f results were scaled so that the sums

Figure 6.2.2.2a. TOPEX Ku Waveform for 1993 Day 257 Data

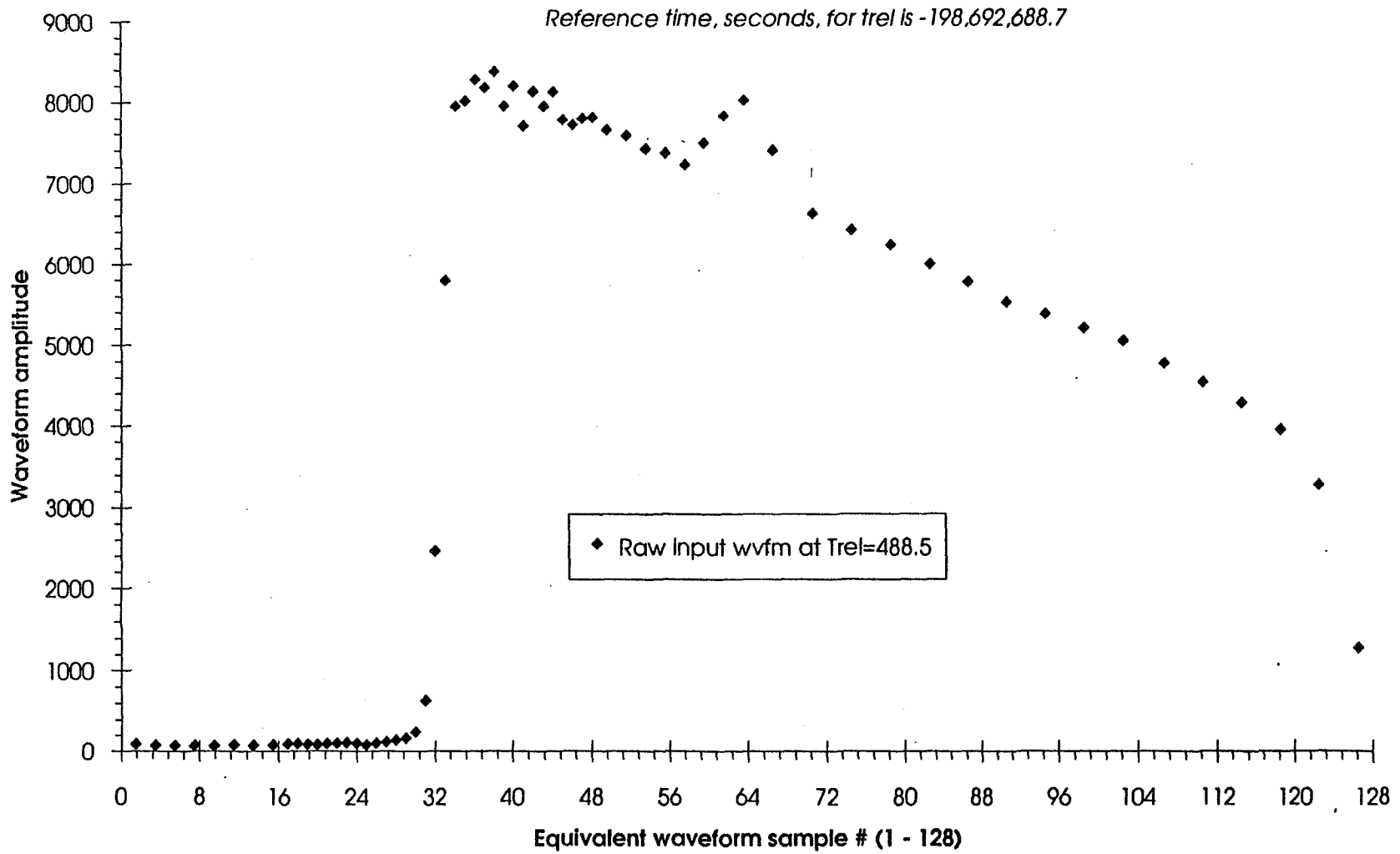


Figure 6.2.2.2b. TOPEX Ku Waveform for 1993 Day 257 Data
(magnified portion of part of the uncompressed waveform region)

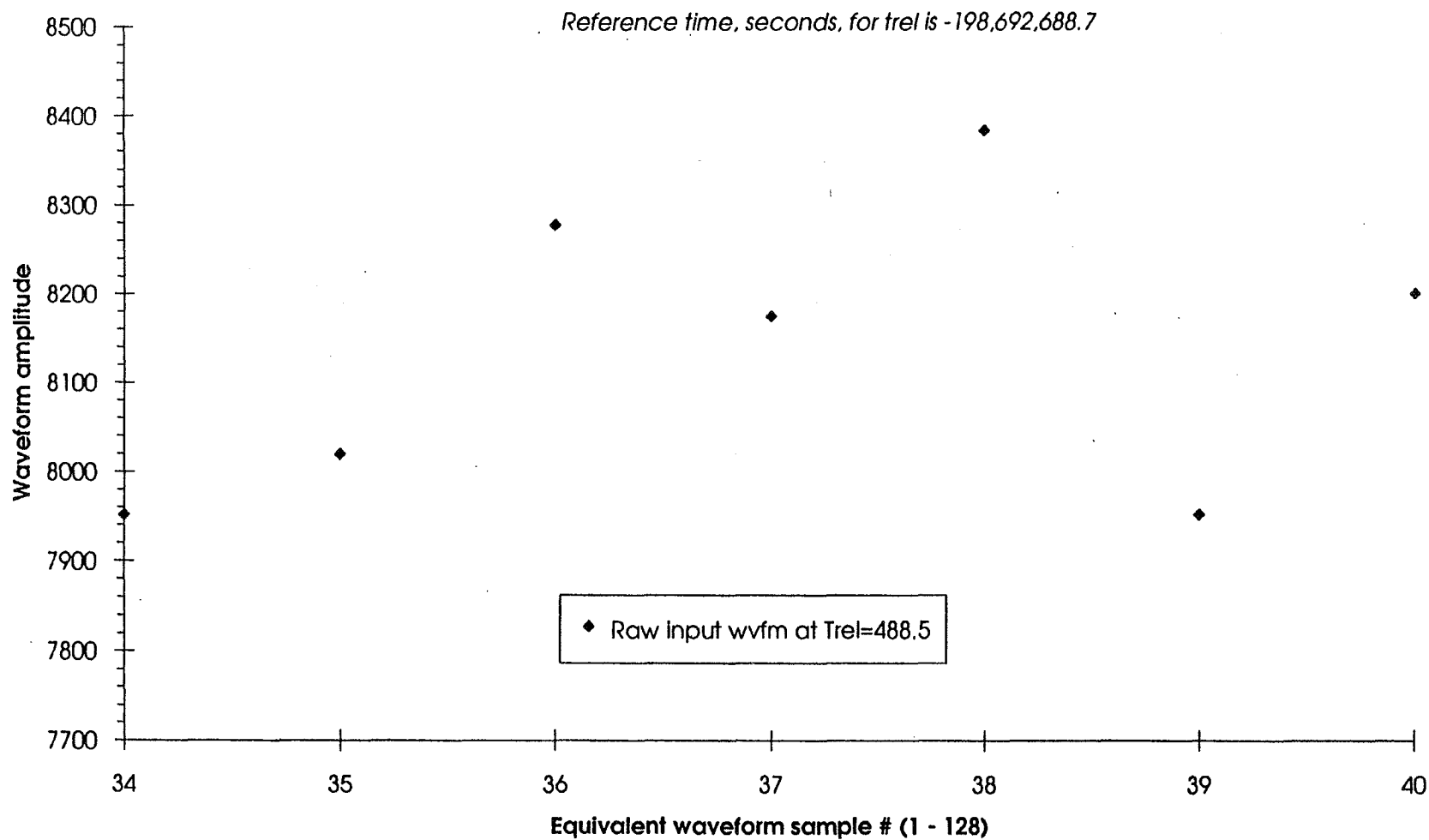


Figure 6.2.2.2c. Calibration Mode 2 Waveform Data for TOPEX Ku-Band Altimeter
10-second waveform averages, two different Cal 2 Modes

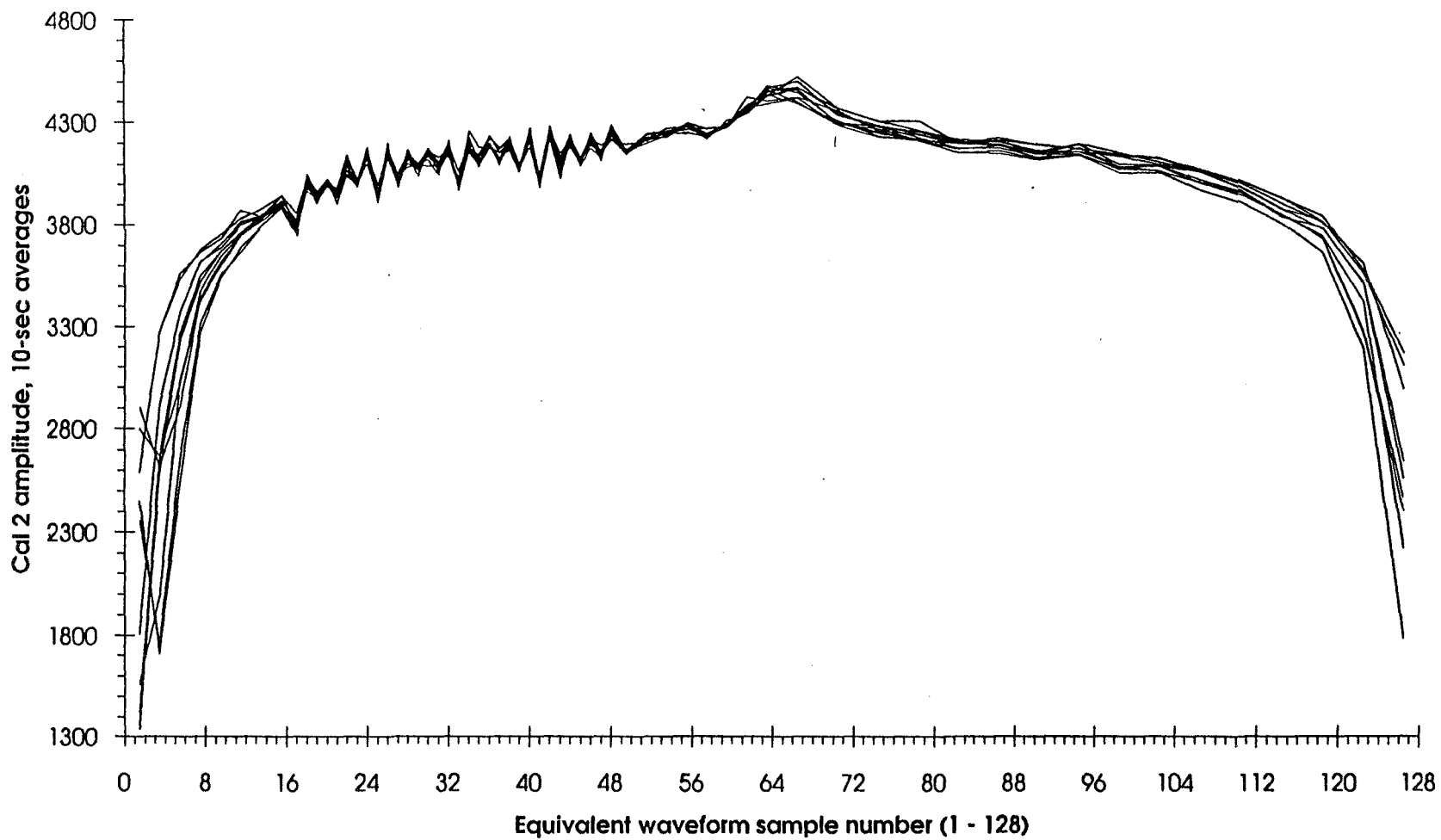


Figure 6.2.2.2d. Jensen Simulation Cal-II Waveforms

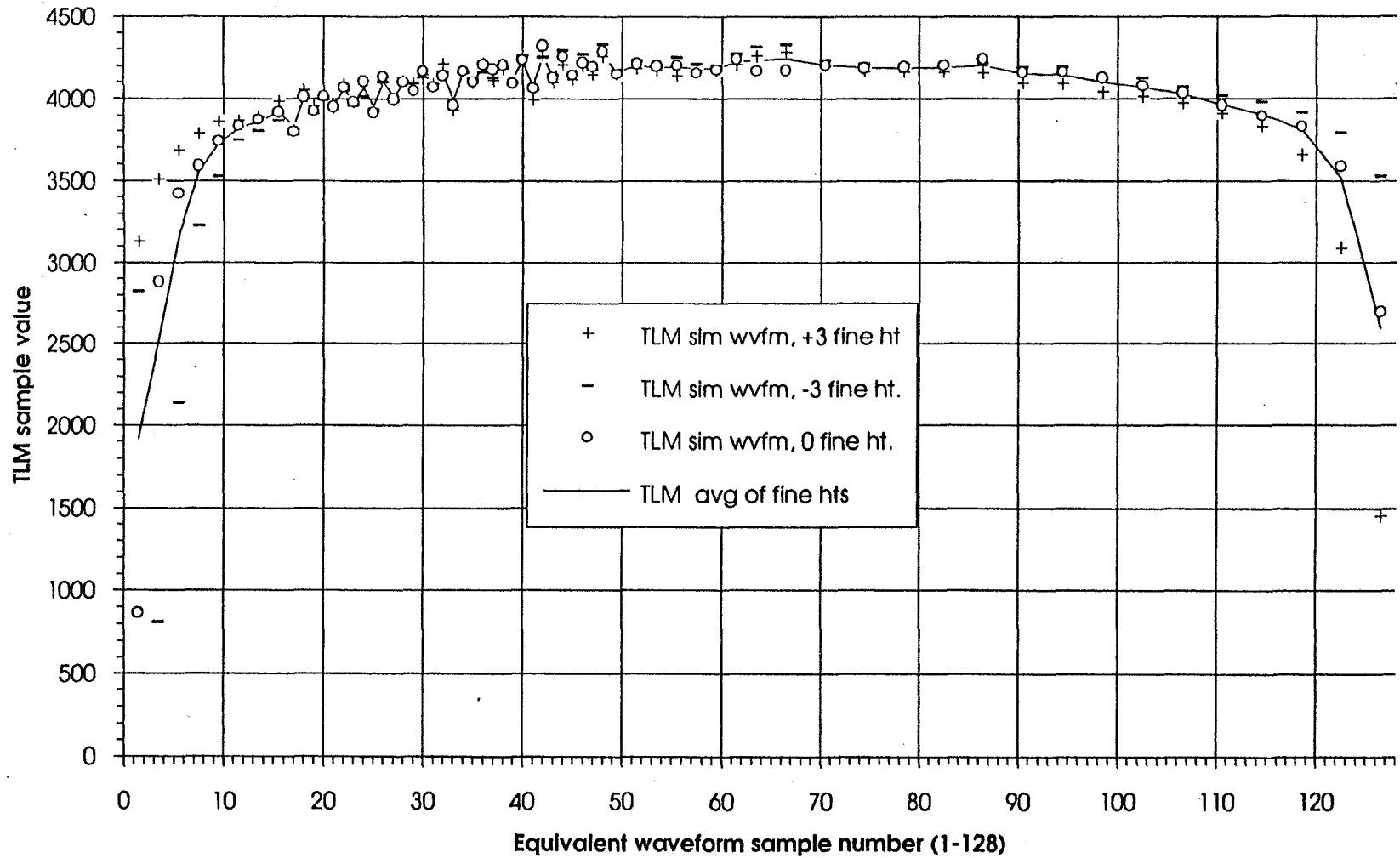


Figure 6.2.2.2e. Jensen Simulation Cal-II Waveforms

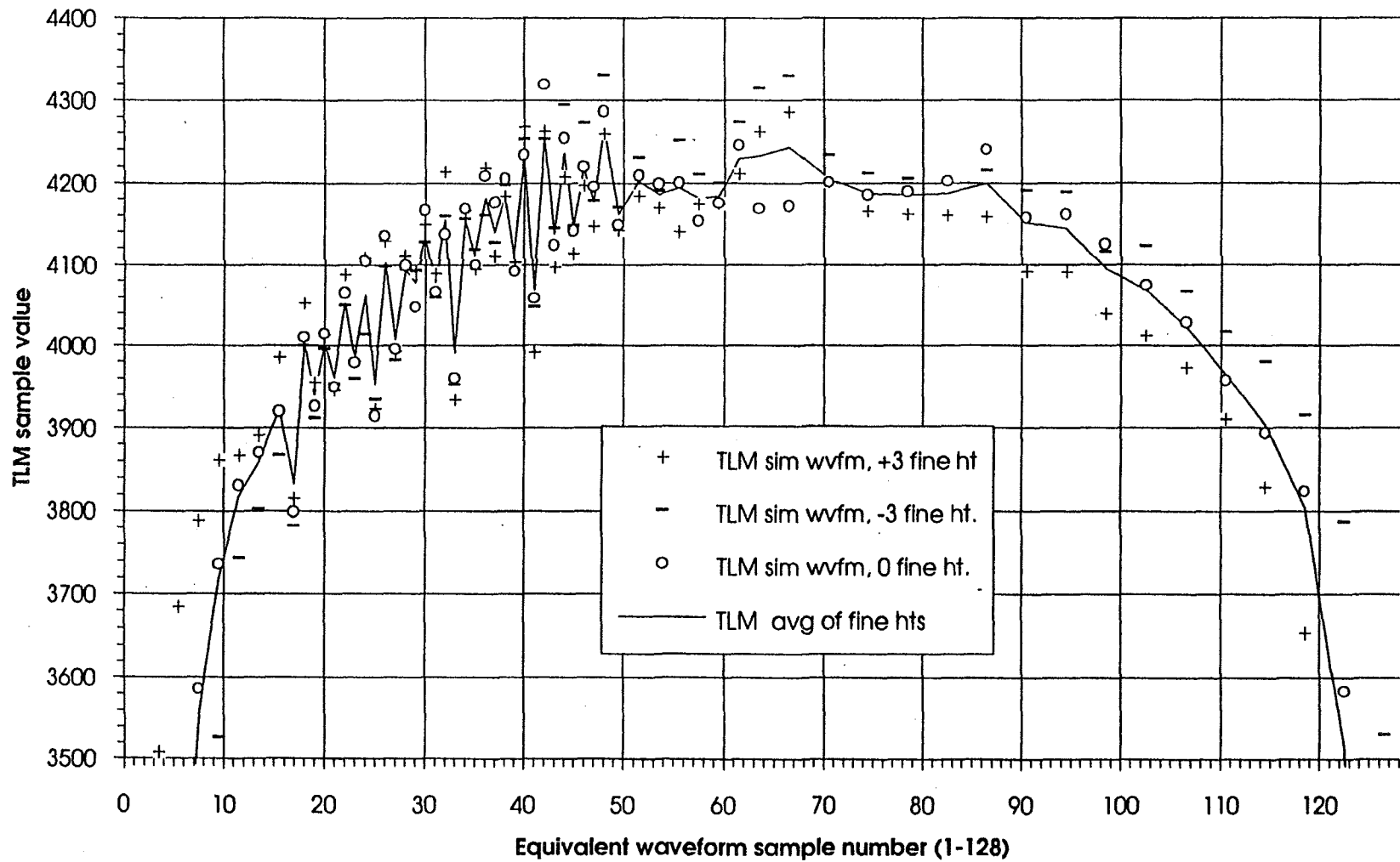
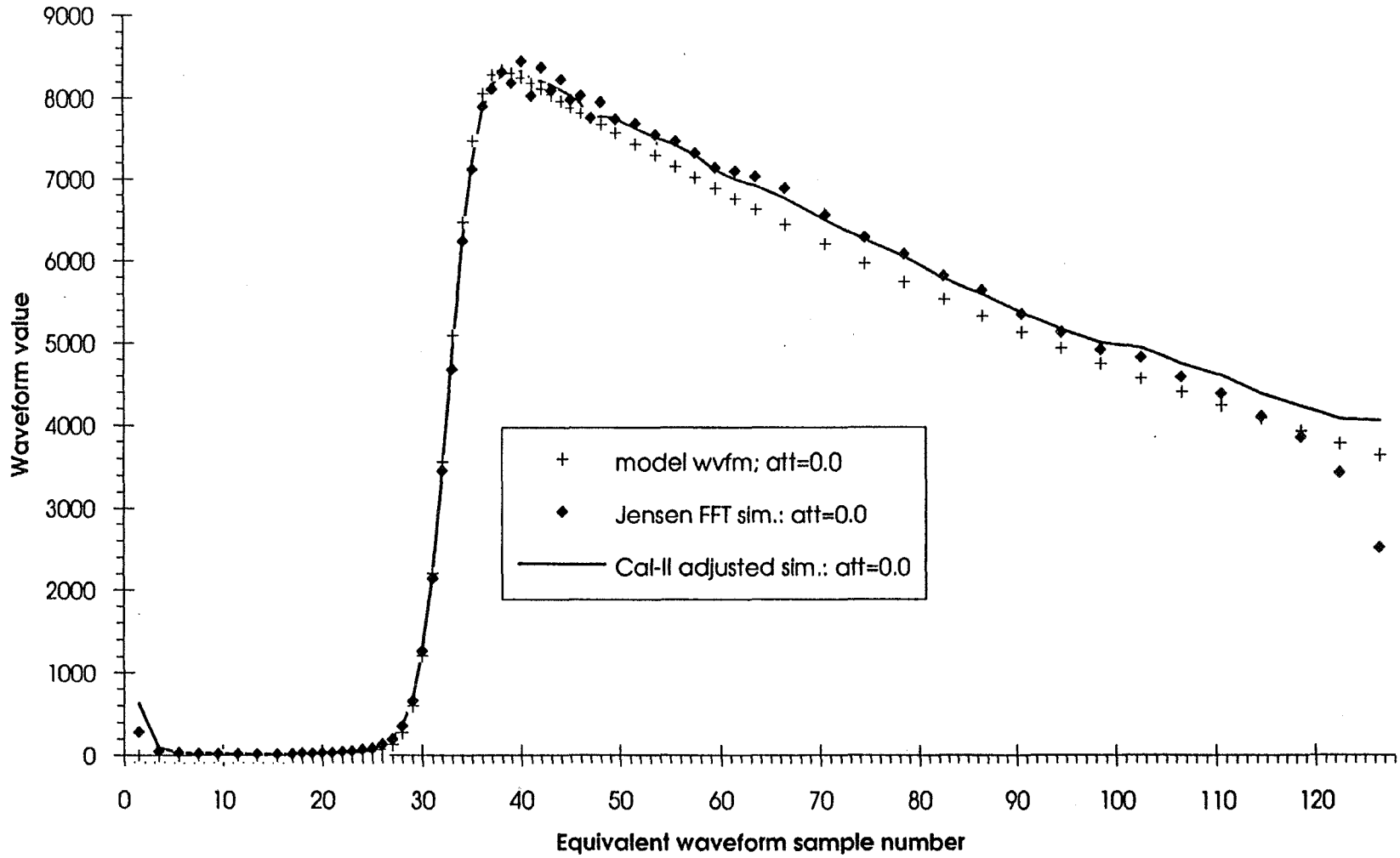


Figure 6.2.2.2f. Modeling Results for TOPEX Ku Altimeter



of telemetry samples 9-40 (corresponding to waveform samples 17-48) are the same for the three curves presented. Figure 6.2.2.2g presents the corresponding information for attitude of 0.2 degrees and Figure 6.2.2.2h is for an attitude of 0.4 degrees. Notice that these figures show the 64 telemetry sample results, but plotted on the equivalent waveform sample range of 1-128.

Comparing input ("+" symbols) to Cal-II-corrected output (solid lines) in Figures 6.2.2.2f - 6.2.2.2h there are two different effects: i) extra signal in the waveform plateau, and ii) non-zero baseline in the noise region of the waveform. Both of these effects may have some correlation with some of the observations of properties of actual TOPEX data. In these comparisons, one should ignore the first and last four TLM samples (equivalent waveform samples 1-8 and 113-128) since they may be affected by the bandpass filter and its wraparound.

The plateau excess can be compensated by a set of multiplicative corrections derived from the Jensen simulations. Fine-height dependence has been ignored to date in these corrections. Further simulation study is needed.

6.2.3 DFB Effects Which Do Depend Upon the Fine-Height Word

6.2.3.1 Relationship between Range Rate and Fine-Height Word

Because some waveform effects to be described depend on the value of the fine-height word, a brief description of the relationship between height rate and fine-height word is provided here. Figure 6.2.3.1 is a sketch of the fine-height word in the tracker. The least significant bit of the coarse-height word is 185.7 cm. When the height rate is negative (the height is decreasing), the height is kept in the upper half of the fine-height word. If the tracked height moves to the lower part of the fine-height word, the coarse-height is reduced by 187.5 cm and the fine-height is increased by 187.5 cm; the sum of the coarse-height and fine-height is the same but the tracked height will have been moved back to the upper half of the fine-height word. Similarly for increasing height the tracked height is kept in the lower half of the fine-height word.

As TOPEX moves from a latitude extreme (either plus or minus 66 degrees) toward the equator, the height rate is negative as depicted in Figure 5.4a. After the equator crossing, the height rate is positive, resulting in four height rate sign reversals per orbit. Table 6.2.3.1 summarizes which half of the fine-height word the height will be in.

Figure 6.2.2.2g. Modeling Results for TOPEX Ku Allimeter

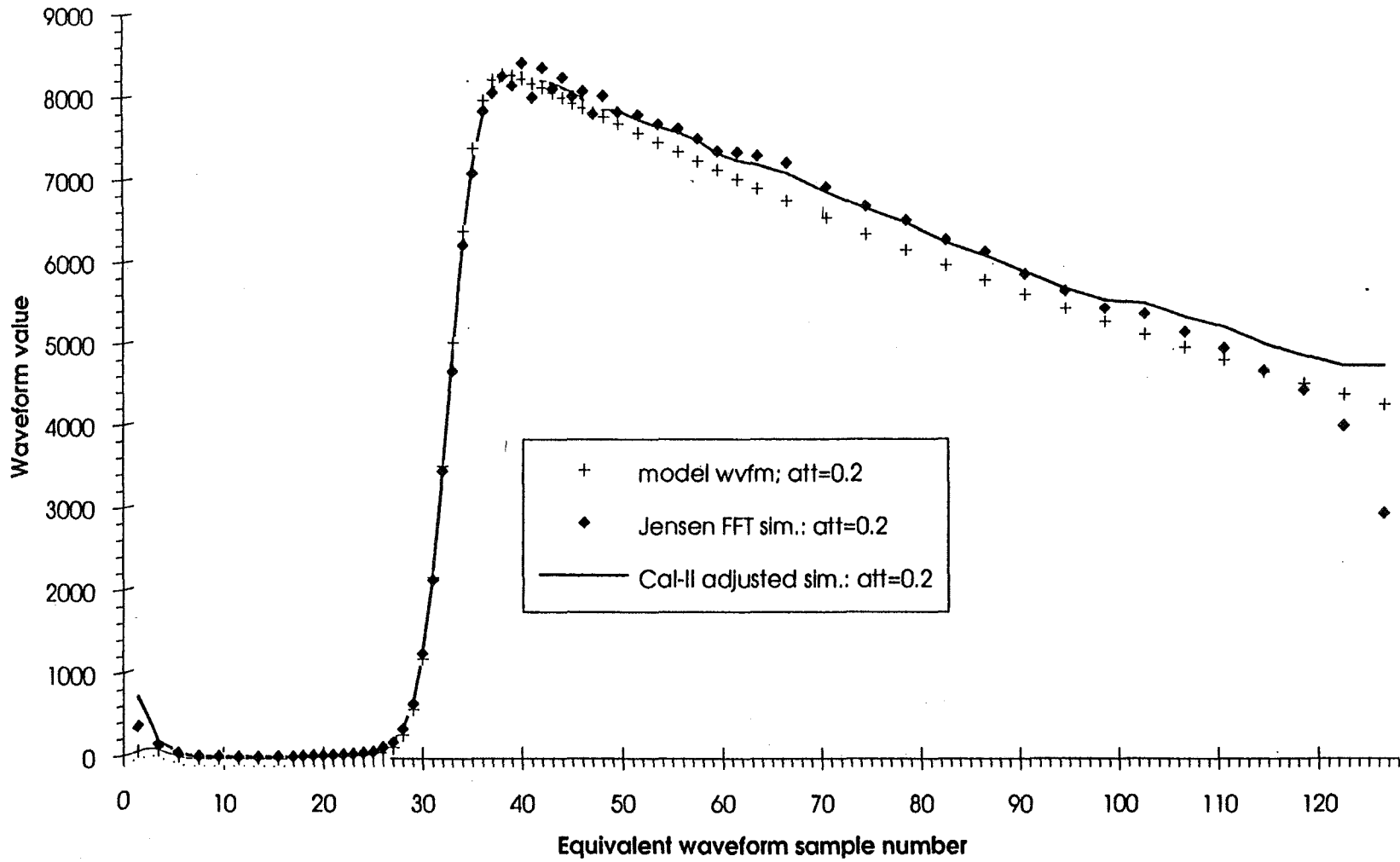
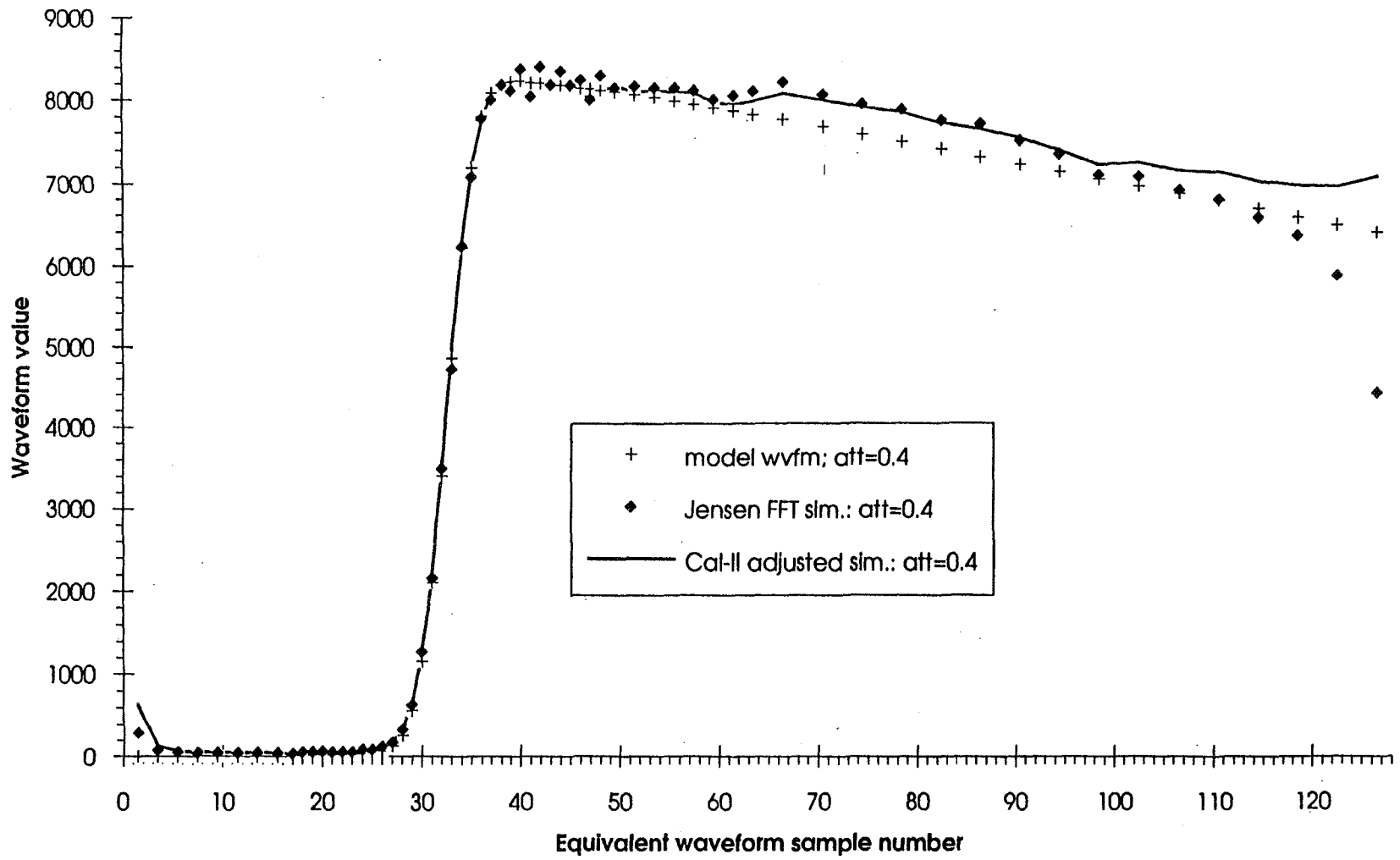


Figure 6.2.2.2h. Modeling Results for TOPEX Ku Altimeter



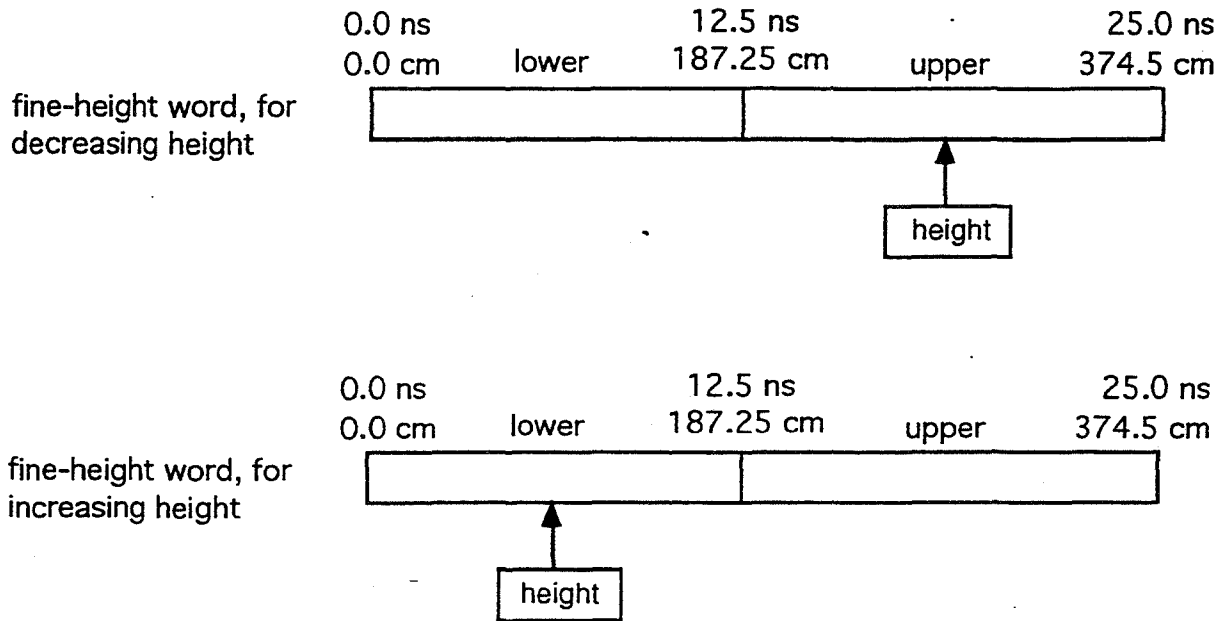


Figure 6.2.3.1 Sketch of Height Location Within Fine Height Word

	Positive Latitude (above equator)	Negative Latitude (below equator)
North-to-South passes	Upper Half (negative height rate)	Lower Half (positive height rate)
South-to-North passes	Lower Half (positive height rate)	Upper Half (negative height rate)

Table 6.2.3.1 Fine Height Word Value Summary

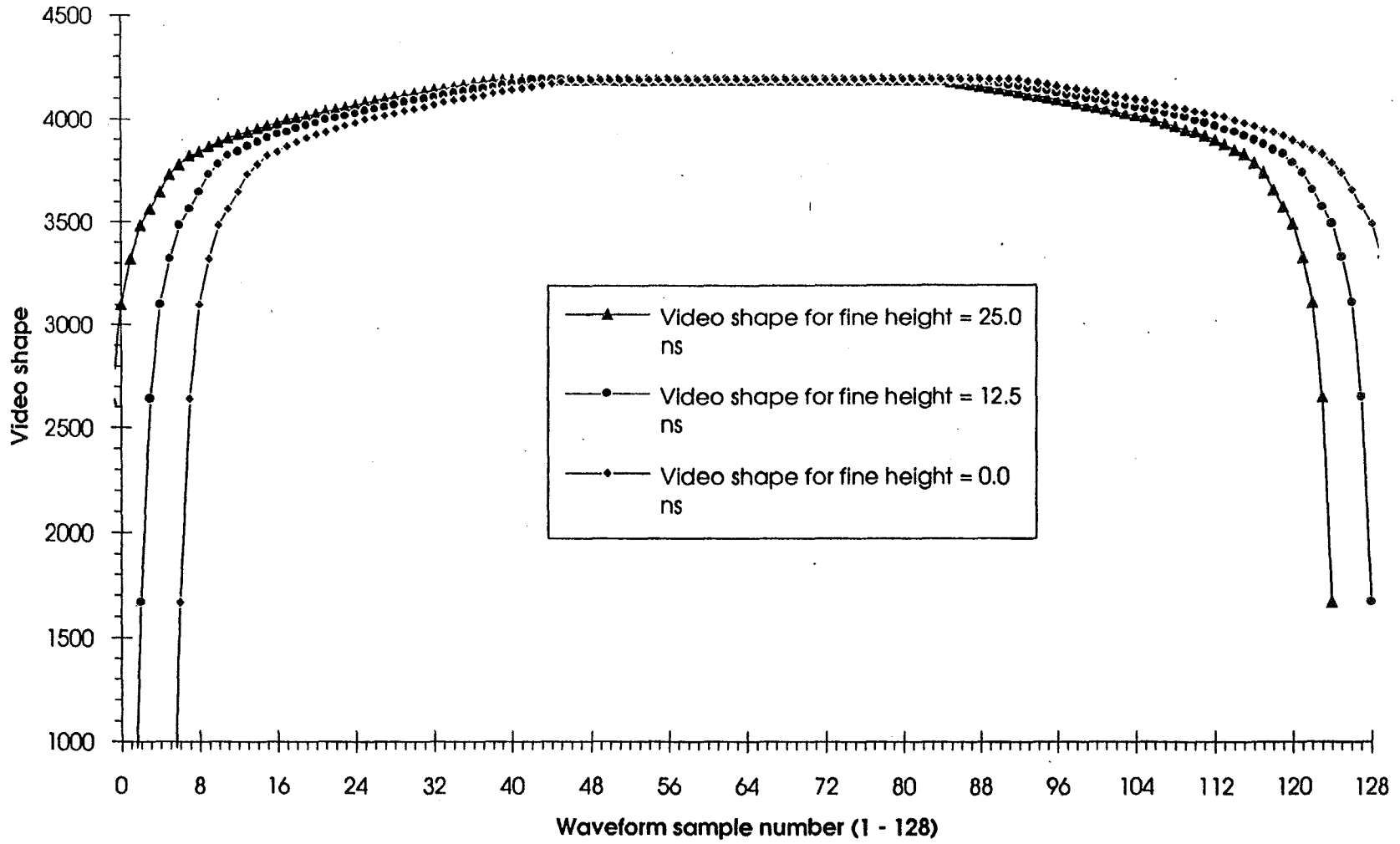
6.2.3.2 Filter Bank End Fall-off

For different fine-height values, the effects of the receiver's video bandwidth shape (the shape resulting from the anti-aliasing filter) is moved horizontally relative to the individual waveform samples. Figure 6.2.3.2 shows an idealized effect for three different fine-height values, and Figure 6.2.2.2d shows the effect as it appears in Calibration Mode 2 data. In this mode, the altimeter looks at noise only, and the AGC adjusts the receiver gain to attain a fixed level of 4096 for AGC minus noise. If the DFB created a replica of receiver input noise, there should be a fixed level seen across the entire band. The anti-aliasing filter modifies this, and the effects are seen at the low and high ends of the bandwidth. In Calibration Mode 2 the fine-height is constantly swept in one direction, incrementing the constantly the low-order bit of the fine-height word (so the fine-height will increase to its maximum, then start increasing again from zero) so that successive averages will show the anti-aliasing filter shape moving relative to the waveform samples. (Recall from Table 6.2.1 that the Cal Mode 2 telemetry compression is the same as for the fine-track mode.)

6.2.3.3 Wraparound effect

At small values of fine height the filter bandpass is shifted upward and some of the energy coming through the filter bandpass will fall past the extent of the filter bank. This extra energy which should be at the end of the pulseshape will be wrapped around to the early waveform samples as sketched in Figure 6.2.2.2f. Figure 6.2.2.2c shows actual data exhibiting the wraparound in low samples. The wraparound affects only waveform samples at the low and high extremes.

Figure 6.2.3.2. TOPEX Video Shape for Different Values of the Fine Height Word



6.2.3.4 Leakage effects

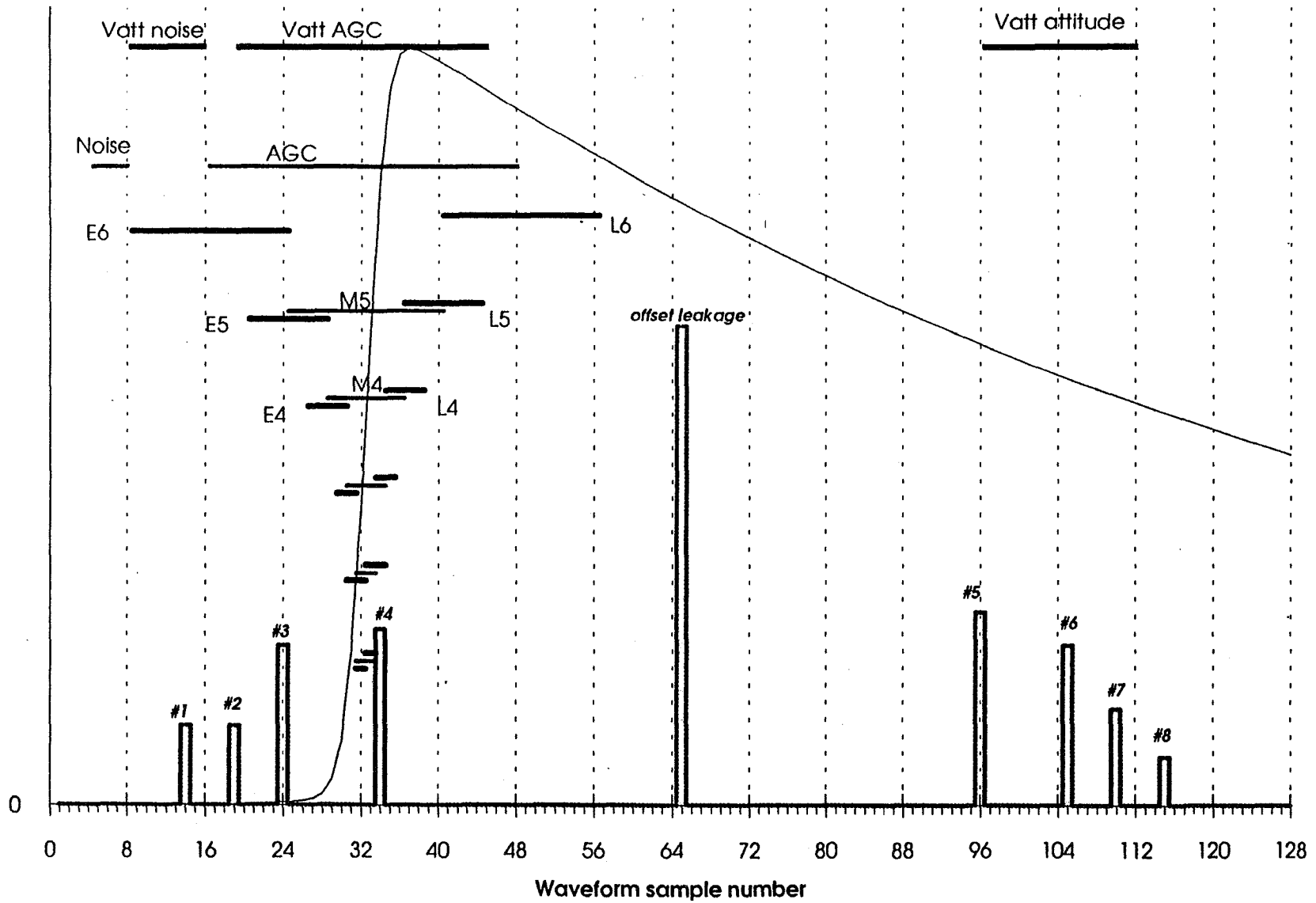
In the investigations of other anomalies in TOPEX waveforms, various low level "spikes" were found in some waveform samples. These were often referred to as leakage. The power of the leakage spikes is independent of receiver gain (AGC), and the location of these spikes in the waveform sample set moves with fine height value. These effects probably enter the altimeter just at or just after the A/D conversion of the I and Q video output of the receiver. Figure 6.2.3.4 sketches the location of these spikes and their relative magnitudes for the fine-height word at the middle of its range (i.e., at the highest height word value for positive height rate, or the lowest height word value for negative height rate). All these leakage effects are small, about 200 counts or less, compared to the AGC value of 4096 counts and the waveform peak of the order of 8000 counts. Figure 6.2.3.4 also indicates the locations of various gates (where gate designates the average value of a specified range of waveform samples) including the early (E), middle (M), and late (L) gates used in tracking. E5, M5, L5 and E4, M4, L4 are the track gates for gate index values 5 and 4, and are indicated by labeled horizontal lines in the figure. The E, M, L gates for gate index values 3, 2, and 1 are shown but labels are not attached in order avoid an excessively cluttered figure.

One way to see the leakages more clearly in the altimeter was to examine Standby Mode waveforms in a transmitter test mode. In Standby, the 64 telemetry samples contain the center 64 (of the total 128) uncompressed waveforms. In the transmitter test mode the height is continuously incremented, either up or down, so the fine height word will sweep over either the upper or the lower half of its range depending on the sign of the height rate. Only the leakages affecting track-mode telemetry samples 25-56 can be seen in this test mode, and the test must be run in two halves, each with a different sign of height rate, to see the full range over which a leakage spike will move.

Another way to see the leakage spikes has been to run a special Calibration Mode 2 test with the AGC attenuator set at a high level (approximately 25 dB) to attenuate the normal noise signal far enough that the small leakage spikes can be seen more clearly. The difficulty with this test mode is that some of the non-central leakages are made more difficult to see by the factor-of-2 or factor-of-4 compression in the telemetry samples.

Because the leakage spikes are so small and these test modes so relatively noisy, the interpretation of the test data is highly subjective. The characterizations of leakage spike amplitude could be in error by as much as 50%, and the waveform sample locations could be incorrect by perhaps one sample. Table 6.2.3.4 lists the leakage spikes by designation, amplitude, and sample number location.

Figure 6.2.3.4. TOPEX Altimeter Gates and Center Locations of Leakage Spikes



Spike Designation	Amplitude, Counts	Waveform Sample # Range	TLM Sample # Range (track mode)
Offset Leakage	300	61-69	47-49
1	50	10-18	6-10
2	50	15-23	8-15
3	100	20-28	12-20
4	110	30-38	22-30
5	120	92-100	55-57
6	100	102-109	58-60
7	60	106-114	59-61
8	30	111-119	60-62

Table 6.2.3.4 Characterization of TOPEX Waveform Leakage Spikes

Offset leakage spike

There is leakage in the center of the waveform sample set, at sample 65 ± 4 depending on fine height word, which is designated as offset leakage in Table 6.2.3.4. This offset leakage is difficult to separate from the zero-frequency leakage (from truncation in digital FFT), but the offset leakage does move with fine-height word (unlike the zero-frequency leakage which does not). This offset leakage is believed to result from a slight offset in biasing of the A/D converter, based on some tests with existing engineering model and breadboard hardware. The engineering model DFB had the offset leakage whose behavior was approximately the same as the flight unit. The breadboard DFB did not originally exhibit the offset leakage but the offset leakage could be made to appear by changing the value of the biasing resistor on the A/D converter in the I channel. The resistor was adjusted until the breadboard DFB offset leakage matched that of the engineering model; this work indicates that the flight unit offset leakage is about 3/8 of the least significant bit in the I-channel A/D.

Other (numbered) leakage spikes

In the flight unit Side A there are several other spikes which are of the order of 100 counts or less, and these are designated by numbers 1 to 8 in Table 6.2.3.4. These spikes are probably caused by low level signal leakage into the receiver chain after the AGC adjustments but before the actual FFT process. There is no AGC effect on their amplitude above noise, but there does seem to be some temperature variation of their amplitudes. This temperature variation was found by reexamining some of the test data. The positions of most of these leakage spikes can be correlated with harmonics of the low voltage power supply switching frequencies, specifically 300, 400, 450, and 500 kHz; the power supply is known to generate these frequencies, based on unit EMF test. Notice that spikes # 4 and #5 are approximately equidistant

from the zero-frequency sample at the center of the 128 waveform sample set. Similarly spikes #3 and #6, #2 and #7, and #1 and #8 are also pairwise equidistant about the center. These particular (numbered) leakage spikes are present only in the flight unit Side A, but were only discovered and investigated after TOPEX launch. Side A had been chosen as the prime altimeter because of minor concerns on reliability of some components (*i.e.*, switches and UCFM).

The most worrisome of the numbered leakage spikes in Table 6.2.3.4 is #4 because of its position relative to the TOPEX tracking gates; this can be seen in Figure 6.2.3.4. All the spikes in Figure 6.2.3.4 will move by ± 4 samples relative to their plotted center positions, depending on the value of the fine height word, and this moves spike #4 in and out of the track gates. Some simulation studies at both JHU/APL and WFF indicate that the tracking errors arising from leakage spike #4 should generally be 1 centimeter or less for most operating conditions of general interest, but further study is needed.

6.3 Correction/Compensation for Waveform Effects

6.3.1 Waveform Samples to Avoid

Because of the zero-leakage and the offset leakage effects, any ground-based waveform processing should avoid using waveform sample 65 and at least 4 samples to either side of 65. Waveform fitting at WFF has skipped (by assigning zero weights to) telemetry samples 45 - 50, corresponding to waveform samples 57 - 72. Likewise, to avoid effects of fall-off and wraparound, telemetry samples 1 - 4 and 61 - 64 (corresponding to waveform samples 1 - 8 and 113 - 128) have been avoided in all WFF waveform fitting work.

6.3.2 Multiplicative and Additive Factors

The several waveform effects can be partially compensated or corrected by sets of multiplicative and additive waveform factors. For each telemetry sample $T_{S,i}$ there is an additive adjustment A_i and a multiplicative adjustment G_i to produce a corrected (compressed) waveform $W_{C,i}$,

$$W_{C,i} = G_i \times (T_{S,i} + A_i),$$

for i from 1 to 64. The multiplicative adjustments, which are obtained from a combination of the Cal Mode 2 data and additional modeling, compensate for the sawteeth, zero-frequency leakage, plateau excess, and end fall-off.

The additive adjustments A_i compensate for the leakage effects but only in a way that averages over all possible fine height values. The spikes in Figure 6.2.3.4 are for the fine height at the middle of its entire range (*i.e.*, at the highest value in the lower

half or the lowest value of the upper half). Since the fine height value is not available for ground post-processing (the fine height value was added to the coarse height in the Engineering Units conversion early in the TOPEX ground processing flow, and is not available as a separate entity after that conversion step) so that the spikes have to be treated as a probabilistic smear over all their possible positions. Figure 6.3.2 shows the spikes of Figure 6.2.3.4 as smeared over ± 4 samples. It would be possible to halve the width of the smear by treating data differently for increasing than for decreasing height rate, but that has not been done to date.

Table 6.3.2 gives the TOPEX Ku and C-320 multiplicative and additive correction factors which are currently in the routine TOPEX ground processing at JPL. The additive factors are based on somewhat earlier leakage analyses than Figure 6.2.3.4 and 6.3.2 and Table 6.2.3.4. Specifically, spikes #7 and #8 were not used, and the two offset leakage spikes were used. These differences should be unimportant, because the offset leakage is not in any of the gates, and spike #7 contributes only a very small amount to the Vatt attitude gate used in attitude corrections in the ground-based processing. The Table 6.3.2 factors are currently used in various waveform fitting analyses at WFF. Although these factors are given for all the telemetry samples, the samples # 1 - 4, 45-50, and 61 - 64 have been given zero weighting in all WFF waveform fitting or analyses.

6.3.3 Example

Figure 6.3.3 shows a typical input waveform (from scaled telemetry samples), the corrected waveform after application of the multiplicative and additive factors, and the waveform which is least-squares fitted to the corrected waveform. In this figure there is some fall-off and wraparound still visible, and there is still some extra energy in the vicinity of equivalent waveform sample 64. The waveform in this figure is the same 5-second average already shown earlier in Figure 6.2.2.2a. From waveform fitting to the corrected waveform data in Figure 6.3.3, the SWH estimate is 1.41 meters, and the attitude estimate is 0.12 degrees.

6.4 Waveform Effects Status

During the first half year of TOPEX operation (the evaluation period) approximately a half dozen new sets of range (and AGC and SWH) correction constants for the TOPEX data ground-processing system were generated through simulation procedures by the Wallops TOPEX team; each simulation set incorporated then-current knowledge of the various waveform features. Our waveform fitting results, after the final set of constants was produced in May 1993, do seem to confirm the adequacy of that set of processing constants for the range corrections for effects of significant waveheight and attitude. Some small improvements could conceivably be made, based on more extensive analyses, but we see no compelling argument for changes in the ground processing constants.

Figure 6.3.2. TOPEX Allimeter Gates and Smeared Locations of Leakage

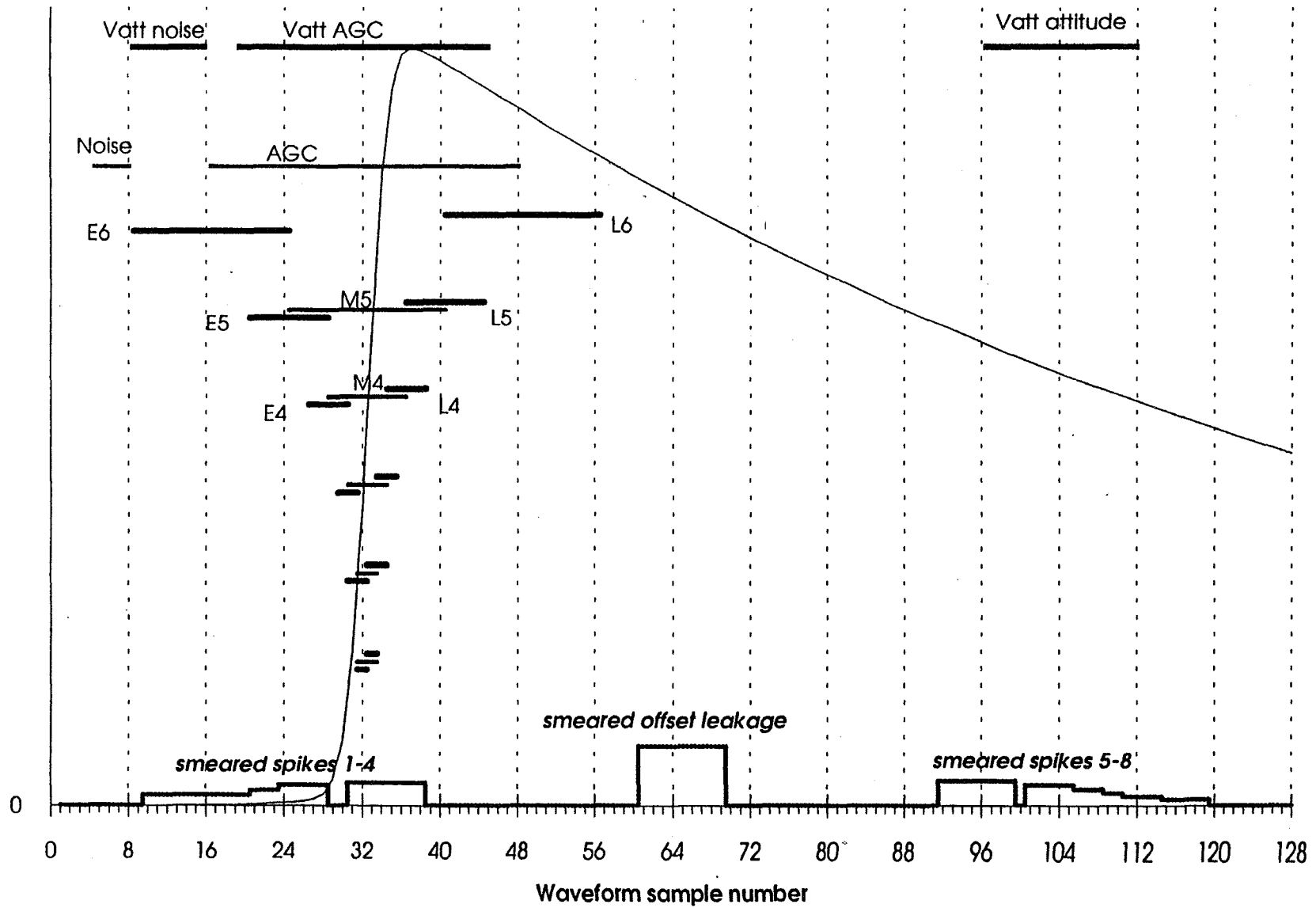
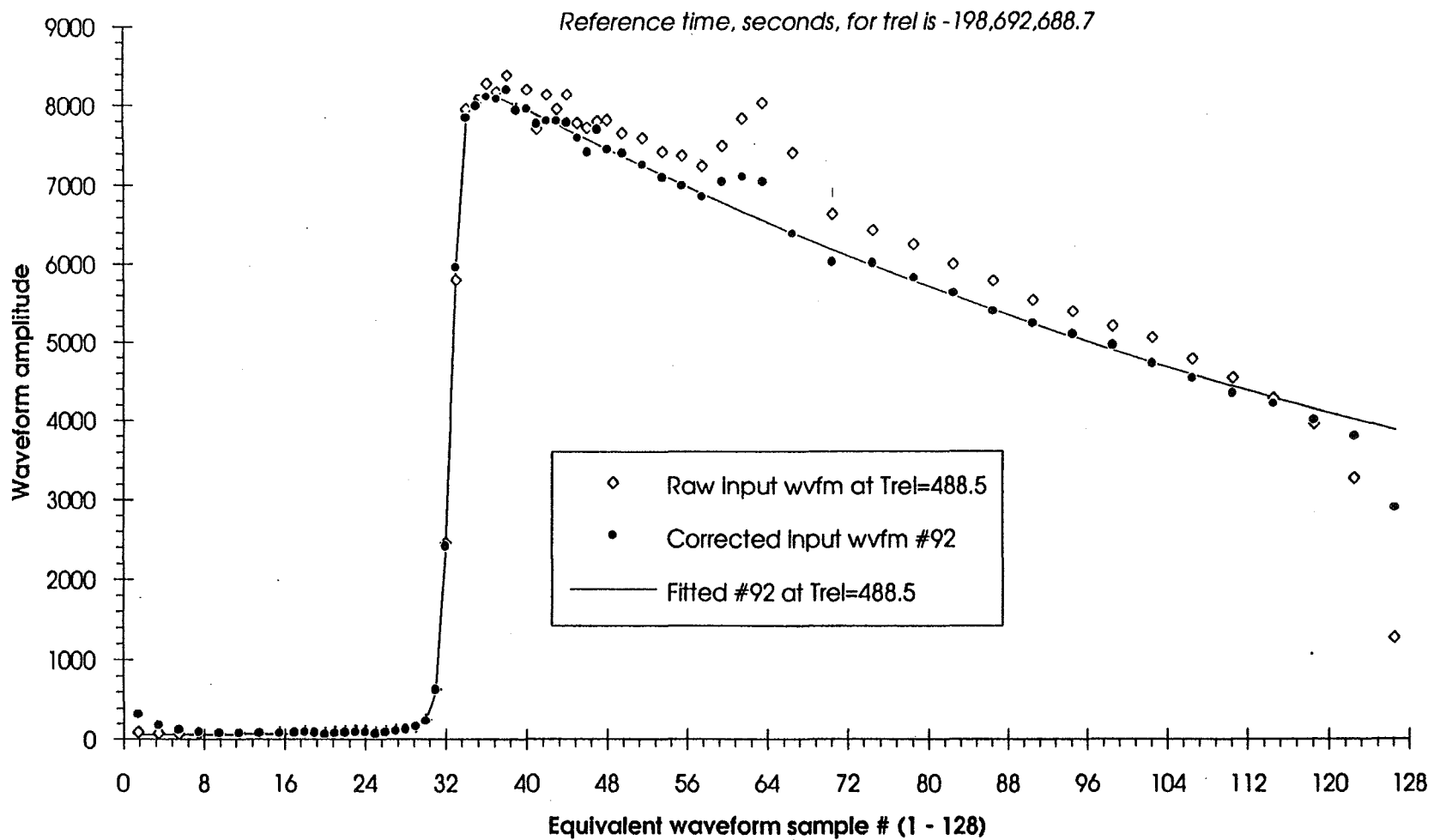


Table 6.3.2. TOPEX Waveform Multiplicative and Additive Correction Factors

Telemetry sample #	Multiplicative factors	Ku additive factors	C additive factors	Telemetry sample #	Multiplicative factors	Ku additive factors	C additive factors
1	3.355	0	0	33	1.007	0	0
2	2.327	0	0	34	0.958	0	0
3	1.638	0	0	35	0.981	0	0
4	1.178	0	0	36	0.956	0	0
5	1.120	-1.39	-0.35	37	0.976	0	0
6	1.083	-2.78	-0.69	38	0.960	0	0
7	1.065	-2.78	-0.69	39	0.986	0	0
8	1.047	-9.44	-2.36	40	0.953	0	0
9	1.070	-9.44	-2.36	41	0.966	0	0
10	1.025	-9.44	-2.36	42	0.955	0	0
11	1.041	-6.67	-1.67	43	0.955	0	0
12	1.025	-17.78	-4.44	44	0.947	0	0
13	1.036	-17.78	-4.44	45	0.945	0	0
14	1.012	-17.78	-4.44	46	0.941	-15.56	-3.89
15	1.029	-17.78	-4.44	47	0.913	-57.78	-14.44
16	1.009	-11.11	-2.78	48	0.882	-57.78	-14.44
17	1.037	-11.11	-2.78	49	0.868	-57.78	-14.44
18	0.999	-11.11	-2.78	50	0.909	-6.67	-1.67
19	1.023	-11.11	-2.78	51	0.934	0	0
20	1.002	-11.11	-2.78	52	0.932	0	0
21	1.006	0	0	53	0.937	0	0
22	0.992	-11.11	-2.78	54	0.932	0	0
23	1.005	-11.11	-2.78	55	0.945	-2.78	-0.69
24	0.987	-11.11	-2.78	56	0.948	-11.11	-2.78
25	1.027	-11.11	-2.78	57	0.954	-11.11	-2.78
26	0.987	-11.11	-2.78	58	0.936	-11.11	-2.78
27	0.997	-11.11	-2.78	59	0.949	-11.11	-2.78
28	0.981	-11.11	-2.78	60	0.957	-2.78	-0.69
29	0.990	-11.11	-2.78	61	0.983	0	0
30	0.979	-11.11	-2.78	62	1.013	0	0
31	0.997	0	0	63	1.158	0	0
32	0.969	0	0	64	2.273	0	0

Figure 6.3.3. Comparison of Input, Corrected, and Fitted Ku Waveforms for 1993 Day 257
Data



Although it would have been desirable for the waveform features to be smaller, we do find by comparing CAL2 telemetry sample data for more than a year of TOPEX operation that the individual samples are stable to better than 1% of their maximum magnitude and therefore have met the original hardware specification for waveform sampling. Considerable clarification has been gained from various post-launch laboratory testing of engineering model components, but we stress the importance of further testing and understanding of waveform features for any future radar altimeters.

7.0 ENGINEERING MONITORS

7.1 Temperatures

The altimeter has 26 internal thermistors to monitor temperatures near key components. The specifications for the altimeter included the provision that the altimeter operate within temperature ranges of -10 degrees to +45 degrees Centigrade. The spacecraft was to maintain the baseplate temperatures between 0 and +35 degrees C, which it has done through February 1994.

Figure 7.1 comprises the temperature history plots for the 26 thermistors. The lowest temperatures occur after the altimeter has been in IDLE or OFF mode. The highest temperatures are observed to occur during periods of No Yaw Steering.

The minimum/maximum values for each of the thermistors during TRACK mode are summarized in Table 7.1. The temperature values are all within the specified temperature range and are within ranges predicted by the prelaunch spacecraft Hot and Cold balance tests. The thermal control systems of the altimeter and spacecraft appear to be performing very well.

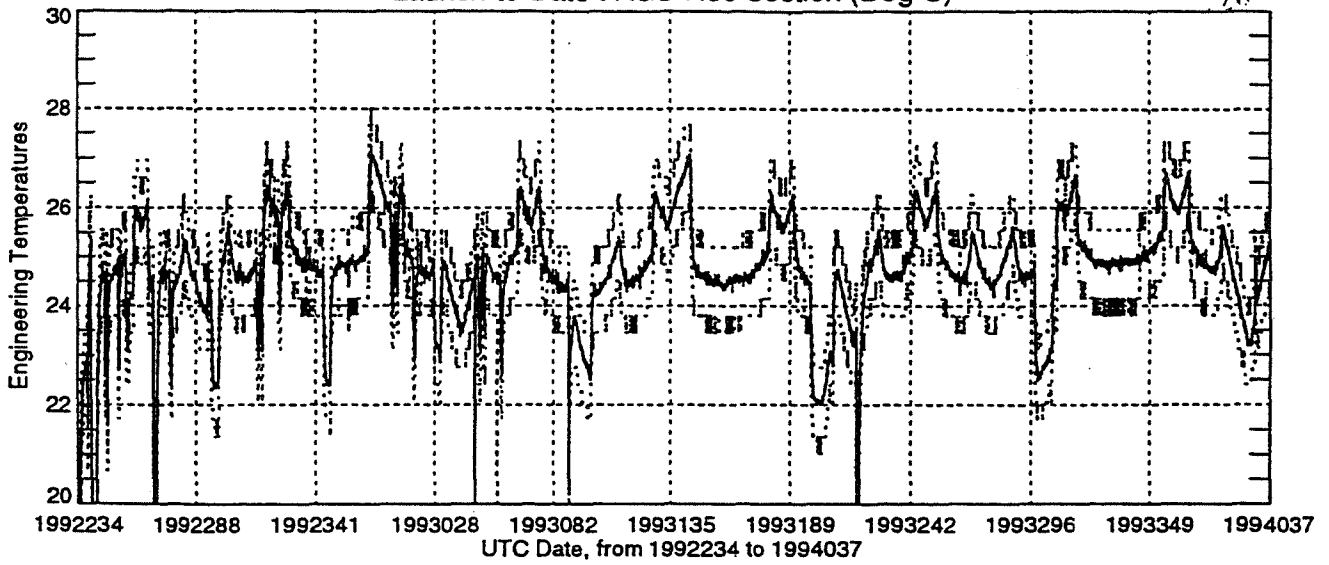
7.2 Voltages, Powers and Currents

The altimeter has 17 monitors for voltages, powers and currents; the time history of each of these monitors is shown in Figure 7.2. Table 7.2 lists the minimum/maximum on-orbit output for each of the 17 monitors during TRACK mode, and compares them with measured TRACK mode values just prior to launch. All are performing nominally and within specifications.

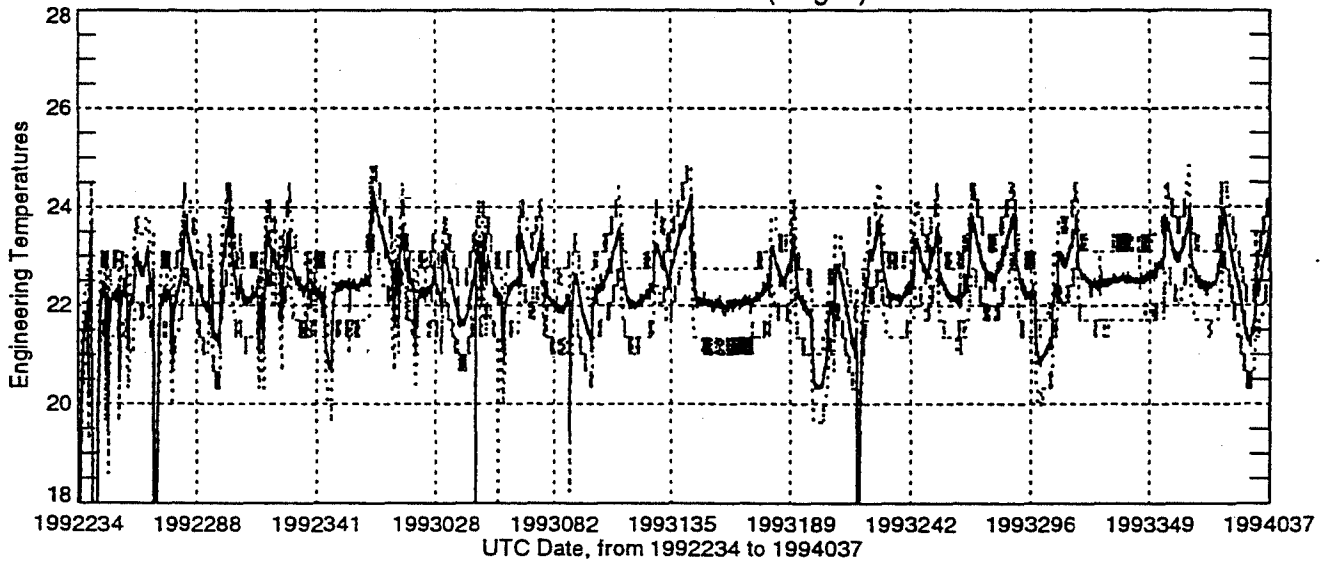
7.2.1 Low Voltage Power Supplies (LVPS)

The time history of the LVPS [+12 V, +28 V, +15 V, -15 V, +5 V(5%), +5 V(1%), -5.2 V and -6 V], as depicted in Figure 7.2, illustrates that these power supplies are steady with little deviation.

Launch-to-Date : AGC Rec Section (Deg C)



Launch-to-Date : SSU (Deg C)



Launch-to-Date : KU MTU IF Preamp (Deg C)

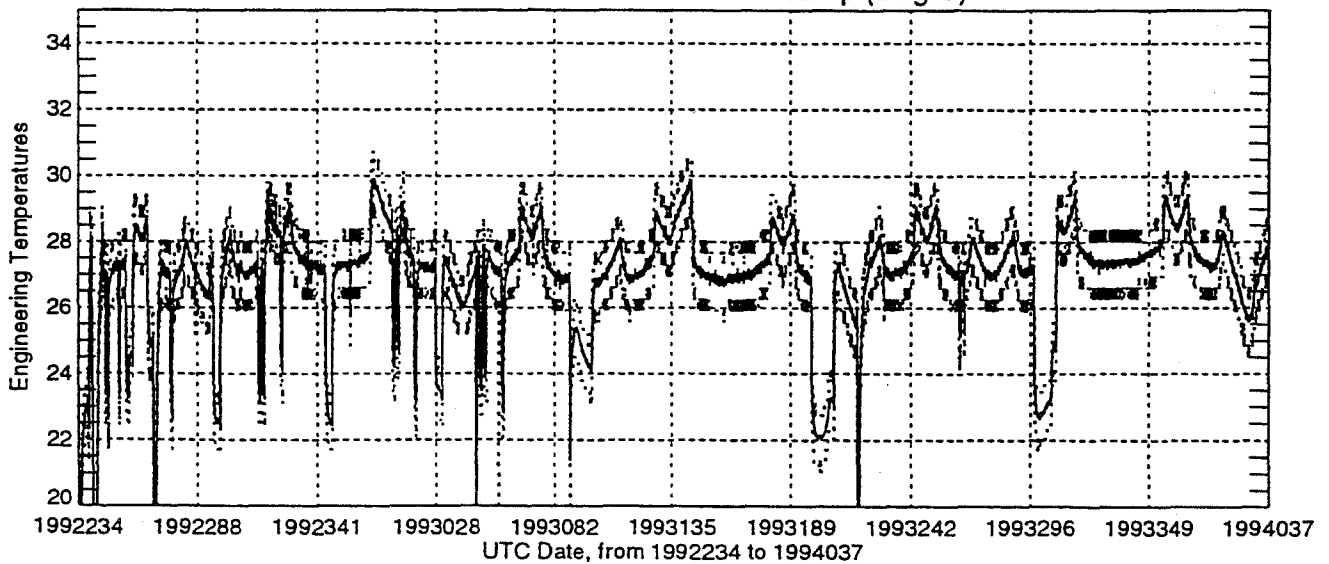
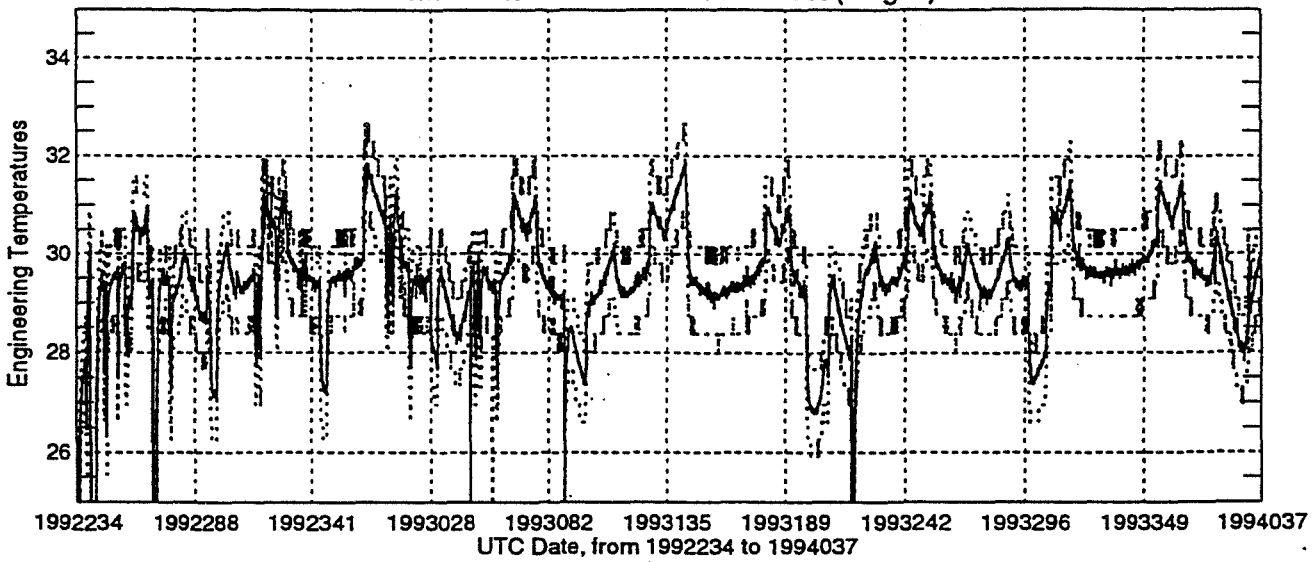
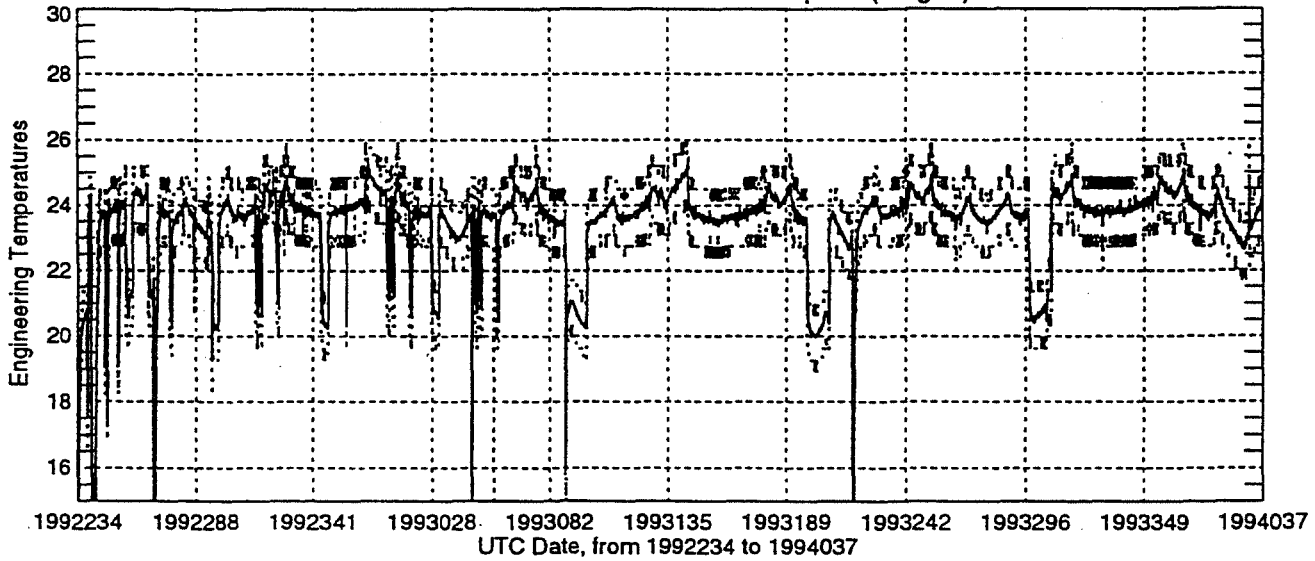


Figure 7.1 Temperature History Plots



Launch-to-Date : TWTA EPC Temp #1 (Deg C)



Launch-to-Date : C MTU Cal Atten (Deg C)

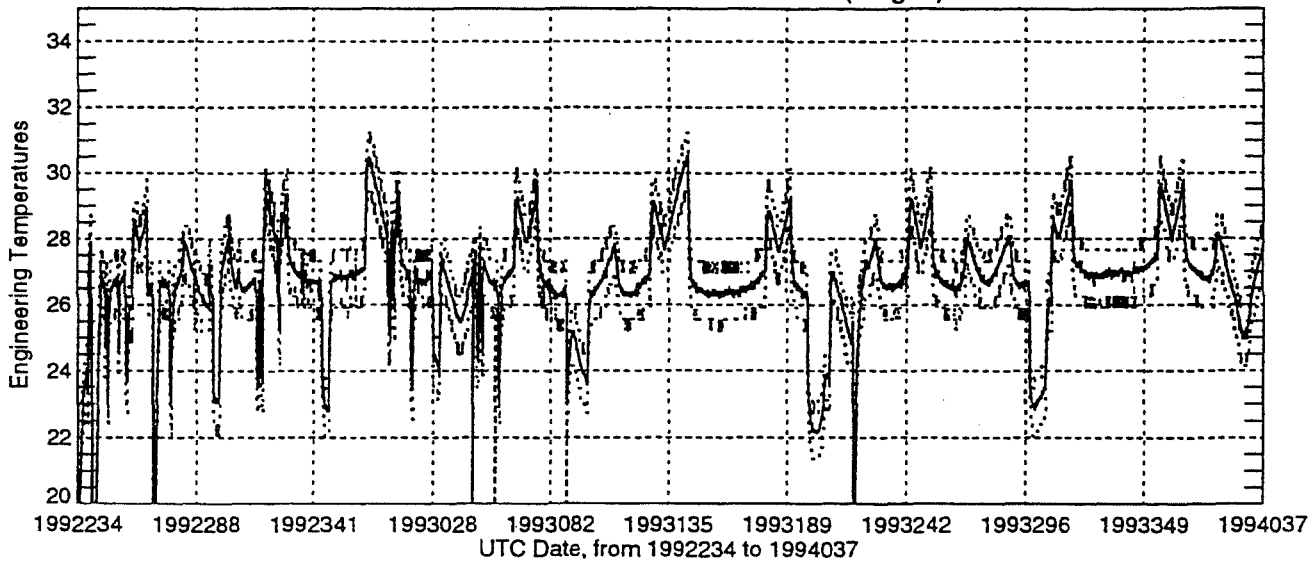


Figure 7.1 Temperature History Plots (cont.)

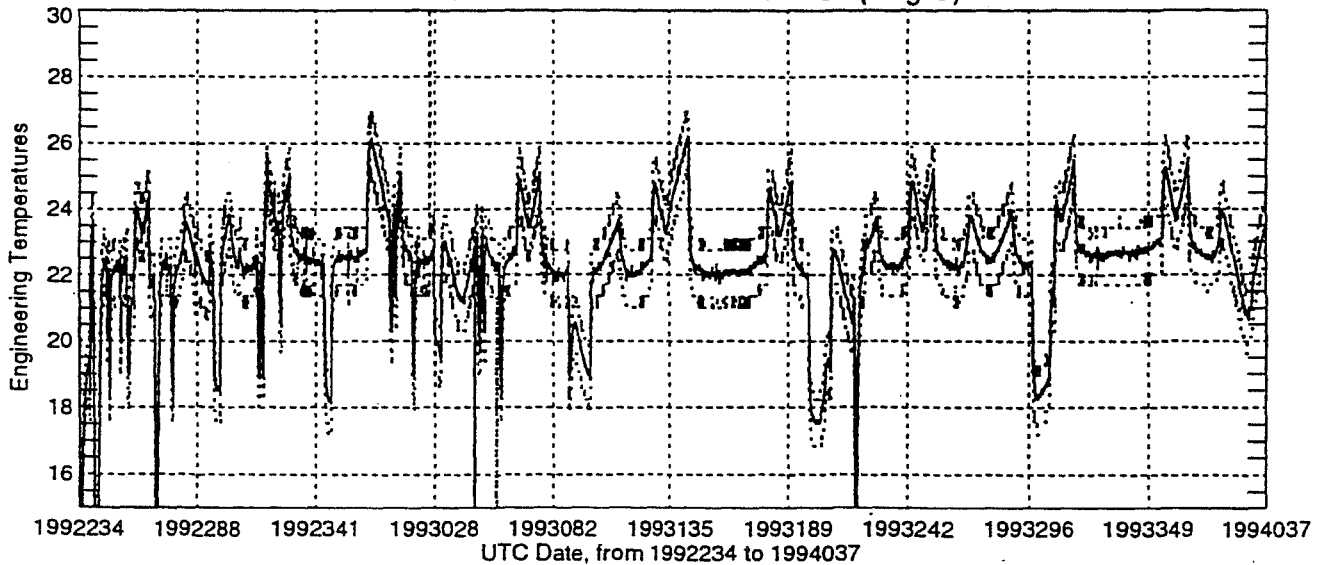
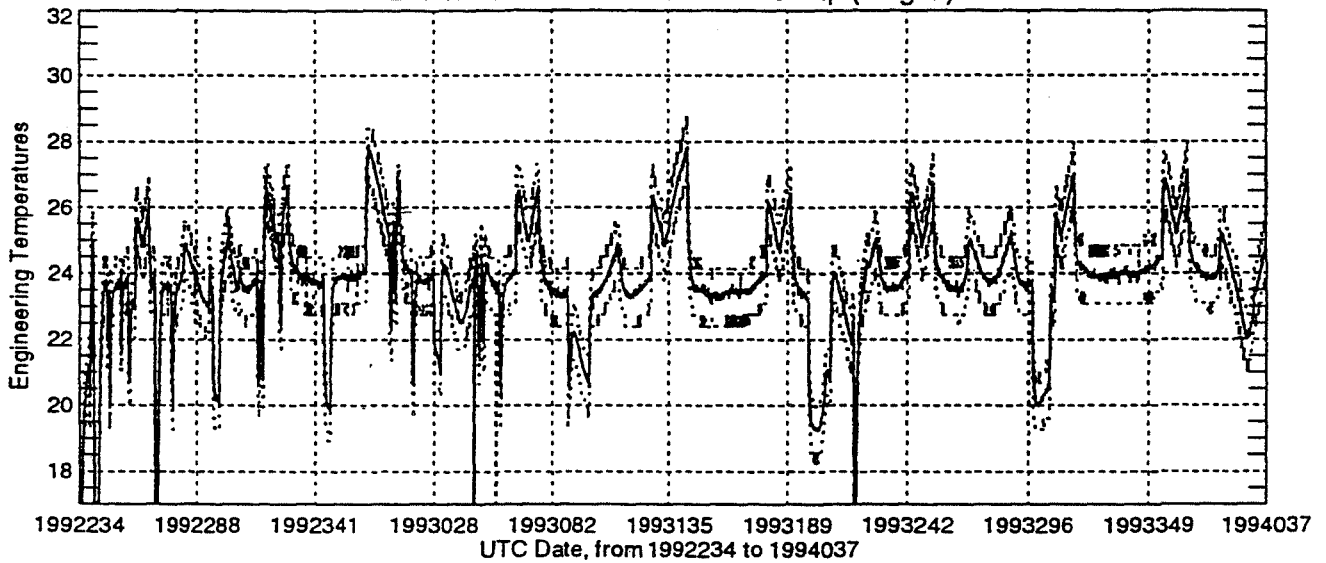
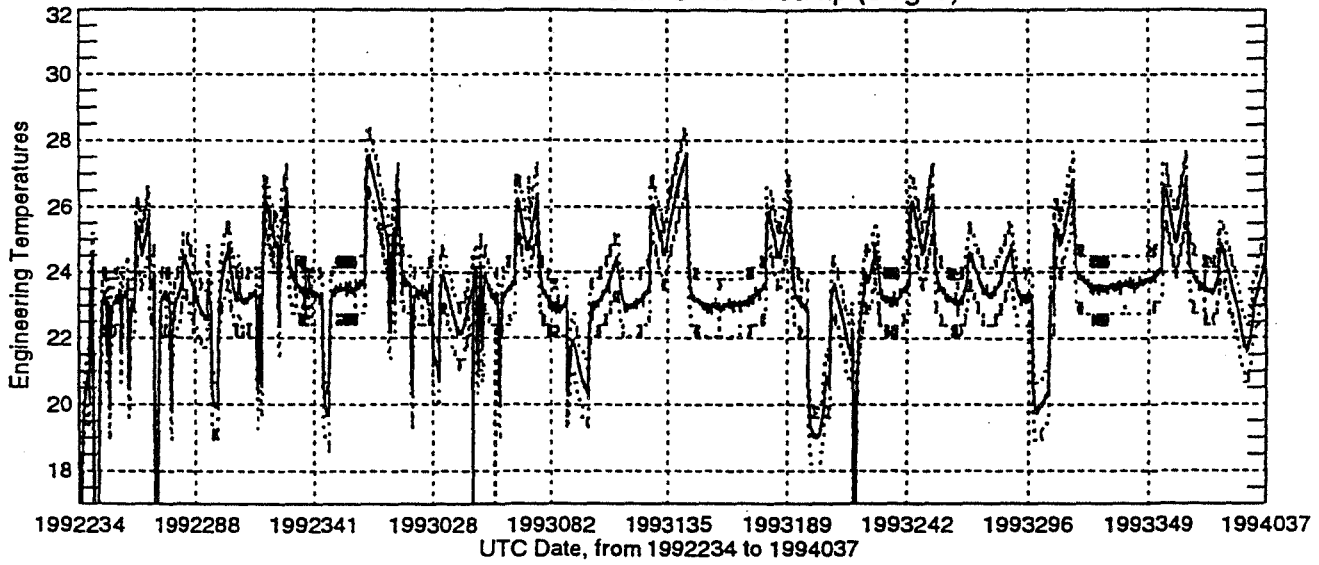


Figure 7.1 Temperature History Plots (cont.)

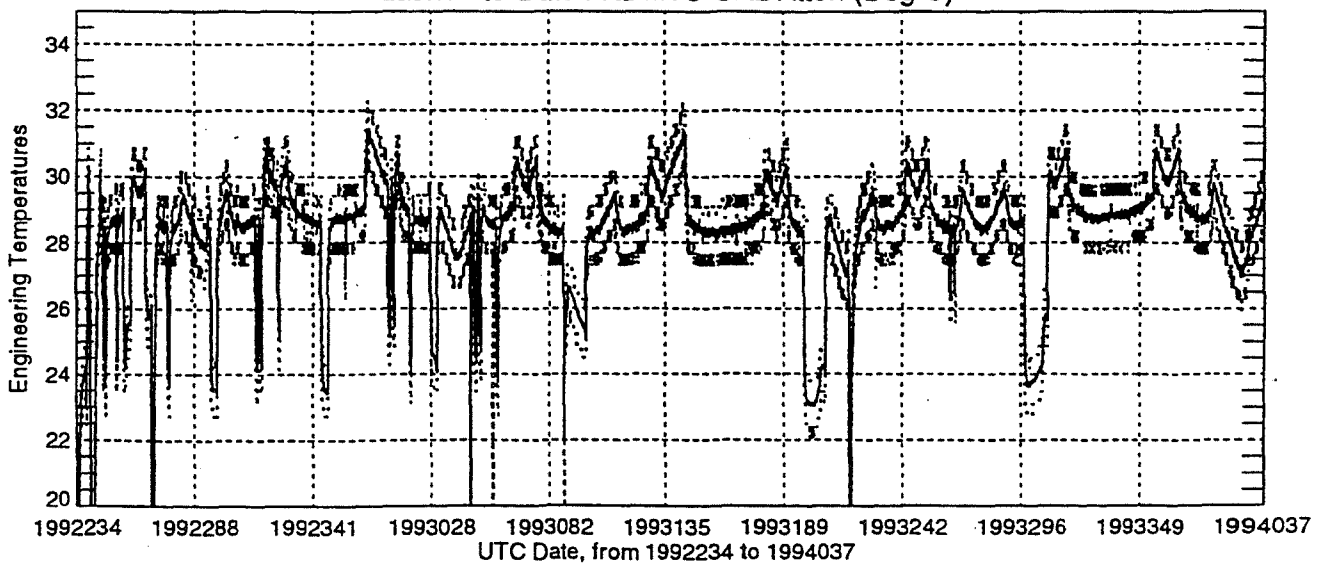
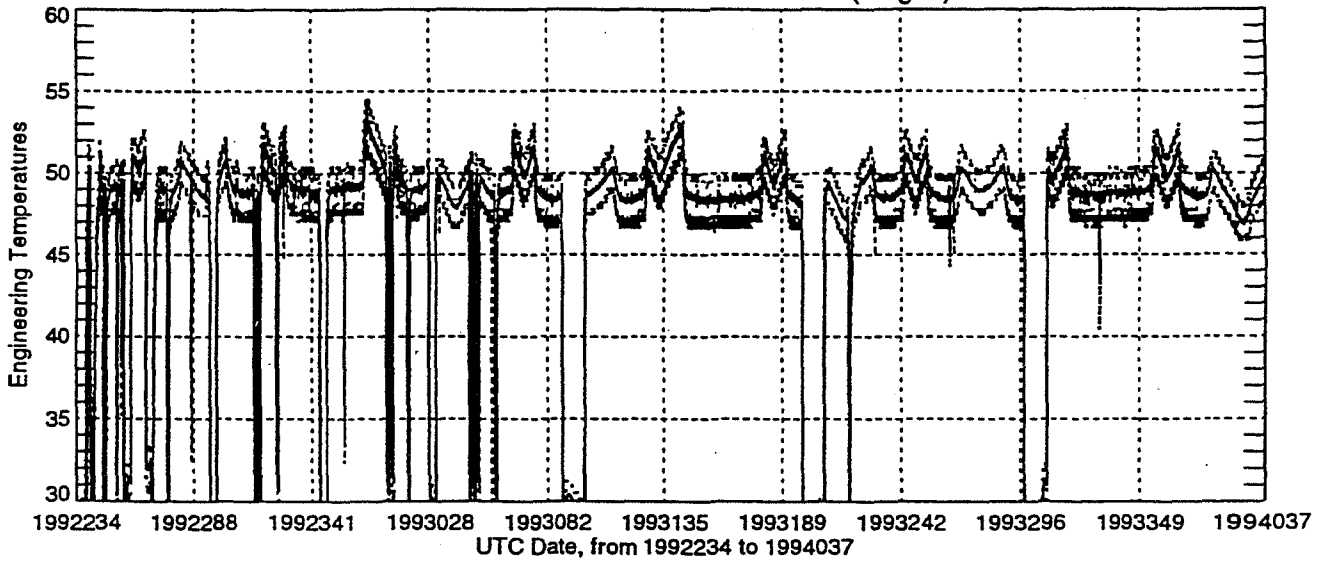
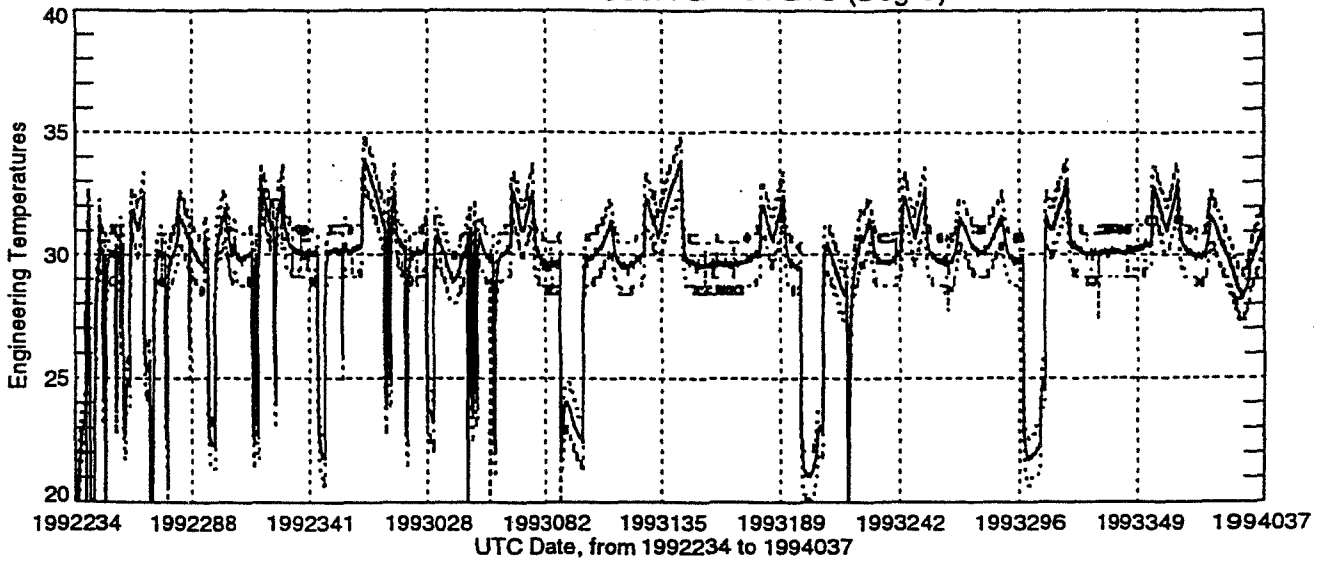


Figure 7.1 Temperature History Plots (cont.)

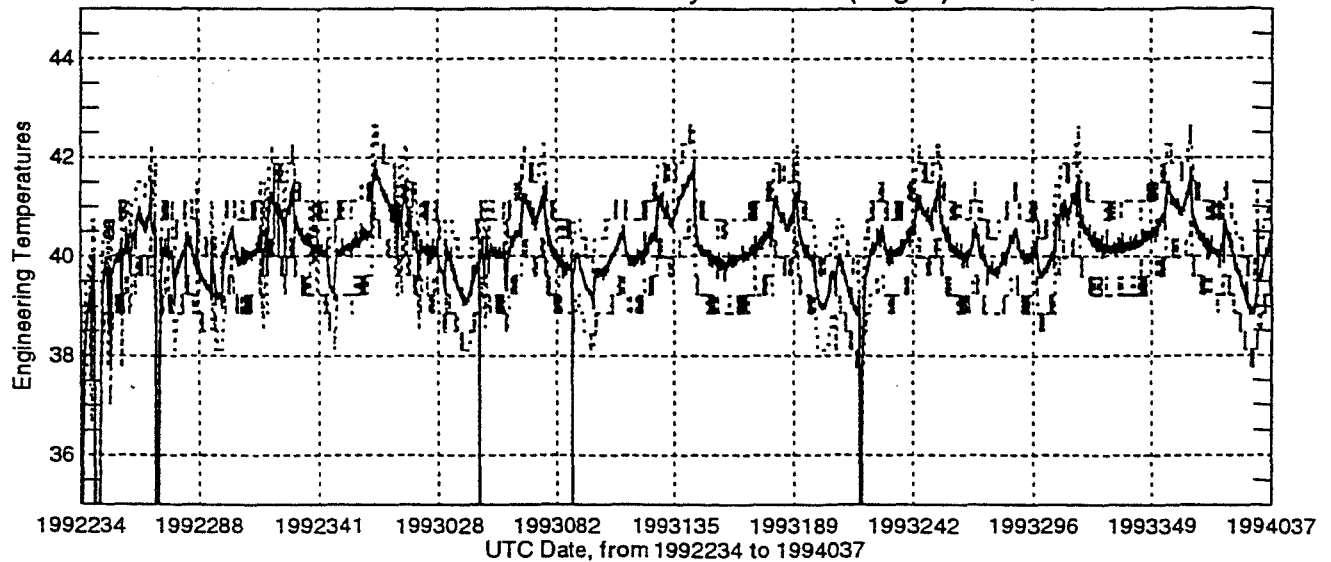
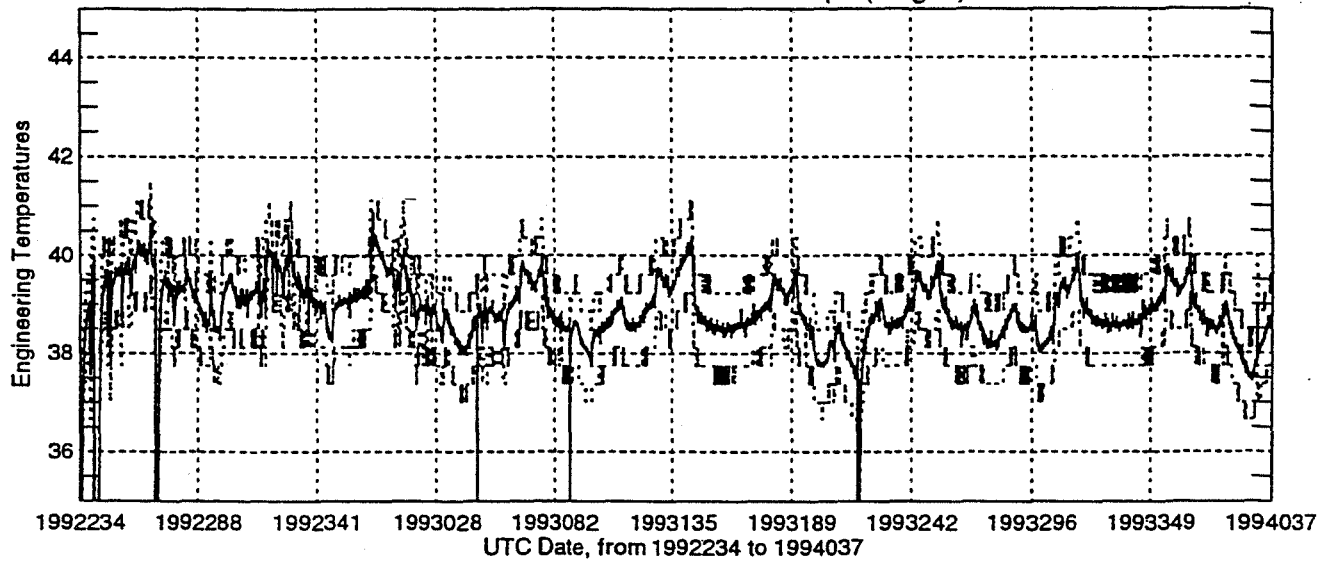
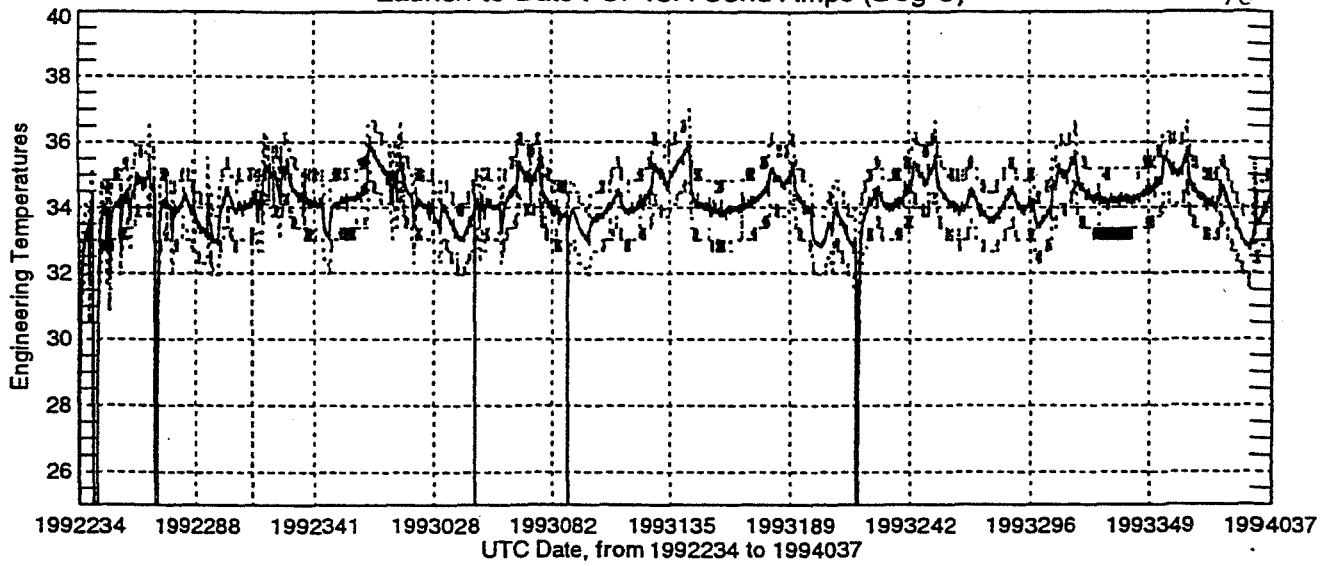


Figure 7.1 Temperature History Plots (cont.)

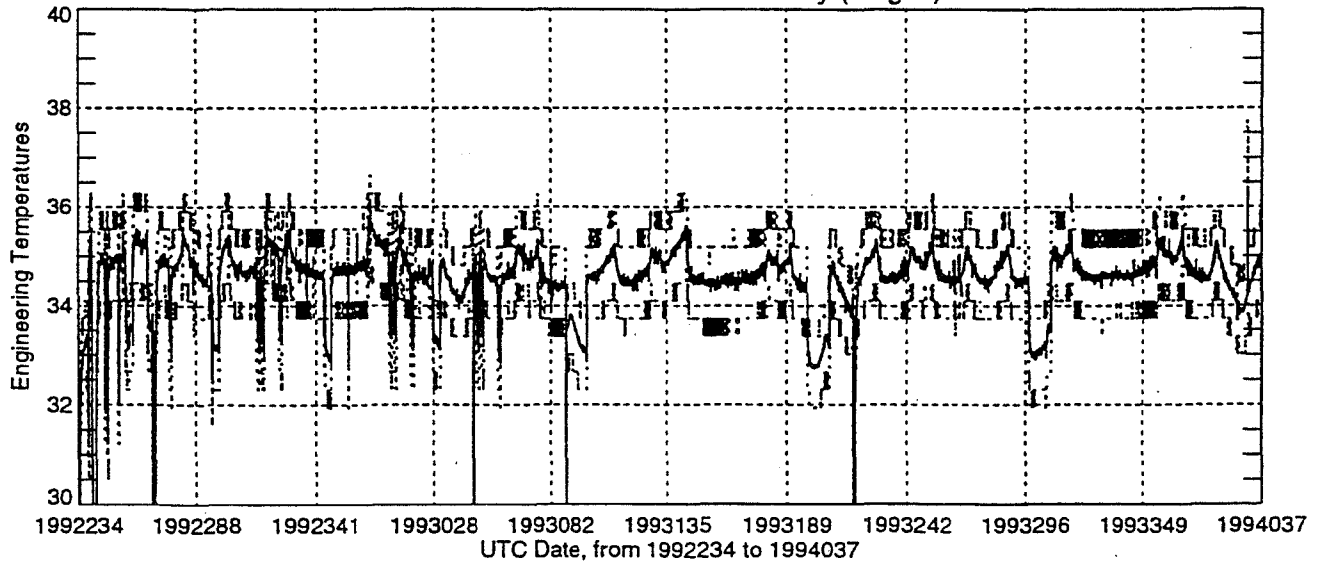
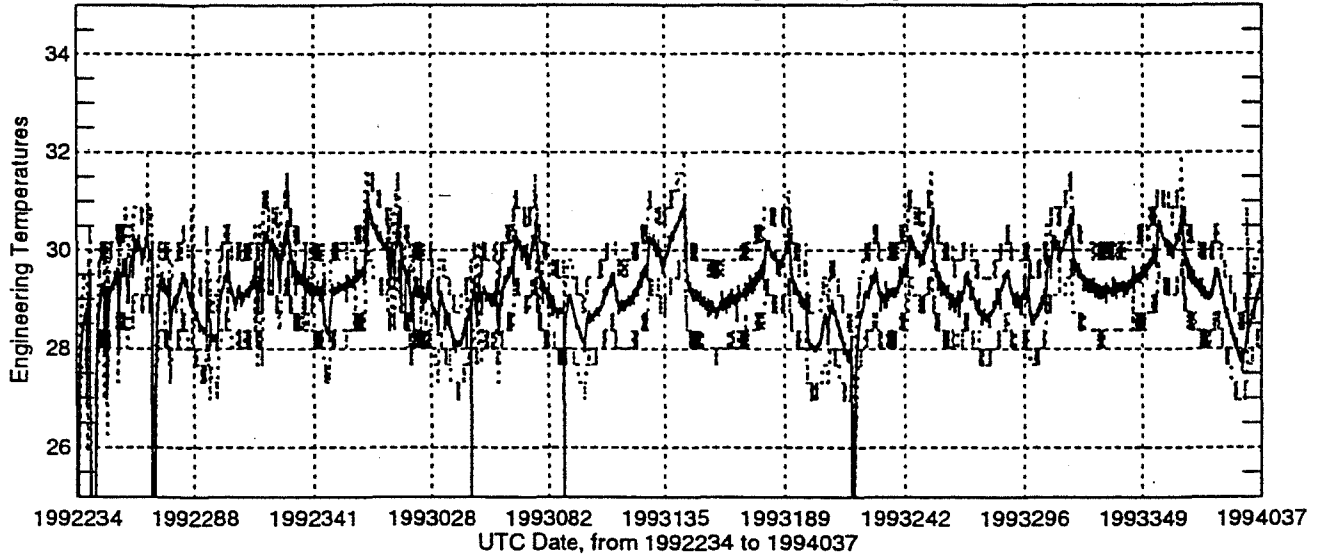
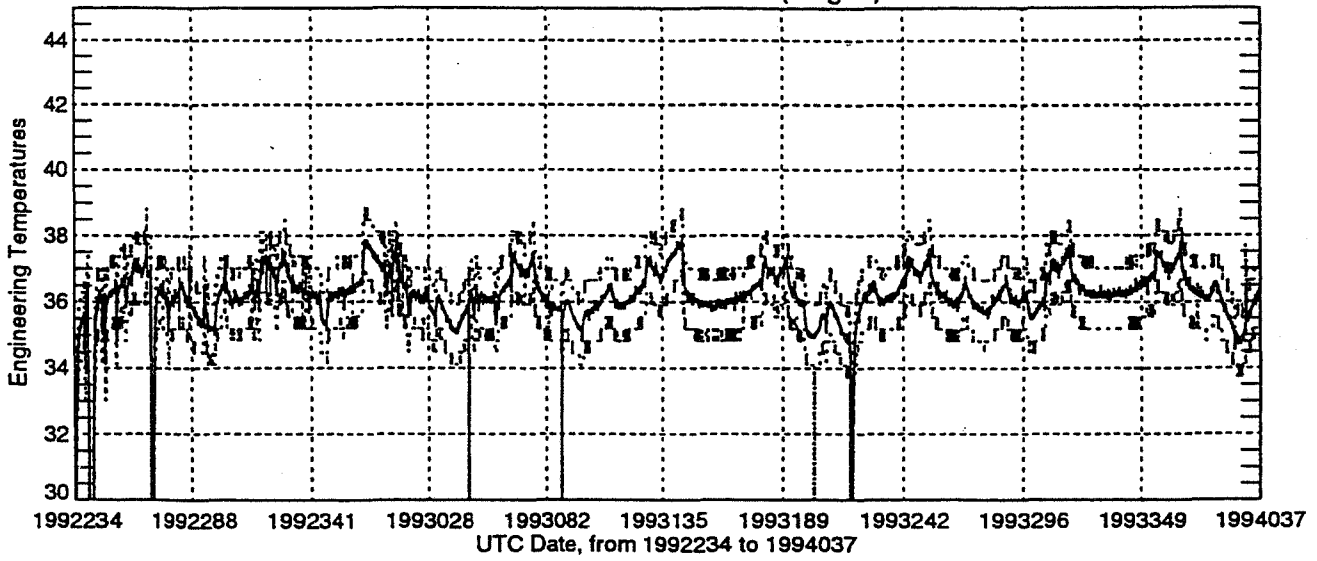
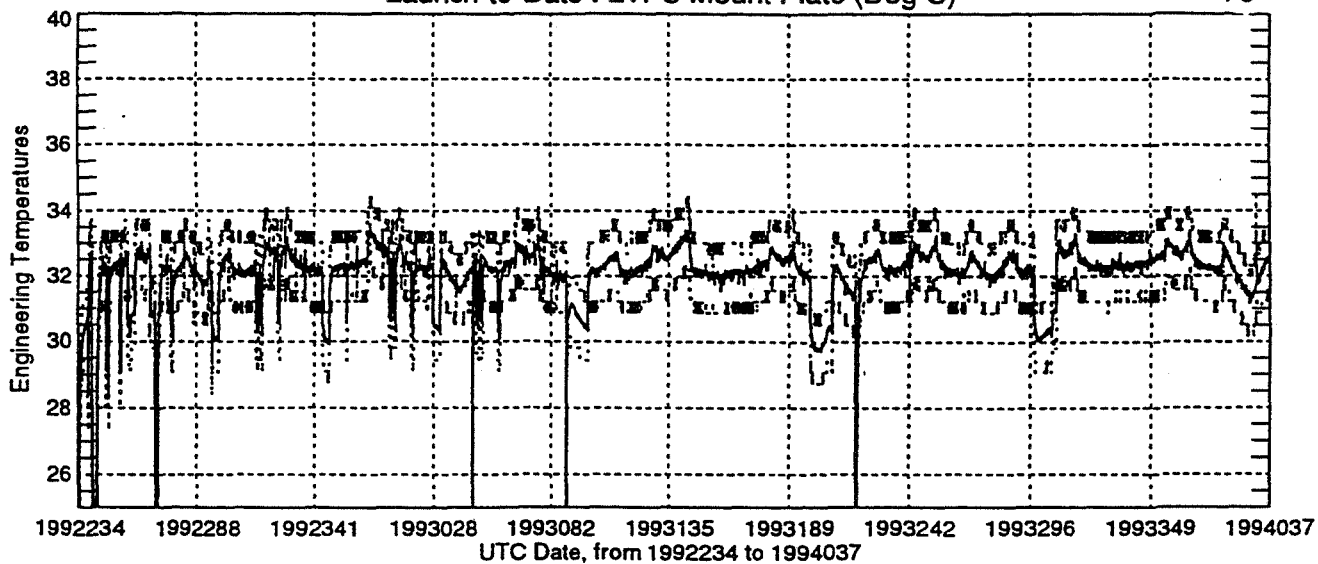


Figure 7.1 Temperature History Plots (cont.)



Launch-to-Date : LVPS Boost Reg (Deg C)

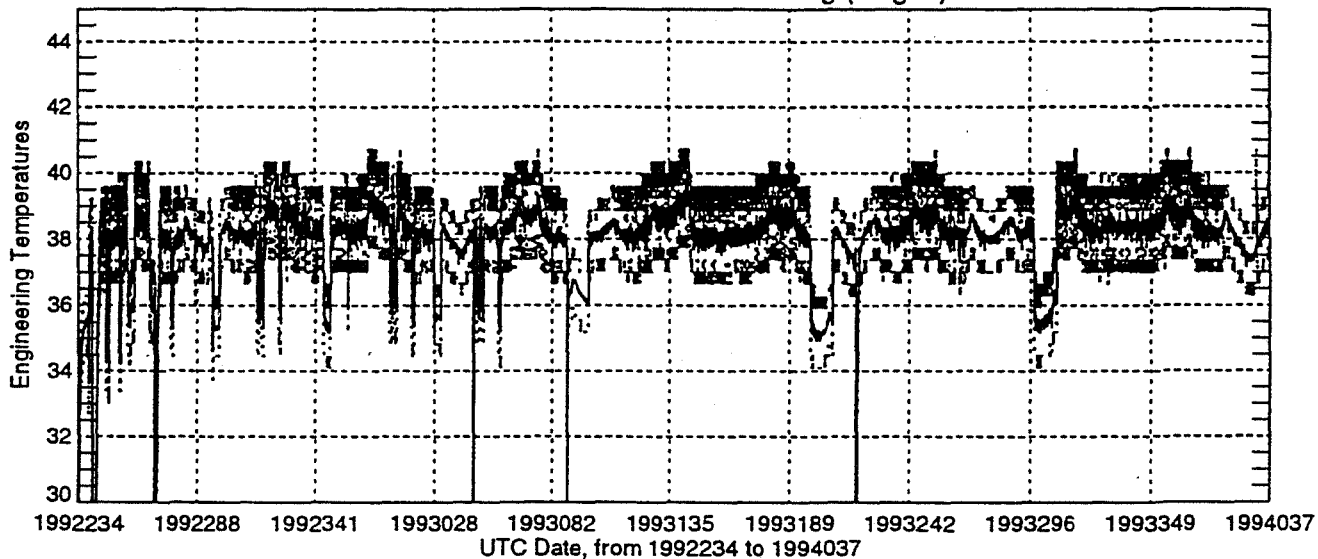


Figure 7.1 Temperature History Plots (cont.)

Thermistor Location	Minimum (°C)	Maximum (°C)
Receiver AGC Selection	23.5	28.0
SSU	20.4	24.8
Ku MTU IF Preamp	25.0	30.6
Receiver IQ Video Select	28.4	32.9
Ku TWTA EPC	22.0	26.0
C MTU Cal Attenuator	24.5	31.2
C MTU RF Preamp	22.0	28.4
C MTU IF Preamp	22.3	28.7
C MTU Transmit Power Monitor	21.0	27.0
C SSA GaAs FETS	28.3	34.9
C SSA Power Converter	45.9	54.6
Ku MTU Cal Attenuator	27.2	32.2
Ku MTU Transmit Power Monitor	24.0	29.6
UCFM	24.2	28.0
Ku MTU RF Preamp	26.5	31.3
Downconverter	29.5	34.9
SP DFB Butterfly Board	42.8	46.6
SP DFB Memory	38.8	43.0
SP ICA Condition Amps	32.5	37.2
SP ICA A/D Converter	37.0	41.2
SP Synchronizer	38.8	42.7
SP ATA	34.8	38.9
SP Housing	27.5	32.0
DCG Gate Array	33.2	37.8
LVPS Transformer Mounting Plate	31.0	34.4
LVPS Boost Regulator Assembly	36.2	40.7

**Table 7.1 Thermistor Minimum/Maximum Temperatures
During TRACK Mode**

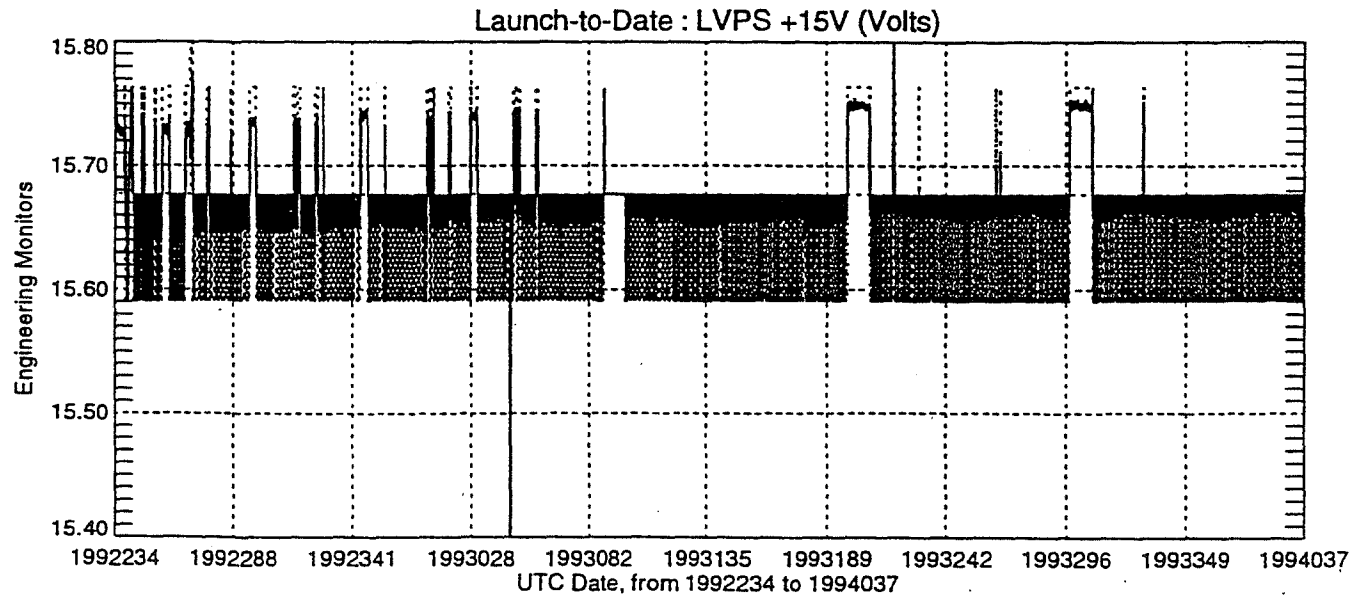
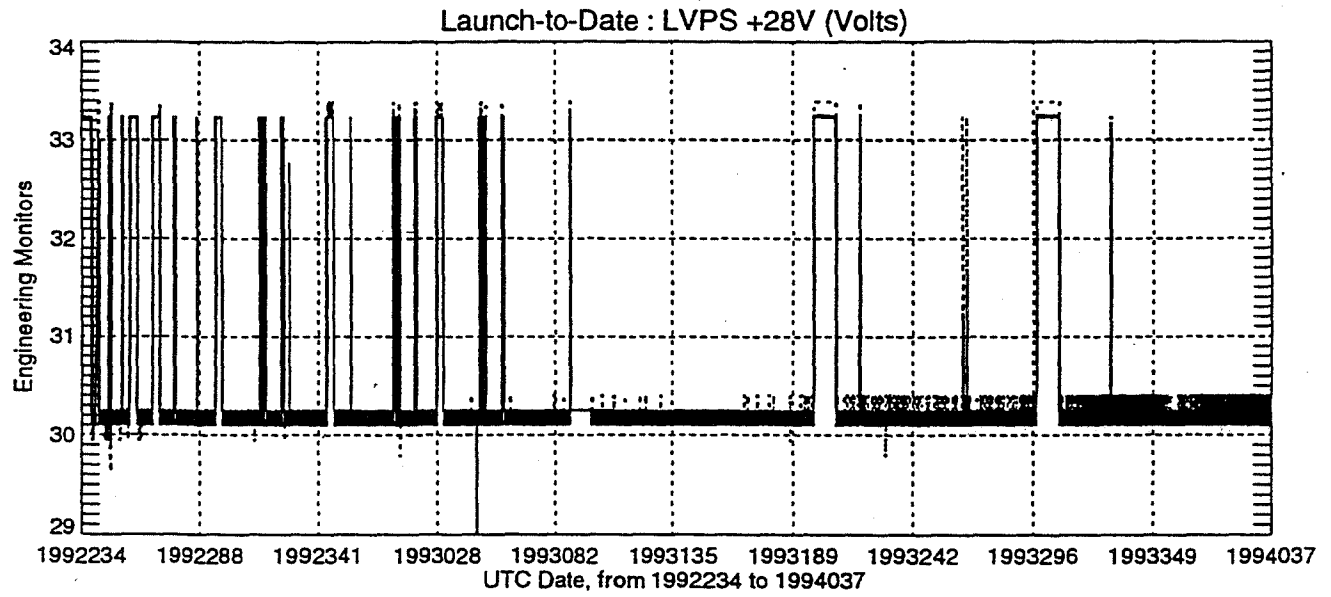
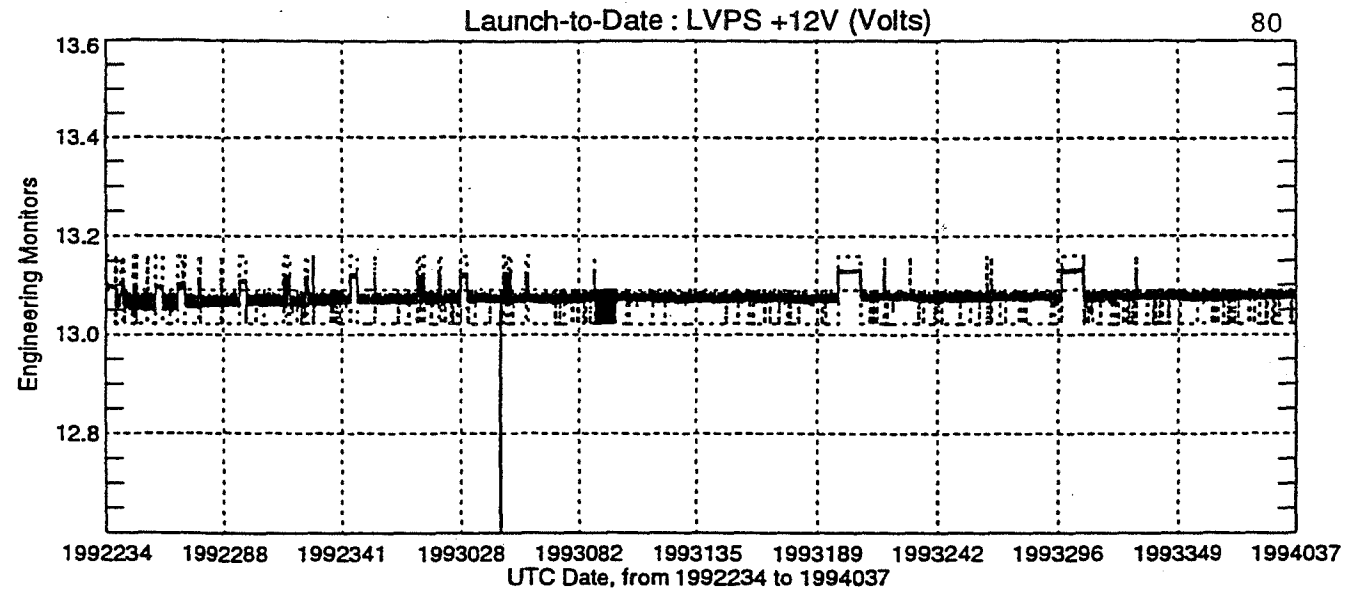
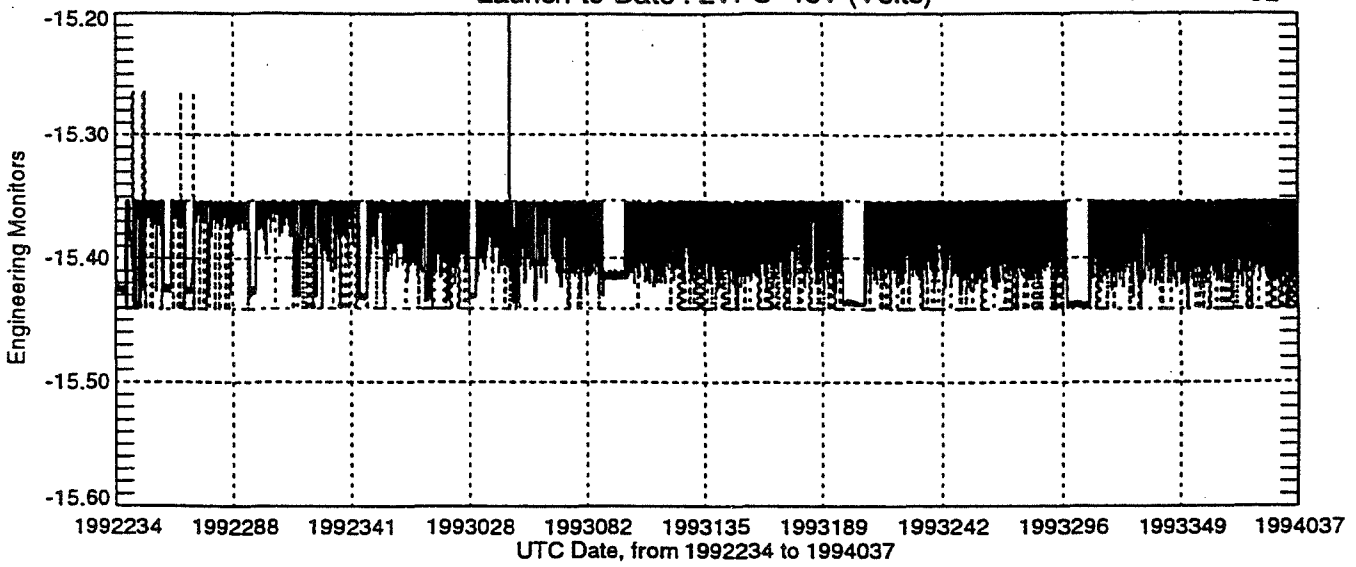
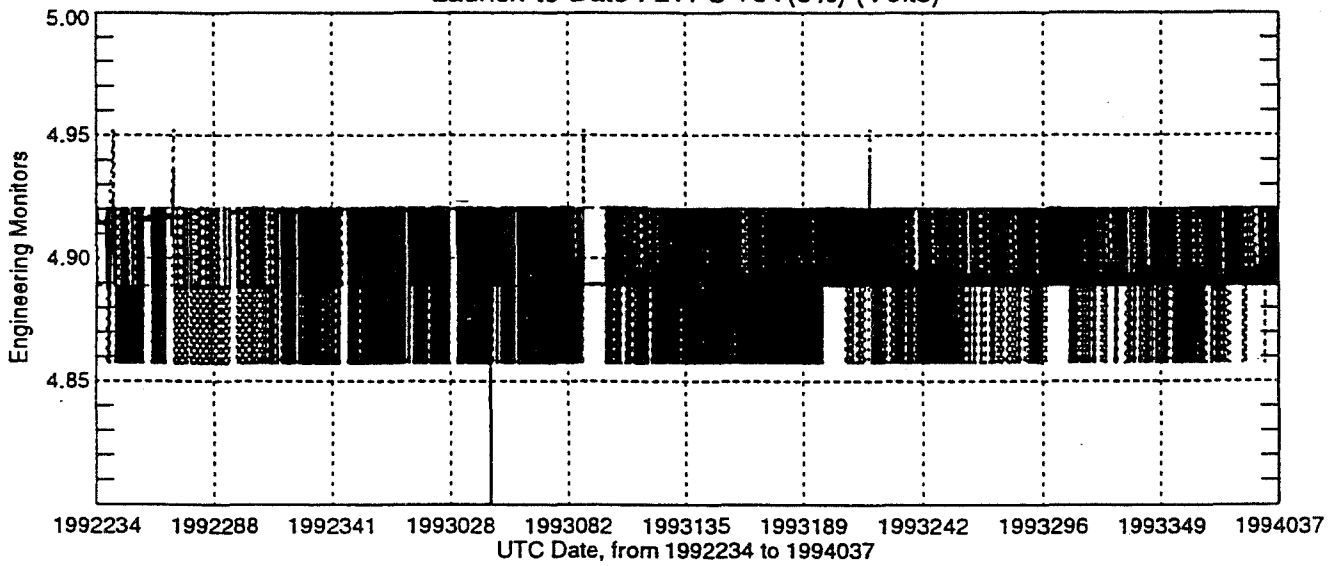


Figure 7.2 Monitor History Plots

Launch-to-Date : LVPS -15V (Volts)



Launch-to-Date : LVPS +5V(5%) (Volts)



Launch-to-Date : LVPS +5V(1%) (Volts)

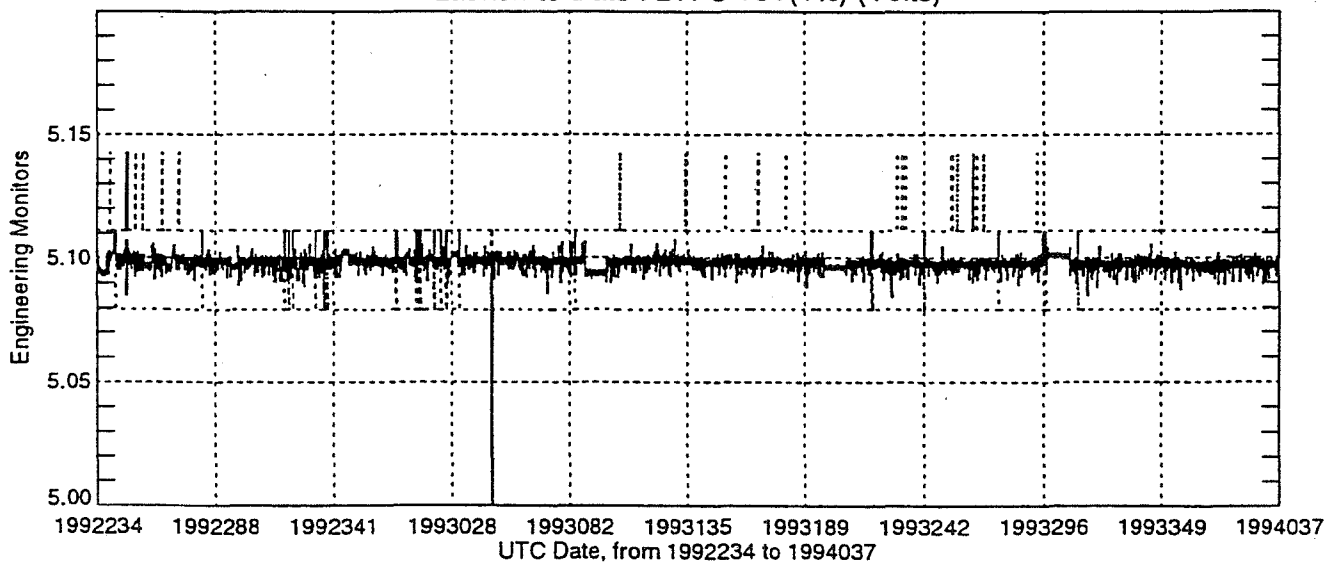


Figure 7.2 Monitor History Plots (cont.)

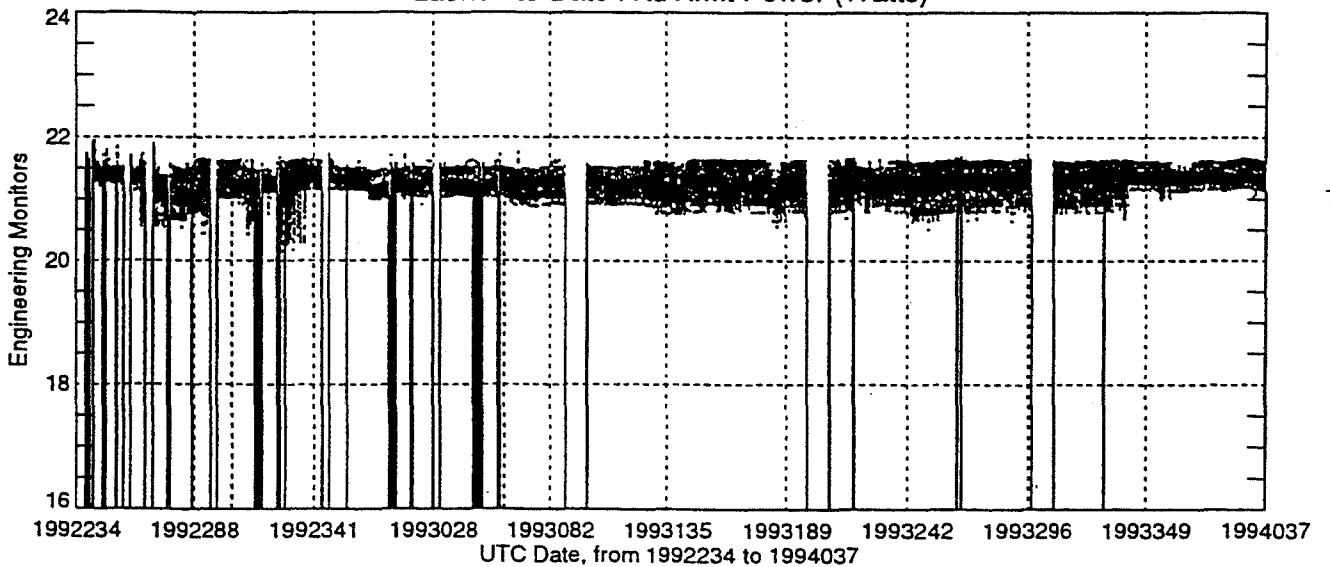
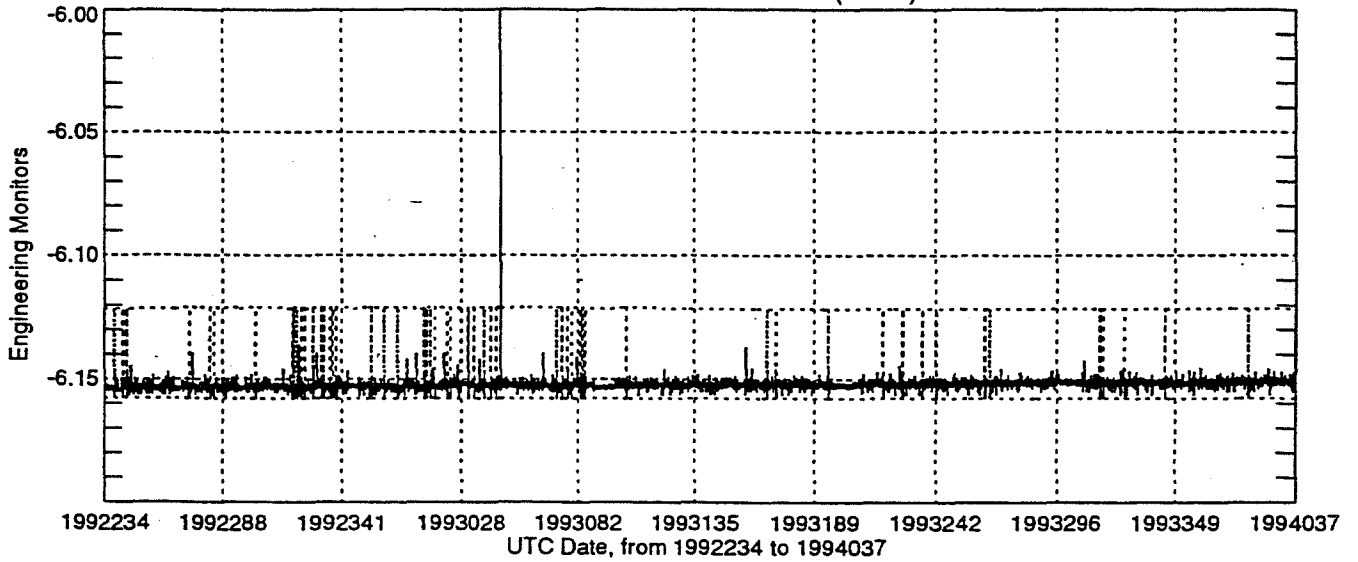
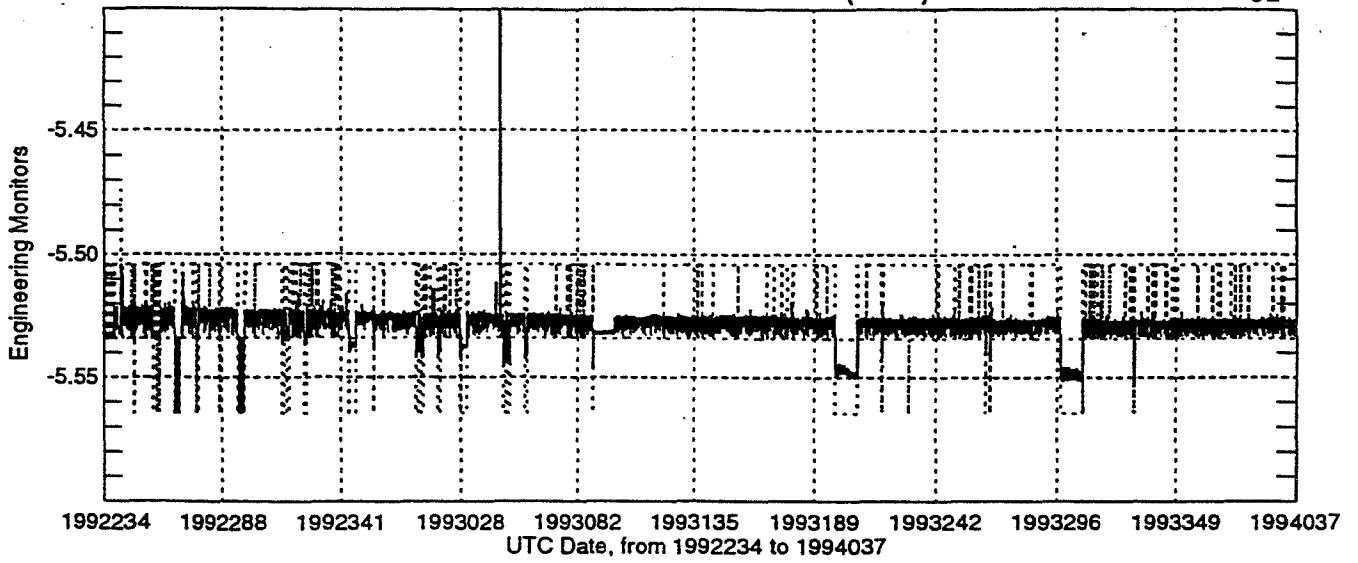
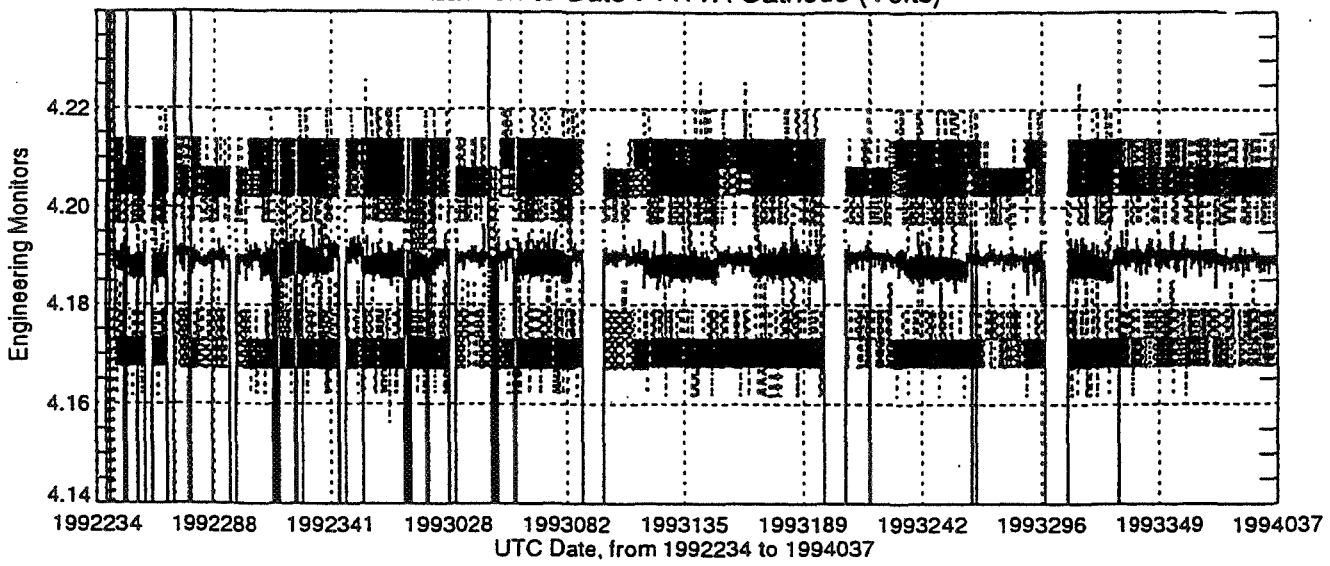
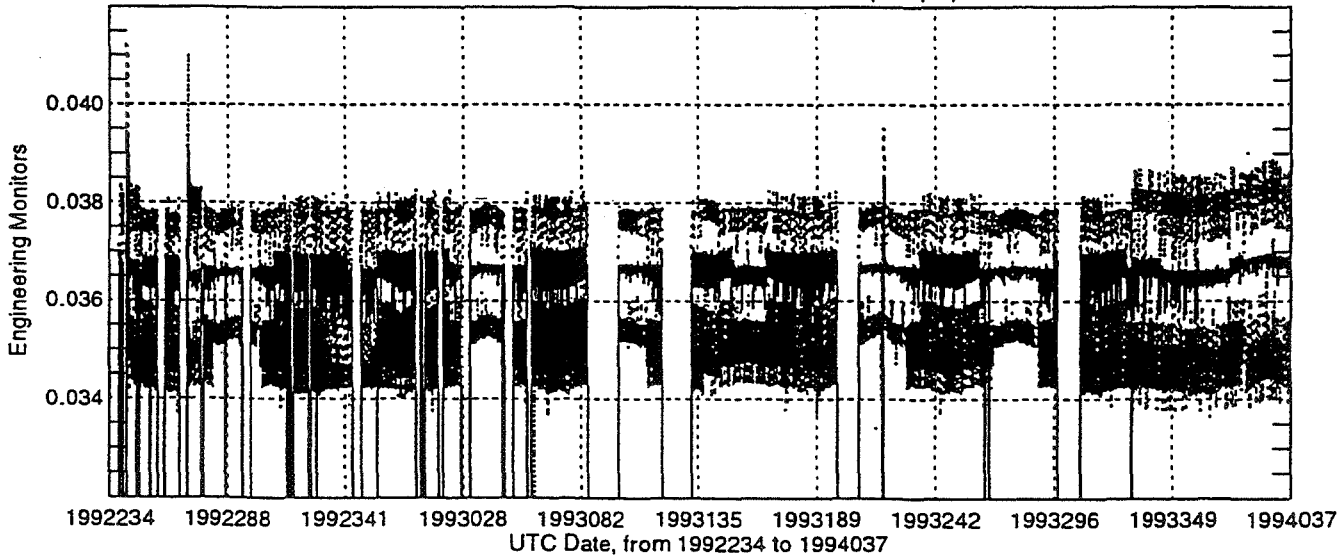


Figure 7.2 Monitor History Plots (cont.)



Launch-to-Date : TWTA Cathode (Amps)



Launch-to-Date : TWTA Helix (Amps)

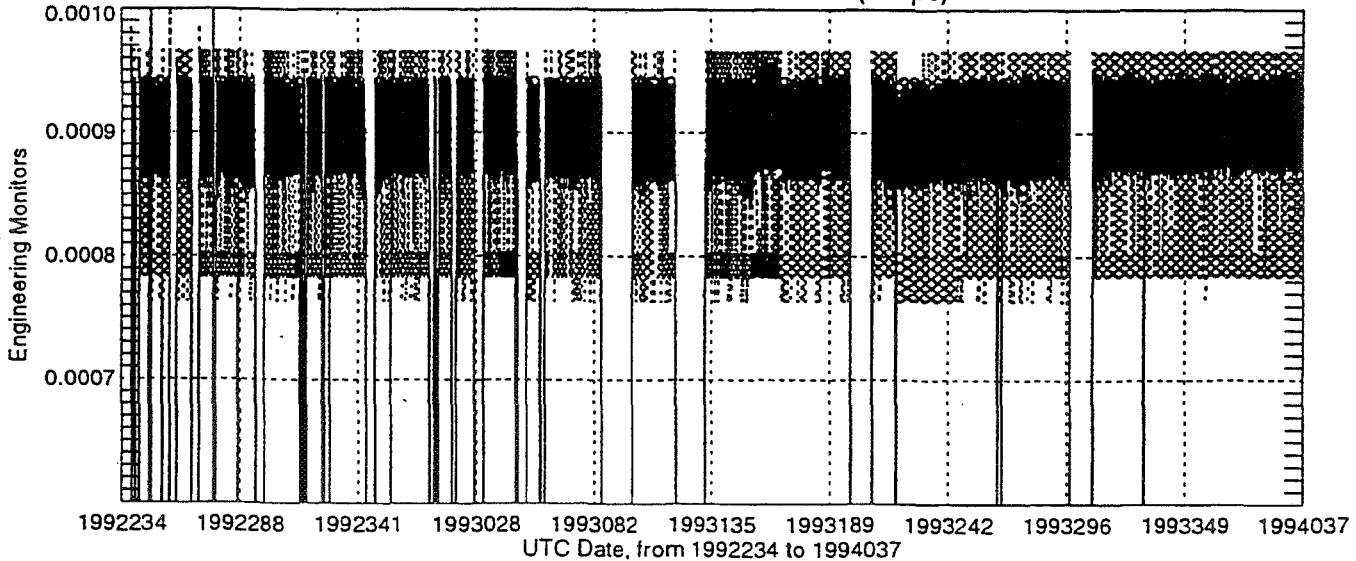
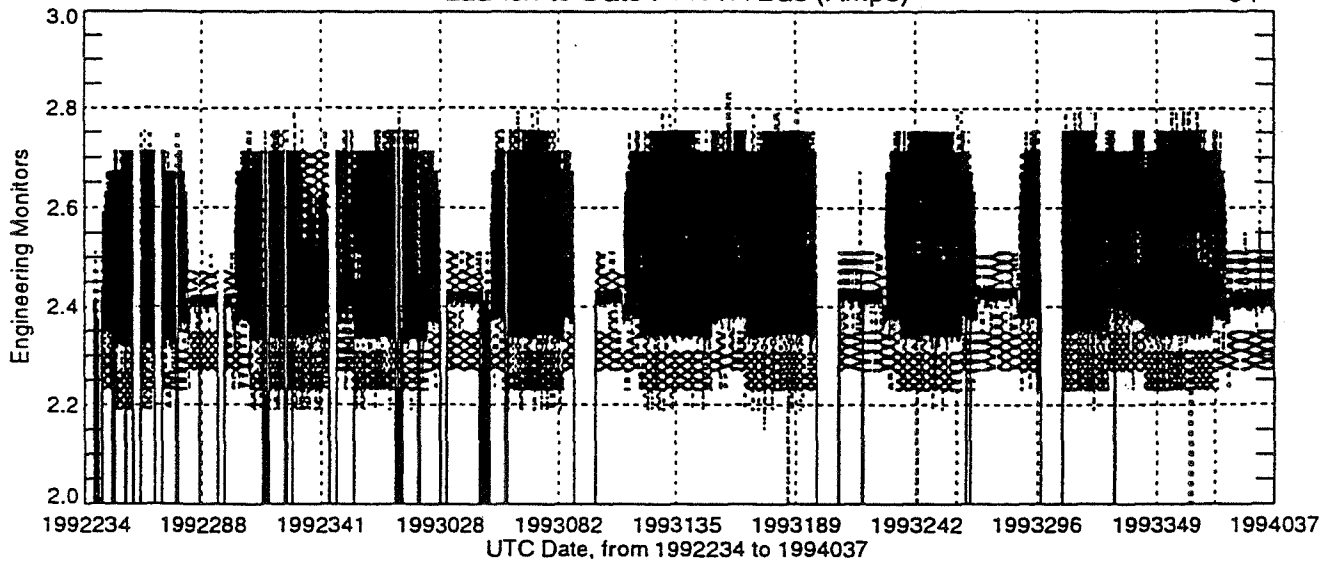
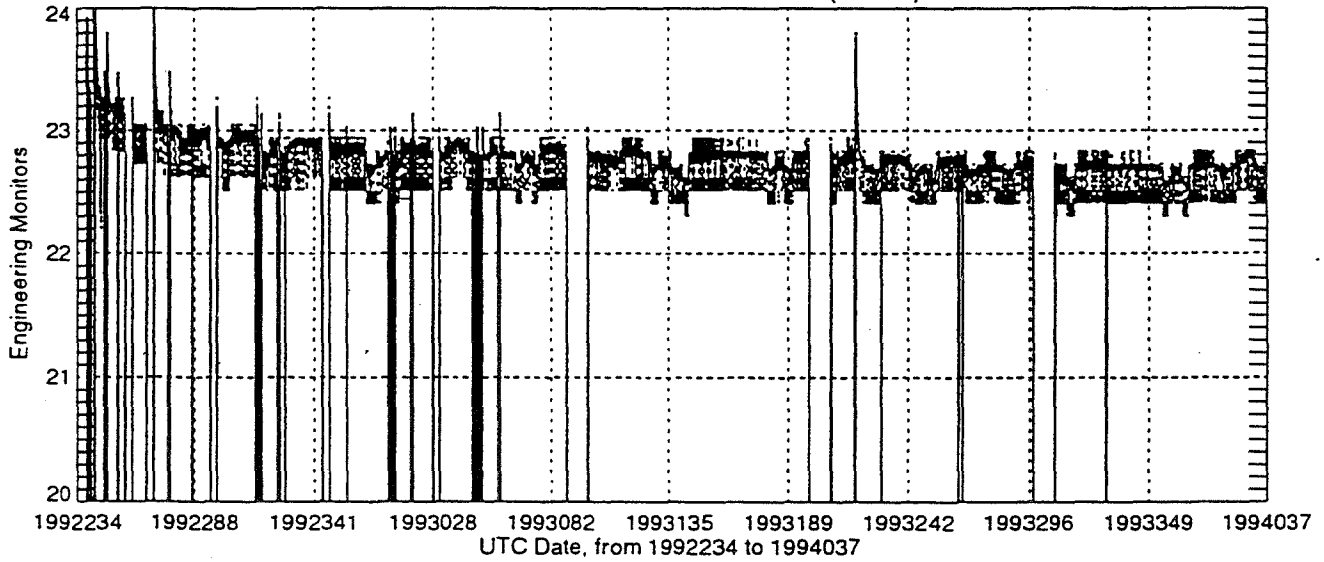


Figure 7.2 Monitor History Plots (cont.)

Launch-to-Date : TWTA Bus (Amps)



Launch-to-Date : C Xmit Power (Watts)



Launch-to-Date : CSSA Input RF (DBm)

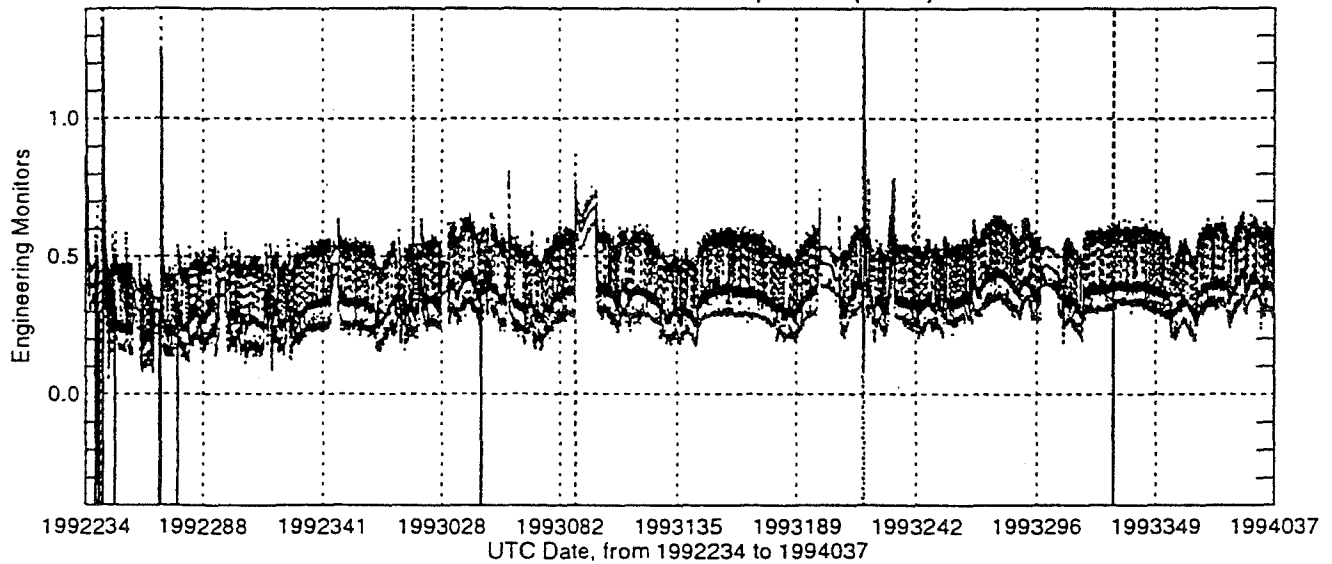


Figure 7.2 Monitor History Plots (cont.)

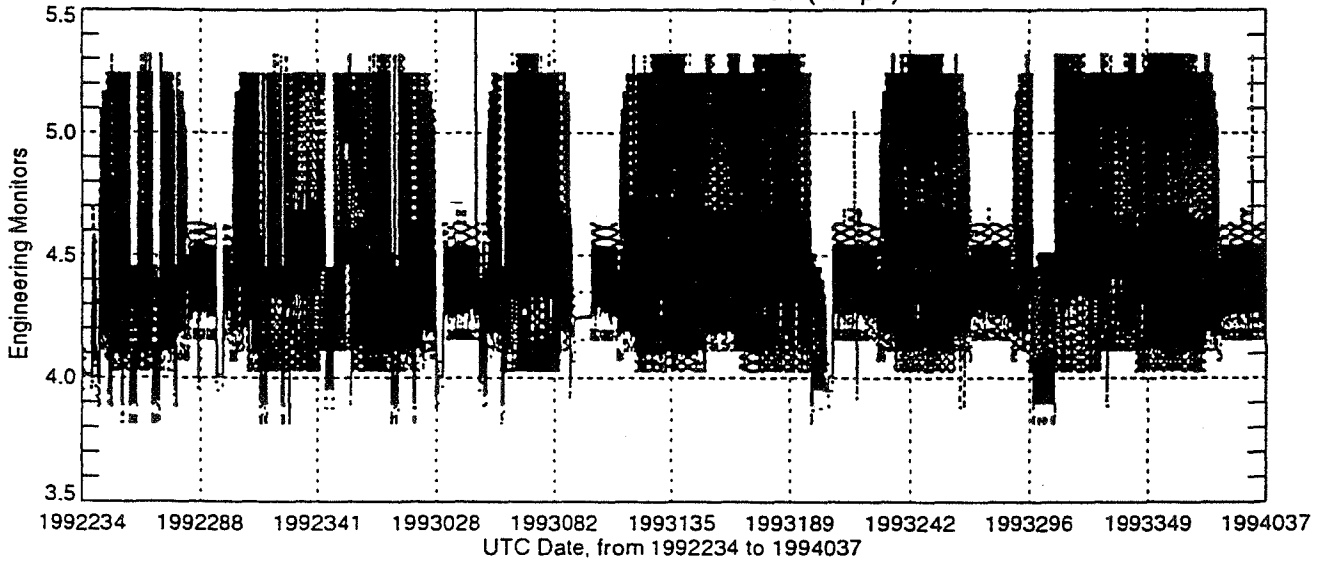
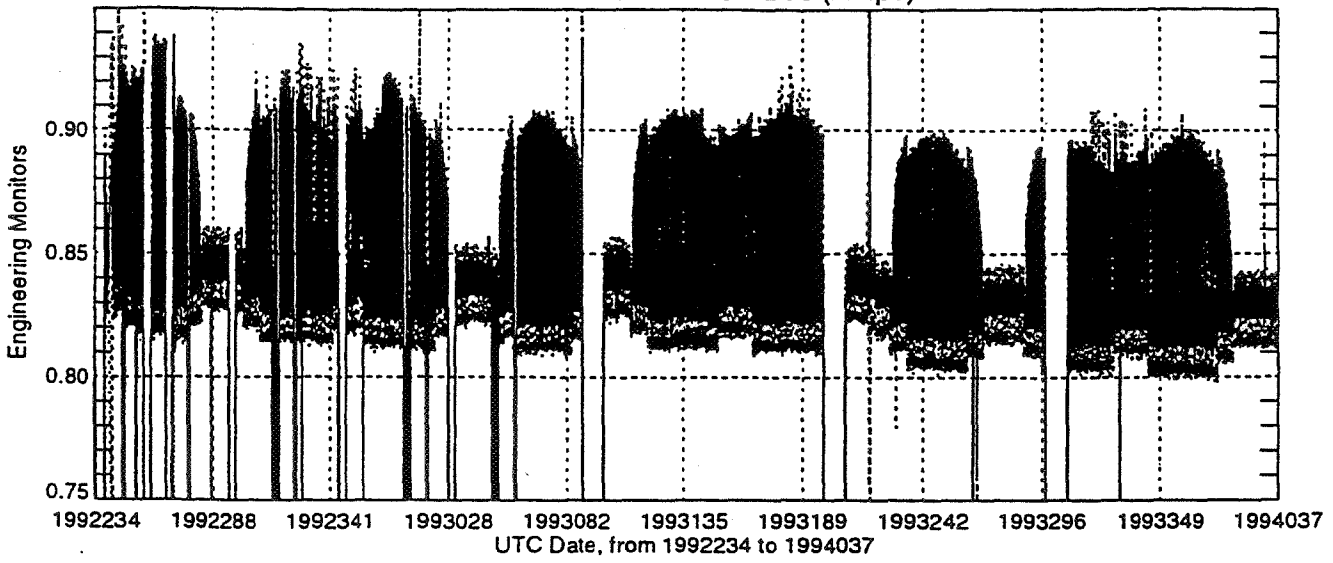


Figure 7.2 Monitor History Plots (cont.)

Parameter	Ambient Limited Performance Tests at Launch Site (May 10, 1992)		On-Orbit	
	Minimum	Maximum	Minimum	Maximum
Volt. Mon. - LVPS +12 VDC (Volts)	13.02	13.09	13.05	13.14
Volt. Mon. - LVPS +28 VDC (Volts)	29.93	30.37	30.10	30.40
Volt. Mon. - LVPS +15 VDC (Volts)	15.59	15.66	15.59	15.68
Volt. Mon. - LVPS -15 VDC (Volts)	-15.40	-15.35	-15.44	-15.35
Volt. Mon. - LVPS +5 VDC 5% (Volts)	4.87	4.89	4.86	4.92
Volt. Mon. - LVPS +5 VDC 1% (Volts)	5.08	5.11	5.10	5.10
Volt. Mon. - LVPS -5.2 VDC (Volts)	-5.53	-5.52	-5.53	-5.52
Volt. Mon. - LVPS -6 VDC (Volts)	-6.16	-6.14	-6.15	-6.15
Analog - Ku MTU Transmit Pwr. Monitor (Watts)	21.11	21.36	18.00	22.00
Analog - Ku TWTA Cathode Voltage (Volts)	4185.	4205.	4187.	4193.
Analog - Ku TWTA Cathode Current (Amps)	0.0350	0.0369	0.0363	0.0371
Analog - Ku TWTA Helix Current (Amps)	0.00083	0.00095	0.00087	0.00095
Analog - Ku TWTA Bus Current (Amps)	2.33	2.59	2.33	2.50
Analog - CMTU Transmit Power Monitor (Watts)	21.88	22.94	22.45	23.00
Analog - C SSA RF Power (dBm)	0.18	0.53	0.22	0.44
Analog - C SSA Bus Current (Amps)	0.835	0.951	0.815	0.860
Analog - LVPS Altimeter Bus Current (Amps)	4.05	4.79	3.90	4.70

Table 7.2 Comparison of Pre-Launch and On-Orbit Engineering Parameters During TRACK Mode

7.2.2 Ku Transmit Power

The Ku band transmit peak power is monitored by a power detector monitor located in the Ku band Microwave Transmission Unit. It generates a voltage proportional to power which is inserted in the engineering telemetry data stream.

The time history of the Ku Transmit Power shows that the power levels have generally remained between 20.7 and 21.6 watts. Minor variations in Ku Transmit Power can be attributed to tracking versus acquisition cycles for which the PRF is different. Variations in PRF cause variations in Power monitor output.

In late November 1992 (days 326-339 in Figure 7.2), larger Ku transmit power variations were indicated. In general, these variations were less than 1 watt (21.25 to 20.70 W) but, occasionally, the monitor dipped all the way to 18 watts for a very short period. After about 2 weeks of these occasional "glitches", they have not reappeared.

When the glitches occurred they were not correlatable with any other altimeter measurement. The Helix current would be the best monitor for verifying power changes, but due to its noisy characteristics, it could not be correlated with the power drop. Also, some of the small changes occurred during calibration modes but, due to their relatively small magnitude (less than 0.1 dB), they could not be positively correlated with AGC changes.

Three possible causes for the glitches are: 1) the power monitor was erroneously indicating these changes possibly due to noise; 2) the telemetry or telemetry interface was erroneously reporting the power; 3) the output power of the TWTA was indeed varying. Although we cannot positively prove either of the above, it is believed that: 1) it probably was not the monitor since we had not seen the glitches before, they have cleared up, and the circuitry does not seem to lend itself to this phenomena; 2) the telemetry is an unlikely source since no other values appear to have been affected; 3) most likely there was real variation in the TWTA power. The TWTA could have become slightly gassy creating minor arcs, corona could have been occurring due to out-gassing of some other part of the spacecraft, or several other typical TWTA phenomena could have been occurring. This condition has not recurred, but it still remains a concern. The cause is unknown and close monitoring continues.

The minor variations in Ku Transmit Power can be attributed to tracking modes versus acquisition mode where the PRF is different. Variations in PRF cause variations in Power monitor output.

7.2.3 TWTA

The time history of the TWTA Cathode Voltage, TWTA Cathode Current, TWTA Helix Current and TWTA Bus Currents, as depicted in Figure 7.2, illustrates that these values have remained steady throughout the mission. The times of larger noise, e.g., days 75-105 and days 125-155, correspond to periods of occultation.

7.2.4 C Transmit Power

The time history of the C Transmit Power shows a linear decrease during the first 90 days, from 23.10 watts to 22.80 watts. This decrease may be due to the characteristics of the GaAs FETS used, and may be a long-term trend towards stabilization. Since that time, there has been a small linear decrease of an additional 0.20 watts. A long term stabilization effect was expected before launch based on test data and known GASFET characteristics.

7.2.5 CSSA

The CSSA Input RF Power time history displays a trend similar to the C Transmit power, but in the opposite direction. There has been an increase of about 0.2 dBm since the beginning of the on-orbit mission. Most of the observed short-term variations in CSSA Input RF are probably due to temperature variations in the power monitor located inside the CSSA; it is not a very precise monitor.

The CSSA Bus Current has remained steady throughout the mission, with the noisier amperage values occurring during periods of occultation when the spacecraft bus voltage varies more. Bus current inversely follows the spacecraft bus voltage.

7.2.6 LVPS Bus Current

The LVPS Bus Current has remained steady, becoming noisier during periods of occultation.

8.0 SYNOPSIS OF ENGINEERING ASSESSMENT

Data have been presented showing that the range noise is within the instrument specifications. The two-frequency altimeter ionospheric corrections do behave as expected, temporally and geographically. Significant waveheight estimation is also consistent with expectations, and the track acquisition time is adequate.

The NASA altimeter's Ku radar backscatter cross-section $\sigma^0(\text{Ku})$ is apparently shifted by about 0.7 dB relative to values observed by Geosat, but this may be partly due to the Geosat data processing's not having taken into account Earth curvature. The NASA altimeter's C-band cross-section $\sigma^0(\text{C})$ is about 3.4 dB higher than $\sigma^0(\text{Ku})$.

The internal calibration mode has shown very small drifts in AGC, and several calibration-based changes in AGC have been entered into the routine ground data processing; these AGC drifts are to be expected, and are well within a reasonable drift magnitude.

A number of SEUs have been observed and the altimeter has automatically recovered from most of these. In nine of these, manual intervention was required; the ground monitoring has been improved to reduce the amount of data lost from anomalous SEU occurrences.

The NASA altimeter is responding correctly to all commands which it has received. The programmability has been successfully demonstrated by an uploaded software patch to improve SEU recovery. The altimeter's routine operation now uses an uploaded parameter file, and the current parameter set's values are included in this report.

There were a variety of small waveform effects produced by the altimeter's digital filter bank, and these have been described and values estimated for the size of the effects. The waveform samplers are performing within the specification of stability to within 1% of the waveform maximum, and no significant changes in the waveform effects have been detected over the past year and a half of operation of the NASA altimeter.

The engineering monitors (temperatures, voltages, currents, and powers) appear to indicate generally nominal performance, within specifications, although one 14-day period (1992, days 326-339) of Ku transmit power variations was described, in Section 7.2.2.

In brief, this report concludes that Side A of the NASA Radar Altimeter is fully operational and within prelaunch specifications. There are no indications of developing problems, and the performance requirements are being met. The Wallops Flight Facility TOPEX personnel are continuing to monitor and analyze the altimeter's performance.

Other Documents in this Series

- Volume 1** TOPEX Radar Altimeter Development Requirements and Specifications, Version 6.0, August 1988 (Published May 2003)
- Volume 2** WFF Topex Software Documentation Overview, May 1999 (Published May 2003)
- Volume 3** WFF TOPEX Software Documentation Altimeter Instrument File (AIF) Processing, October 1998 (Published July 2003)
- Volume 4** TOPEX SDR Processing, October 1998 (Published July 2003)
- Volume 5** TOPEX GDR Processing, July 2003
- Volume 5, Ver. 1.0** GFO Radar Altimeter Processing at Wallops Flight Facility, August 2003
- Volume 6** TOPEX NASA Altimeter Operations Handbook, September 1992 (Published September 2003)
- Volume 7** TOPEX Mission Radar Altimeter Engineering Assessment Report, February 1994 (Published September 2003)

REPORT DOCUMENTATION PAGE

Form Approved
OMB No. 0704-0188

Public reporting burden for this collection of information is estimated to average 1 hour per response, including the time for reviewing instructions, searching existing data sources, gathering and maintaining the data needed, and completing and reviewing the collection of information. Send comments regarding this burden estimate or any other aspect of this collection of information, including suggestions for reducing this burden, to Washington Headquarters Services, Directorate for Information Operations and Reports, 1215 Jefferson Davis Highway, Suite 1204, Arlington, VA 22202-4302, and to the Office of Management and Budget, Paperwork Reduction Project (0704-0188), Washington, DC 20503.

1. AGENCY USE ONLY (Leave blank)		2. REPORT DATE February 1994	3. REPORT TYPE AND DATES COVERED Technical Memorandum	
4. TITLE AND SUBTITLE Topography Experiment (TOPEX) Software Document Series TOPEX Mission Radar Altimeter Engineering Assessment Report			5. FUNDING NUMBERS Code 972	
6. AUTHOR(S) D.W. Hancock III, G.S. Hayne, C.L. Purdy, R.L. Brooks				
7. PERFORMING ORGANIZATION NAME(S) AND ADDRESS (ES) NASA Radar Altimeter Team Observational Science Branch Laboratory for Hydrospheric Processes GSFC/Wallops Flight Facility Wallops Island, VA 23337			8. PERFORMING ORGANIZATION REPORT NUMBER 2003-03169-0	
9. SPONSORING / MONITORING AGENCY NAME(S) AND ADDRESS (ES) National Aeronautics and Space Administration Washington, DC 20546-0001			10. SPONSORING / MONITORING AGENCY REPORT NUMBER NASA/TM-2003-212236, Vol. 7	
11. SUPPLEMENTARY NOTES TOPEX Contact: David W. Hancock III, NASA GSFC/Wallops Flight Facility Wallops Island, VA 23337				
12a. DISTRIBUTION / AVAILABILITY STATEMENT Unclassified - Unlimited Subject Category:42 Report available from the NASA Center for AeroSpace Information, 800 Elkridge Landing Road, Linthicum Heights, MD 21090; (301) 621-0390.			12b. DISTRIBUTION CODE	
13. ABSTRACT (Maximum 200 words) This document describes the GSFC/WFF analysis of the on-orbit engineering data from the TOPEX radar altimeter, to establish altimeter performance. In accordance with Project guidelines, neither surface truth nor precision orbital data are used for the engineering assessment of the altimeter. The use of such data would imply not only a more intensive and complete performance evaluation, but also a calibration. Such evaluations and calibrations are outside the scope of this document and will be presented in a separate Verification Report.				
14. SUBJECT TERMS			15. NUMBER OF PAGES 95	
			16. PRICE CODE	
17. SECURITY CLASSIFICATION OF REPORT Unclassified	18. SECURITY CLASSIFICATION OF THIS PAGE Unclassified	19. SECURITY CLASSIFICATION OF ABSTRACT Unclassified	20. LIMITATION OF ABSTRACT UL	